Experimental and modelling studies on fuel-NO_x formation during flameless combustion of biogenous fuels

Von der Fakultät Energie-, Verfahrens- und Biotechnik
der Universität Stuttgart zur Erlangung der Würde eines
Doktors der Ingenieurwissenschaften (Dr.-Ing.)
genehmigte Abhandlung

vorgelegt von
Mariusz Zięba
aus Ruda Śląska, Polen

Hauptberichter:	Prof. Dr. techn. G. Scheffknecht
Mitberichter:	Prof. Dr.-Ing. R. Weber, TU Clausthal

Tag der mündlichen Prüfung: 02.12.2022

Institut für Feuerungs- und Kraftwerkstechnik
der Universität Stuttgart
2023

This work is dedicated to my beloved wife Katharina
and our lovely children, Paula and Jakob

Nomenclature

Latin Symbols	*Unit*	*Description*
GCV	kJ/kg	Gross Calorific Value
K	-	Recirculation rate
$\dot{m}$	kg/s	Mass flow
NCV	kJ/kg	Net Calorific Value
n	-	Air ratio
u_j	m/s	Cartesian velocity component
S_ϕ	var.	sources/sinks of the conservation variable ϕ
x_i	m	Cartesian coordinate in the i-direction
Y_i	-	elemental mass fraction for element i

Greek Symbols	*Unit*	*Description*
$\in$	m^2/s^3	dissipation rate of turbulent energy
ρ	kg/m^3	density
μ	kg/(m·s)	laminar dynamic viscosity
ϕ	var.	mass specific conservation variable
ξ	-	Mixture fraction

Subscripts

Index	*Description*
air	combustion air
ar	as received
daf	dry and ash free substance
dry	dry substance
FG	flue gas
fuel	fuel
g	gasifier
i	index
ox	oxidizer
stp	standard temperature and pressure
tot	total
wf	water free substance

Abbreviation	*Description*
AR	Air Ratio
CFD	Computational Fluid Dynamics
CHP	Combined heat and power
CR	Conversion ratio
DDGS	Dried distillers' grains with soluble
EDC	Eddy Dissipation Concept
EDCM	Eddy Dissipation Combustion Model
EU	European Union
FBN	Fuel bound nitrogen
FLOX®	Flameless oxidation – registered trademark
GHG	Greenhouse gas
HiTAC	High Temperature Air Combustion
HR	Heating rate
IFRF	International Flame Research Foundation
IFK	Institute of Combustion and Power Plant Technology
LCVG	Low calorific value gases
MILD	Moderate and Intense Low oxygen Dilution
MCS	Methane containing syngas
MFS	Methane free syngas
NDIR	Non-dispersiv Infrared
NG	Natural gas
NPN	Non-protein nitrogen
PAH	Polycyclic aromatic hydrocarbons
PCDD/F	Polychlorinated dibenzodioxins and furans
PFR	Plug flow reactor
PM	Particular matter
PME	Oil methyl ester fuel
PN	Protein nitrogen
PSR	Perfectly stirred reactor
RANS	Reynold averaged Navier-Stokes equations
SCR	Selective Catalytic Reduction
SNCR	Selective Non-Catalytic Reduction
TFN	Total-Fuel-Nitrogen
VOC	Volatile organic compounds

Abstract

Flameless oxidation technology (FLOX®) has already demonstrated great potential in reducing thermal nitrogen oxides while burning natural gas. Due to the high stability of the combustion process, the FLOX® technology has been further developed to burn various low calorific value gases (LCVG).

The work presented in this thesis focuses on the optimization of such flameless burners for LCVG as well as on a profound analysis of the combustion processes, with a special emphasis on the fuel-NO_x formation and reduction mechanisms.

The test results have shown that when combusting NH_3 doped synthetic gases, the NH_3 to NO_x conversion is highly dependent on the CH_4 concentration in the fuel. It significantly increases when increasing the CH_4 content. The CO/H_2 ratio has no measurable influence on the NH_3 conversion. When gasifying solid biomass and combusting the product gases in the flameless burner, it has been observed that the final NO_x emission depends on the initial N content in the fuel, the gasifier parameters, and the final stoichiometry of the burner. For the fuels with lower N content, the NO_x emissions, thus N to NO_x conversion ratios, are comparable to other common combustion technologies. However, for high-N content fuels, the conversion ratios are higher. It has been observed that the higher temperature and air ratio in the gasifier, the better NO_x emission can be achieved in the flameless burner. Due to very good mixing conditions, it is possible to operate the flameless burners for LCVG at very low excess oxygen, simultaneously achieving CO emissions at the level of a few ppm.

Numerical modeling using CFD software has been performed to optimize the design of various burners. The most important parameter when optimizing the geometry for LCVG is the internal recirculation rate, which stabilizes the combustion process. The methodology to calculate the recirculation has been introduced to the software code by the calculation of the local recirculation rate for quantitative analysis of the flue gas flow pattern.

It has been shown that the CFD analysis with a global chemistry model is a sufficient tool for the proper geometry design to optimize the fluid flow in a flameless burner. However, for the NO_x modelling a two-stage numerical model has been developed comprising the reactive flow modelling using CFD and detailed chemistry modeling using reactor network model for pollutant formation analysis. Two different detailed chemistry schemes have been validated, identifying both suitable to predict NO_x emissions for methane containing gases. Three different mixing approaches have been applied and validated, showing that the proper mixing representation is crucial when modelling gases with lower CH_4 content.

It has been shown that CH_4 influences the kinetics of combustion causing significant delay in the fuel oxidation and it simultaneously blocks ammonia decomposition. The later the decomposition is taking place the more air is entrained in the jet, the more nitrogen is converted to NO_x. For methane rich fuels the mixing is faster than the combustion reactions. The combustion is kinetically controlled. For methane free fuel the combustion occurs

immediately – what is mixed is also burned, causing the ammonia to react immediately after introducing into the combustor under fuel rich conditions. The process is diffusion controlled. Therefore, for the methane free gases the precise representation of mixing processes is deciding for correct NO_x predictions.

Kurzfassung

Die flammlose Oxidationstechnologie (FLOX®) hat bereits ein großes Potenzial bei der Reduzierung von thermischen Stickoxiden bei der Verbrennung von Erdgas gezeigt. Aufgrund der hohen Stabilität des Verbrennungsprozesses wurde die FLOX®-Technologie weiterentwickelt, um verschiedene niederkalorische Gase (LCVG) zu verbrennen. Die in dieser Dissertation vorgestellten Arbeiten und Ergebnisse konzentrieren sich auf die Optimierung solcher flammlosen Brenner für niederkalorische Gase sowie auf eine tiefgreifende Analyse der Verbrennungsprozesse, mit besonderem Schwerpunkt auf den Brennstoff-NO_x Bildungs- und -Reduktionsmechanismen.

Die Versuchsergebnisse haben gezeigt, dass bei der Verbrennung von synthetischen, mit NH_3 angereicherten Gasen, die Umwandlung von NH_3 zu NO_x stark von der CH_4-Konzentration im Brennstoff abhängt. Sie nimmt mit zunehmendem CH_4-Gehalt deutlich zu. Das CO/H_2-Verhältnis hat dagegen keinen messbaren Einfluss auf den NH_3-Umsatz. Bei der Vergasung von fester Biomasse und der nachgelagerten flammlosen Verbrennung der Produktgase wurde beobachtet, dass die NO_x-Emission vom ursprünglichen N-Gehalt im Brennstoff, den Vergaserparametern wie Temperatur und Luftüberschuss sowie der Stöchiometrie des Brenners abhängt. Bei Brennstoffen mit geringerem N-Gehalt sind die NO_x-Emissionen, also die Umwandlungsraten von N zu NO_x, vergleichbar mit anderen gängigen Verbrennungstechnologien. Bei Brennstoffen mit hohem N-Gehalt sind die Umwandlungsraten jedoch höher. Es wurde beobachtet, dass je höher die Temperatur und die Luftzahl im Vergaser ist, desto niedrigere NO_x-Emission erreicht werden können. Aufgrund der sehr guten Durchmischungsbedingungen ist es möglich, die flammlosen Brenner für LCVG mit sehr geringem Sauerstoffüberschuss zu betreiben und gleichzeitig CO-Emissionen im Bereich von wenigen ppm zu erreichen.

Numerische Modellierung mittels CFD-Software wurde durchgeführt, um das Design verschiedener Brenner zu optimieren. Der wichtigste Parameter bei der Optimierung der Geometrie für LCVG ist die interne Rezirkulationsrate, da die Rezirkulation den Verbrennungsprozess stabilisiert. Die Methodik zur Berechnung der Rezirkulation wurde durch die Berechnung der lokalen Rezirkulationsrate zur quantitativen Analyse des Strömungsfeldes in den Softwarecode eingeführt. Es hat sich gezeigt, dass die CFD-Analyse mit einem globalen Chemiemodell ein ausreichend gutes Werkzeug für die Auslegung der Brennergeometrie ist, um die Strömungsfelder in einem flammlosen Brenner zu optimieren. Für die NO_x-Modellierung wurde jedoch ein zweistufiges numerisches Modell entwickelt,

das die reaktive Strömungsmodellierung unter Verwendung von CFD -Software und eine detaillierte chemische Modellierung unter Verwendung eines Reaktornetzwerkmodells zur Schadstoffbildungsanalyse umfasst. Zwei unterschiedliche detaillierte Reaktionsmechanismen wurden validiert, wobei beide als geeignet identifiziert wurden, NO_x-Emissionen für methanhaltige Gase vorherzusagen. Es wurden drei verschiedene Mischansätze angewendet und validiert, die zeigen, dass die präzise Mischungsdarstellung bei der Modellierung von Gasen mit geringerem CH_4-Gehalt entscheidend ist. Es hat sich gezeigt, dass CH_4 die Verbrennungskinetik beeinflusst, was zu einer erheblichen Verzögerung der Brennstoffoxidation führt und gleichzeitig die NH_3-Zersetzung blockiert. Je später die Zersetzung stattfindet, desto mehr Luft wird im Brennerstrahl mitgerissen, desto mehr Stickstoff wird in NO_x umgewandelt. Bei methanreichen Brennstoffen ist der Mischprozess schneller als die Verbrennungskinetik. Die Verbrennung ist kinetisch kontrolliert. Bei methanfreiem Brennstoff erfolgt die Verbrennung sofort – was gemischt wird, wird ebenfalls verbrannt, wodurch das NH_3 unmittelbar nach dem Einbringen in die Brennkammer unter brennstoffreichen Bedingungen reagiert. Der gesamte Prozess ist diffusionskontrolliert. Daher ist für methanfreie Gase die richtige Modellierung von Mischungsprozessen entscheidend für korrekte NO_x-Vorhersagen.

1 Introduction

The use of biomass as an energy source plays a significant role in the transition towards a CO_2 neutral economy. For several years, the major CO_2 emitting countries have focused on the increased use of renewables in their power, heat, and transportation sectors to decrease their overall CO_2 footprint. Moreover, with the rising global temperature, and considering the already noticeable impact of global warming on our lives, more and more countries are intensifying their efforts to decrease the global CO_2 emissions.

The EU has recently revised its climate strategy and has decided to reduce the CO_2 emission by at least 55% by 2030 to reach a complete climate neutrality by 2050, thereby fulfilling the commitments made under the Paris Agreement [1].

It has become clear that such a significant reduction of emissions will require efforts in all sectors, and that the transition toward climate neutrality can only be managed with a contribution from all countries. The desired scenario includes a drastic reduction of the greenhouse gas (GHG) emissions and, ultimately their removal, as shown in Figure 1.

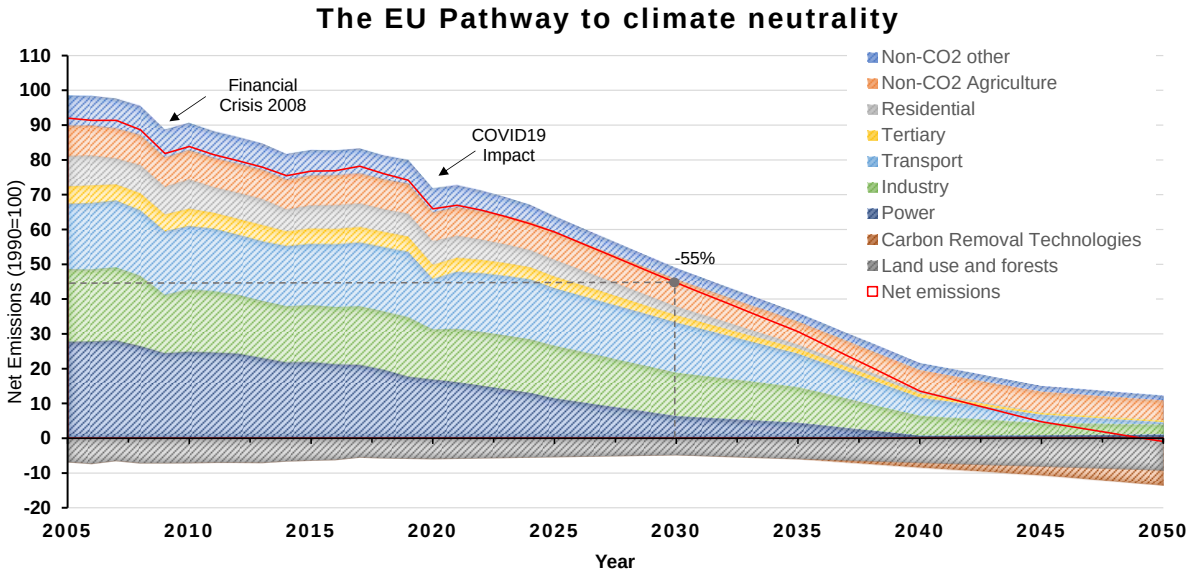

Figure 1 The EU's pathway to climate neutrality (chart prepared based on the data published in [1])

Biomass, as a renewable and easily stored energy source, plays an important role in this transition. Although the share of bioenergy in the total energy consumption stabilized over the last years, and most future scenarios predict no increasing share of biomass, the long term will be characterized by better mobilization of agricultural residues and organic wastes [1]. The increase in low-grade biofuels' share of total energy is mainly driven by the high competition with non-energy markets [2]. In recent years, a sustainable use of biomass increasingly came into focus and the strong expansion of agricultural areas for energy crops has been questioned.

The German Federal Environment Agency formulated the main principles of the sustainable use of bioenergy as follows [3]:

- In agriculture, priority must be given to food production.
- The energy use of biomass should to a large extent take place without the cultivation of energy crops.
- The focus should be placed on unavoidable residue or waste mass flows that are coupled to food production.
- The biomass used for energy conversion should not be in competition with possible recycling. Such recycling also includes ecologically beneficial scenarios such as humus formation resulting from leaving crop residues on the agricultural land.

Based on these principles, following usage hierarchy can be derived (Figure 2).

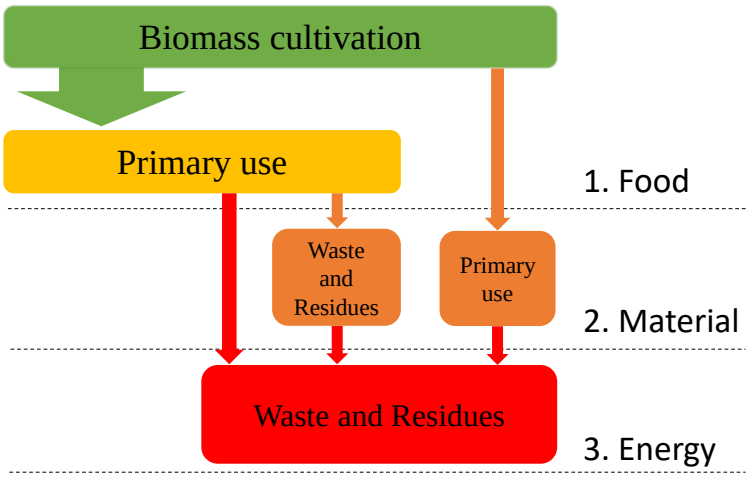

Figure 2 Biomass usage hierarchy. Based on [3]

As the availability of renewable bio feedstock as an energy source is very limited, it should be ensured that the utilization occurs at a maximum efficiency and a minimum impact to the environment. In the case of thermal conversion of biomass in systems for heat (industrial processes or domestic needs) and power generation, it means a highly efficient conversion using processes that are tailored to the particular fuel used. Such a task becomes more difficult the more bio-residues, including waste solids and waste gases, are used.

A clean and efficient use of biomass or biowastes for heat and power production is usually associated with certain challenges originating in the fuel properties. Depending on the biomass composition, the main issues are usually related to the relatively low melting point of the ash, the corrosive character of the deposits, corrosive flue gases and emissions of various pollutants. Furthermore, a low calorific value of the fuel or large fluctuations in its quality might also cause problems. These aspects are also relevant for gaseous fuels, such as waste gases from landfills or synthetic gases from biomass gasification processes.

The main pollutants emitted to the atmosphere during combustion of solid biomass are particulate matter (PM) and nitrogen oxides (NO_x). Other emissions such as volatile organic compounds (VOC) and polycyclic aromatic hydrocarbons (PAH) are also considerable [4].
The PM emitted from residential biomass combustion has been identified as a major contributor to the air pollution worldwide with a serious impact on air quality, climate and human health [5]. It has also been found that the ultra-fine particles emitted are mainly composed of alkali metal compounds (mineral matter-ash) whereas large agglomerates were found to contain mainly carbon and are considered to primarily be soot particles [6]. It also has to be noted that the particular matter emitted during biomass combustion exhibits a severe toxic and carcinogenic potential [7].
The NO_x emissions during combustion of biomass have a comparably large impact on the environment as particulate matter emissions [4]. In solid biomass fired systems, the oxidation of fuel-bound nitrogen is the main source of NO_x emissions. Therefore, the more nitrogen bound in the fuel, the higher the NO_x emission that can be expected [8]. As agricultural residues and organic wastes usually include more nitrogen than does woody biomass, it is more challenging to control the emissions when burning such low-grade fuel.
To overcome all these disadvantages, and to use biomass sustainably, there is a need for technology development comprising combustion systems that can handle low-grade biofuels, ensure complete combustion to avoid such pollutants like CO, VOC, PAH and minimize the emissions of PM and NO_x.
Among all technologies developed over the last three decades, one has the potential to address most of these aspects, allowing for clean combustion of low-grade biofuels. The flameless oxidation technology (FLOX®), originally developed for the combustion of natural gas, has been adapted for combustion of low calorific value (LCVG) biogases [9]. The work done by Schuster, and described in [9], focused on the development of a particular flameless burner integrated in a commercially available combustion system equipped with a pre-gasifier. The main driver behind the research was the idea that flameless oxidation allows the application of a much wider range of fuels in a system that was originally designed for wood chips. The decoupling of the gasification process from the process of combustion was promising in terms of PM and NO_x emissions. The application of a flameless combustor for the product gases should ensure the minimization of incomplete combustion products by simultaneously lowering excess air and thus increasing the efficiency. It should also have a further positive impact on reducing NO_x emissions.
The work presented in this doctoral thesis builds on the results of Schuster [9] and complements them with topics that provide a more in-depth analysis of phenomena behind the FLOX® technology.

1.1 Biomass as fuel

In the following, the state-of-the-art of the different technological aspects considered in this thesis is provided. This includes fundamentals on the biomass composition and the related impact on the subsequent technological conversion processes, as well as the different approaches to thermal biomass conversion routes.

1.1.1 Biomass classification

The term biomass refers to all non-fossil organic substances (i.e., carbon-containing matter). The differentiation of biomass from fossil fuels begins with peat, the fossil secondary product of rotting [10]. In an engineering sense, the term biomass usually refers to all substances of an organic origin such as dead plant or animal material suitable for use as a substrate of a secondary energy carrier's production, or as a fuel for direct heat or power generation.

Depending on its origin, biomass may be categorized as primary, secondary and tertiary biomass [10]. Primary biomass originates in the direct utilization of solar energy through photosynthesis. This is mainly the case in plants (e.g., energy plants), but also in residues such as waste wood from forestry or industrial waste wood. Secondary biomass originates in the indirect utilization of solar energy only. It is formed by the conversion of organic matter, mainly in animals, in the form of sewage sludge. Tertiary biomass is produced by one or more technical processing steps of the primary, and partly of the secondary, biomass. This category includes paper and pulp, or cotton clothing.

Another approach to biomass fuel classification was introduced by the European Committee for Standardization CEN within the standard EN ISO 17225-1:2014-09 [11]. The aim of this international standard is to provide clear and unambiguous classification principles for biogenic solid fuels, and thus provide a tool that enables efficient trade in biofuels and easy communication between seller and customer, as well as a means of communication with equipment manufacturers. According to this standard, the solid biomass fuels can be grouped in five main categories. These major groups are further divided into several other groups and subgroups.

Woody biomass is the biomass of trees, bushes, and shrubs. These include forest and plantation wood, industrial residue wood and by-products, as well as used wood.

Herbaceous biomass comes from plants with a non-wood-like stem that die at the end of the growing season. These include grains and their by-products, such as cereals.

Fruit biomass is biomass from the parts of the plant that form or contain the seeds.

Aquatic biomass comes from so-called aquatic plants or hydrophytes. These are plants that have adapted to life in an aquatic habitat. The fifth group includes various ***biomass blends*** and ***mixtures***. The groups are further divided into several other groups and subgroups, indicating the origin of the material. The retracing of fuels to their origin according to the proposed scheme of the standard is an essential element of an effective quality assurance management, and an important fuel assessment factor for solid biofuels [12].

In addition to the biomass fuels described in this standard, there is also a significant potential of biomass fuel in the organic components of municipal and industrial waste [13].

1.1.2 Biomass characterization

Another fuel assessment method is the fuel characterization by a direct determination of specific fuel properties. From the engineering point of view, the most important properties are the technical combustion properties, elementary composition, and the physical-mechanical properties of the fuel. These three groups of parameters have a decisive influence on the conversion of solid biomass. The parameters listed in Table 1 influence the thermochemical and the pollutant formation processes, thus determining the design of the dedicated conversion systems.

Table 1 Solid biomass fuel properties and their impact in the utilization chain [12, 14, 15]

Quality parameter	Main impact
Technical combustion parameters [15]	
Calorific Value	Energy content of fuel, energy density, dimensioning of combustion plant
Moisture content	Heating value, storability (losses by biodegradation, self-ignition), fuel weight, combustion temperature, plant design
Volatile Matter	Reactivity of the biomass, plant design
Fixed Carbon	Reactivity of the biomass, plant design
Ash content	Particulate matter (PM) emissions, residue management and utilization, calorific value
Ash-melting behavior	Slag formation and deposits, operational safety and continuity, maintenance requirements, ash utilization
Elemental composition	
Carbon (C)	Calorific value, oxygen demand, particle emissions
Hydrogen (H)	Calorific value, oxygen demand
Oxygen (O)	Calorific value, oxygen demand
Nitrogen (N)	NO_x and N_2O emission
Potassium (K)	Ash-softening behavior, high-temperature corrosion, particle emission
Magnesium (Mg)	Ash-softening behavior, ash embedding of pollutants, ash utilization, particle emission
Sodium (Na)	Ash-softening behavior, ash embedding of pollutants, ash utilization, particle emission
Calcium (Ca)	Ash-softening behavior, ash embedding of pollutants, ash utilization, particle emission
Phosphorus (P)	Ash-softening behavior, ash embedding of pollutants, ash utilization, particle emission
Sulphur (S)	SO_x emissions, high-temperature corrosion, particle emission
Silicon (Si)	Ash-softening behavior, ash utilization, particle emission
Chlorine (Cl)	Emissions of hydrochloric acid HCl and halogen-organic compounds (e.g., PCDD/F), high-temperature chlorine corrosion, particle emission
Heavy metals	Ash utilization, heavy metal emissions, catalytic impacts (e.g., in PCDD/F formation), particle emission

The *calorific value* is the most important parameter that defines the energy content of the fuel. When defining the calorific value, one can distinguish between the *Gross* (GCV) and the Net

heating value (NCV). GCV refers to the heat released in a combustion reaction, considering that the fuel moisture and combustion-generated water is condensed to a liquid. NCV considers water vapor as a product, and the energy that is needed to evaporate water is not regarded as useful heat.

Moisture content is important for determining the most effective conversion technology for a given biomass. Thermal conversion requires rather low moisture levels, whereas biochemical processes such as anaerobic digestion can handle materials with very high moisture contents, such as municipal bio-waste. Moisture greatly affects the NCV of the fuel, and thus also the fuel combustion behavior, plant management and design. It also has a major impact on the storability of the material.

Volatile matter and *fixed carbon* are related to the reactive part of the solid fuel. Volatile matter is the part of the dry fuel matter that is released at high temperature in the absence of air. On the other hand, the fixed carbon is the fraction of the reactive fuel matter remaining after the volatile fraction is released. The ratio between these two parameters indicates the reactivity of the fuel. Higher reactivity facilitates the ignition process and significantly influences the gasification or combustion processes.

The *ash content* describes the fraction of inorganic residue that remains after complete combustion of the biomass fuel. It affects the PM emissions and, depending on the *ash melting behavior*, it may cause slagging, fouling, corrosion, or erosion in the combustion system. Ash composition affects its final disposal. The ash may be used as fertilizer or in the cement industry [15].

The elemental composition provides more detailed information about the fuel and its impact on the conversion process. The composition of various biomass materials is widely reported in the literature. Detailed analysis of dozens of biomass types can be found in [12, 14–16].

According to these analyses, the three main elements C, H and O represent more than 95 % of the total weight of dry biomass. These elements comprise the main substance of biomass—cellulose, hemicellulose, and lignin [17]. Some biomasses also contain fats (oil-producing plants such as rapeseed) or proteins (cereal grains). The elements C and H are the main energy carriers stored in biomass and determine the calorific value of the combustible dry matter. This energy can be transformed into heat during oxidation processes, which are supported by the oxygen contained in the biomass.

Other elements such as nitrogen (N), potassium (K), phosphorus (P), magnesium (Mg), calcium (Ca) or sulphur (S) represent the main plant nutrients. Chlorine (Cl) in the form of a chloride ion Cl^- can also be counted to this group [18].

Even though these elements are necessary for the life and the growth of plants, they are undesirable in the fuel due to their negative impact on pollutant emissions, deposit formation and corrosion. Woody biomass is characterized by much lower nutrient concentrations in comparison to herbaceous based fuels. Therefore, native wood is the most favorable fuel for thermal conversion processes [19]. The content of the nutrients also changes significantly

within a specific plant, i.e., the bark has a significantly different nutrient content to the woody stem or to the green tree crown. This also means that these three exemplary mentioned types of biomass will have different combustion properties and will place different requirements on the combustion or gasification system. The content of the main nutrients in selected biomasses is shown in Figure 3.

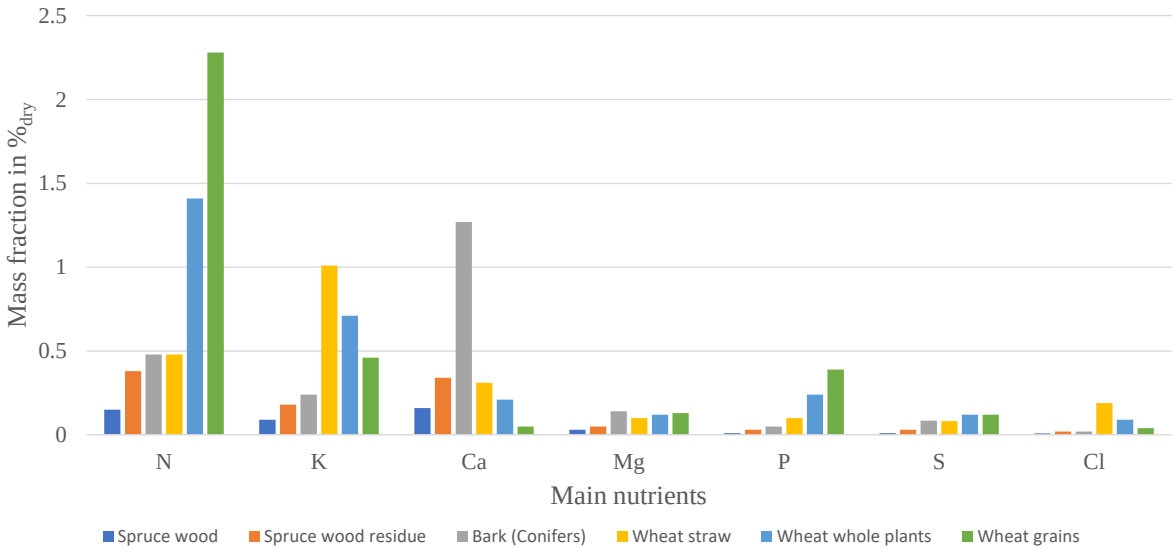

Figure 3 Mass fraction of nutrients in chosen biomasses. Based on data from [10]

The impact of these elements on the conversion processes varies greatly. The N bound in the biomass is the main source of NO_x and N_2O emissions during the combustion of biogenic fuels. There are many structures in which N can be found in biomass. The N compounds in living organic tissues can be classified into two main groups: the protein-N (PN) and the non-protein-N (NPN). A significant part of N is contained in amino acids that form proteins. The NPN contains several functional N compounds such as free amino acids, polypeptides, nucleic acids and various types of alkaloids including cyclic alkaloids (e.g., caffeine) [20]. Furthermore, the structure of chlorophyll, the green photosynthetic pigment, contains meaningful amounts of N. The N content in the biomass varies widely depending on its origin and on where it is located in the plant (due to the different biological functions of the specific plant organs). Woody biomass contains (relatively) less N in comparison to herbaceous biomasses. The lowest concentration, usually N < 0.3 %, is found in the stem wood, which is the “dead part” of the tree. The wood bark usually contains slightly more N than the stem. The N concentrations are usually between 0.3 and 0.5 % in the bark. The highest N concentration is expected in the living part of the tree, i.e., in the needles and leaves, where a much higher protein content can be found. Therefore, all forest residues, which are usually mixtures of wood, bark, smaller branches, leaves, and needles may have significantly higher N content than the pure wood.

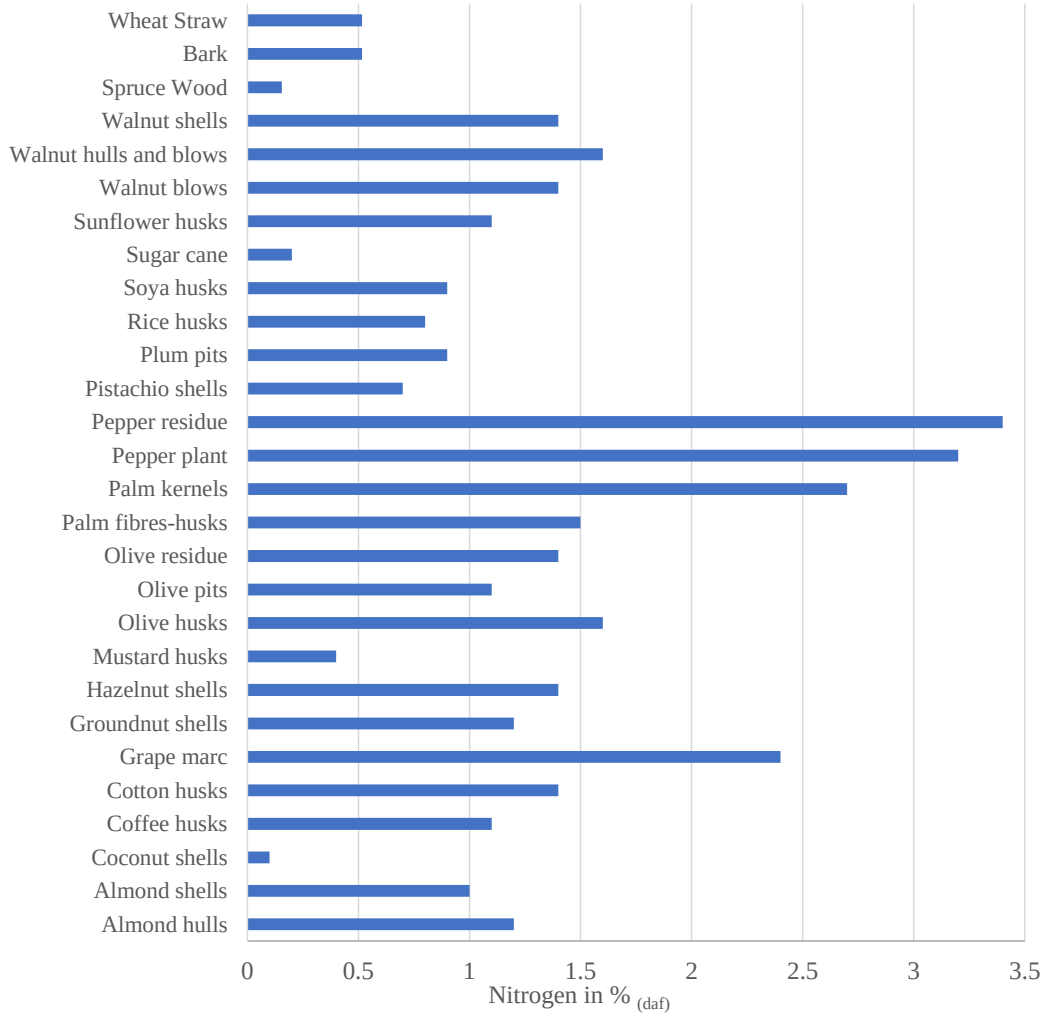

Figure 4 Nitrogen content in various biomass residues. Based on data from [16]

Much higher N contents are expected in herbaceous biomasses. A compilation of the data related to N content in diverse biomass residues is shown in Figure 4. Particularly cereal grains, as an important source of proteins, can contain up to 5 % N. However, it must be noted that only residues from food processing such as straw, husks, shells, pits etc. and not the grains themselves are considered as a fuel, as these are primarily dedicated for food production. Higher N contents of up to 12 % can be measured in animal biomass such as meat bone meal or chicken litters [16, 21]. The impact of the N bound in the biomass fuel on the emissions is the primary focus of this thesis, and the subject of the N evaluation within the biomass gasification and combustion process will be further described in detail in Subchapter 1.2.

The impact of K on thermal conversion varies. This element can form gaseous alkali chlorides (KCl), which condense and form deposits on the heat exchanger surfaces, causing corrosion.

Moreover, during the combustion process it can be released in a gaseous form, which condenses to very fine aerosol particles that are released into the atmosphere. It also has a negative impact on the ash melting behavior, by lowering the ash melting temperature [22]. Beside the alkali chlorides, the Cl can also form toxic substances such as dioxins and furans (PCDD/F) or hydrogen chloride that forms corrosive hydrochloric acid in the colder parts of flue gas systems. All these phenomena are expected when, e.g., straws are used as a fuel.

Ca, according to the literature, can have a positive effect on the ash melting behavior [23]. It also supports the binding of the S in the ash, thus preventing it from being oxidized and released as SO_x to the atmosphere. This phenomenon is well known in solid fossil fuel fired systems. Since the S content in biofuels is usually low (except in rapeseed straw), no significant emissions of SO_x are expected from biomass combustion processes.
P and Mg are available in the biomass, usually in small concentrations. These elements also contribute to PM emissions. While P tends to lower the ash melting temperature, Mg raises it [24].
Silicon (Si) is available in biomass in concentrations up to approximately 2 %. The Si content of < 0.8 % in woody biomass is relatively low. Higher concentrations of up to 1 % are measured in herbaceous biomasses [10]. The highest concentrations are found in biomass fuels that are polluted with soil. Such pollution can be expected e.g., in forest residues and biomass residues from roadsides. In the thermal conversion systems, biomass with high Si content tends to have a low ash melting temperature and causes slagging and fouling related problems. On the other hand, higher Si content can increase the binding of K in the ash, thus decreasing the aerosol emissions [25].

1.1.3 Biomass conversion routes

There are three main possible conversion routes when considering biomass as fuel for heat and power generation. These are shown in Figure 5. Most of them lead to an upgrade of the biomass feedstock into secondary fuel that is characterized by better combustion characteristics than the original material. The most suitable conversion path depends on the quality of the original material as well as on the desired product. Moreover, the biological and physical conversion requires certain kind of biomass applicable for these processes.
Anaerobic digestion and fermentation represent the biological conversion route. Anaerobic digestion is well suited for biomass with a very high moisture content. The main product of this process is biogas – a mixture of methane (CH_4), CO_2 and acid gases. The biogas can be locally utilized after cleaning or can be further upgraded by increasing the CH_4 concentration up to the levels known from the fossil natural gas. Within the anaerobic digestion process, liquid, solid and gaseous residues are produced. The solid residues may either be composted or thermally incinerated, while the liquids can be used as a fertilizer. The gaseous fraction in the form of a

low calorific off-gas from the CH_4 upgrading process has to be combusted to avoid CH_4 emissions escaping to the atmosphere [26].
A fermentation process allows for ethanol to be produced from biomass. This process includes two major steps: sugar extraction or decomposition of biomass structures to sugars, and the fermentation itself. In the second step, the main product – ethanol – is created. Within this process, different types of by-products and residues are generated. Some of them are thermally used, generating heat necessary for the fermentation process itself. Other residues, such as dried distillers' grains with soluble (DDGS) are commonly sold as a high-protein livestock feed [27].
The physical conversion path includes all processes related to the biomass-based oil production such as rapeseed, sunflower, or palm oils. Within such a process, the liquid oil phase is separated from the solid phase. It can be realized by a mechanical pressing or an additive extraction, where the oil content of the oily seed or the still oily press cake is removed using a solvent.
The oil can be used as fuel in its pure form and – after a chemical conversion – as oil methyl ester fuel (PME) in car diesel engines or combined heat and power (CHP) plants. After extraction, a solid residue in the form of a press cake is produced. This residue is commonly used as livestock feed or may also be used via different thermal conversion paths for heat and power generation if it is necessary for the process.

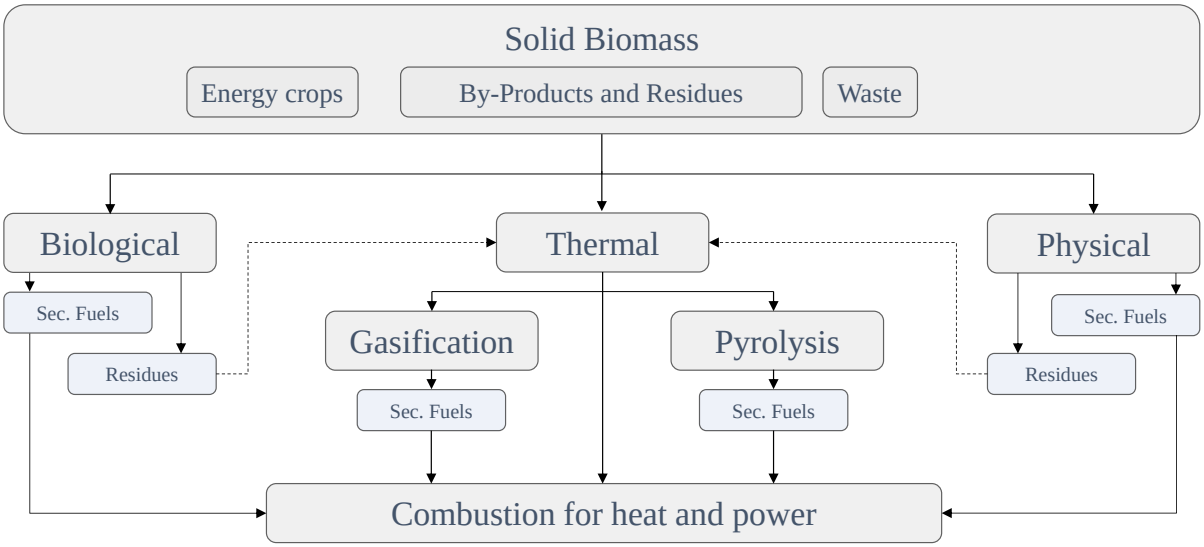

Figure 5 Biomass conversion paths

Since the work developed in this thesis deals with the thermal conversion of biomass materials, a brief introduction to the current technologies is given in the next subchapter.

1.1.4 Thermal conversion of biomass

This section will provide a brief overview of the technologies currently used for the thermal conversion of biomass. The thermal conversion route is the most flexible, and allows for the conversion of various qualities of biomass. Within this route, the final provision of the useful heat occurs either directly via a combustion process (complete oxidation) or by a prior conversion into a secondary energy carrier, which can then be completely oxidized in an independent step. The thermal conversion from using this intermediate step usually provides a fuel of a better quality than the original biomass, allowing for final conversion (complete oxidation) in more complex and efficient systems.

Combustion

Biomass combustion is the oxidation of organic material in the presence of air. The combustion is related to the original solid biomass, the secondary liquid and gaseous energy carriers or to the various residues and wastes produced via other conversion paths. The carbon and hydrogen contained in the fuels is converted to CO_2 and H_2O. During this process, the chemical energy stored in the organic matter is released as heat, thereby forming high-temperature flue gases. This heat can be further used (traditionally for cooking or heating purposes) or it can be transformed into mechanical and further into electrical energy.

Under ideal conditions, all organic material contained in the biomass is combusted when mixed with the appropriate amount of O_2. In a real system, the combustion of biomass is related to several technical challenges, mainly resulting from the fuel characteristics previously described in Subchapter 1.1.2.

Pyrolysis

During pyrolysis, the biomass is heated in an inert atmosphere in the absence of an oxidizing agent. Pyrolysis can either be seen as an independent process leading to the generation of a desired fuel product or as an initial step of every gasification or combustion process [28].

The product of pyrolysis as an independent conversion process is the pyrolysis oil, a non-condensable gas mixture and a solid residue char. The pyrolysis oil is generated during condensation of the gaseous product. The proportions between the products and their composition are highly dependent on the pyrolysis process parameters such as temperature, heating rate and the residence time. The lower the temperature and the slower the pyrolysis, the more charcoal and less pyrolysis oil are produced. When increasing the heating rates and the temperatures, a more intensive decomposition of the biomass material is expected, shifting the process towards condensable liquid products [29]. Depending on the process parameters, one can distinguish between flash, fast and intermediate pyrolysis for bio-oil production and slow pyrolysis for the production of charcoal. The slow pyrolysis includes such processes such as carbonization and torrefaction [30].

Gasification

Gasification is a process of solid or liquid fuel conversion in a gas phase using a gaseous agent, whereby the fuel undergoes only a partial oxidation. The gaseous product is commonly called synthesis gas or syngas. Air, water vapor or pure oxygen can be used as an oxidant agent.

The untreated syngas consists of carbon monoxide (CO), H_2, CH_4 and CO_2, light and heavy hydrocarbons such as tars, and water vapor as well as N. The water vapor and N content is mainly influenced by the oxidation agent used for gasification [31].

Depending on the chemical composition of the biomass treated, undesirable gases and vapors are also included in the syngas. Hydro sulphuric (H_2S) and HCl, vapors of inorganic salts, and N-containing organic compounds are some of the most important examples.

Beside the product gas, a solid residue called char, consisting of unconverted organic and inorganic matter, is generated. The organic fraction of the char is mainly carbon.

In a similar way to the case in pyrolysis, the process conditions can determine the distribution of the products: gasification with air produces a low calorific value gas due to the dilution of N_2, while gasification with oxygen or steam produces a syngas with a medium or high calorific value. The promotion of the reforming or water-gas-shift reactions increases the amount of hydrogen in the gas at the expense of CH_4 and CO.

There are various possibilities for syngas usage. The gas can be applied directly for heat and power production via combustion in boilers, engines, or turbines [32, 33], can be further converted to liquid fuels [34] and applied in e.g., the automotive sector or can be used for the synthesis of other chemicals [35]. Moreover, H_2 generation from biomass syngas and its application for the automotive industry or in fuel cells is also under investigation [36]. All the approaches mentioned lead to a more valuable application of biofuel, which would not be possible for the original biomass.

An example for the combination of pyrolysis and gasification processes is the Bioliq® process, developed at the Karlsruhe Institute of Technology (KIT), which aims to produce synthetic fuels and chemicals from solid waste biomass [37]. In this concept the biomass is converted into bio-crude oil which in further step undergoes gasification. The resulting synthesis gases are processed and cleaned. In the final step via appropriate synthesis a liquid gasoline is created

1.2 Nitrogen chemistry during the thermal conversion of biomass

1.2.1 The origin of nitrogen oxides in combustion processes

The nitrogen oxides formed in combustion plants, commonly referred to as NO_x, mostly consist of NO and, in small amounts, of NO_2. However, at a higher oxygen partial pressure in the atmosphere, an almost complete conversion of NO to NO_2 takes place [38]. Due to this high probability of reaction, limiting concentrations for the group of mono-nitrogen oxides (NO_x) are always given as NO_2.

The nitrogen that forms the NO_x during combustion processes can basically be from two origins i.e., the N introduced with the combustion air and the N contained in the fuel itself.

Within the first group of nitrogen oxides, one can distinguish between the thermal and prompt NO_x formation mechanism.

The *thermal-NOx mechanism* was first described by the Russian scientist, Zeldovich [39]. The NO_x is formed by combining the N contained in the air with the elemental oxygen, or oxygen radical O.

$$N_2 + O \Leftrightarrow NO + N \quad \text{(R 1)}$$

$$N + O_2 \Leftrightarrow NO + O \quad \text{(R 2)}$$

This mechanism was further supplemented with a third reaction, accounting for the influence of OH radicals that can form during combustion [40].

$$N + OH \Leftrightarrow NO + H \quad \text{(R 3)}$$

All three Reactions R1-R3 constitute the extended Zeldovich mechanism. The reactions are highly temperature-dependent, so the higher the combustion temperature, the more NO_x is formed. The dependence of the temperature on the thermal-NO_x formation rate is exponential. A simplified representation of the temperature dependencies on the resulting NOx concentration is shown in Figure 6. Therefore, the reduction of the flame temperature is the most important strategy when decreasing the pollutant emissions. The NO_x formation rate is also pressure and residence time dependent and increases of these two parameters always lead to higher NO_x emissions.

The *prompt-NO mechanism* was introduced by Fenimore [41]. This rapidly formed NO is created mostly under fuel-rich conditions in the regions near the flame zone. Typical levels of prompt-NO in hydrocarbon flames range from a few ppmv to more than 100 ppmv [42]. The contribution to total NO_x formed slightly increases with increasing temperature.

It is primarily formed by a reaction sequence that is initiated by the rapid reaction of hydrocarbon radicals with molecular nitrogen, leading to the formation of amines, or cyan compounds that subsequently react to form NO [42]. The mechanism is usually described by the following reactions:

$$CH + N_2 \Leftrightarrow HCN + N \quad \text{(R 4)}$$

$$CH_2 + N_2 \Leftrightarrow HCN + NH \quad \text{(R 5)}$$

$$CH_2 + N_2 \Leftrightarrow H_2CN + N \quad \text{(R 6)}$$

$$C + N_2 \Leftrightarrow CN + N \quad \text{(R 7)}$$

Significant changes to this mechanisms were introduced in 2018 [43]. However, all calculation performed presented in this work are still based on the older description of prompt-NO mechanism.

Both thermal and prompt-NO mechanisms play a small – or even negligible – role when combusting biomass, and their contribution to the overall NO_x emission further decreases with increasing N content in the fuel [44]. In this context, the fact that older prompt mechanism has been used does not meaningfully affect the results of the study.

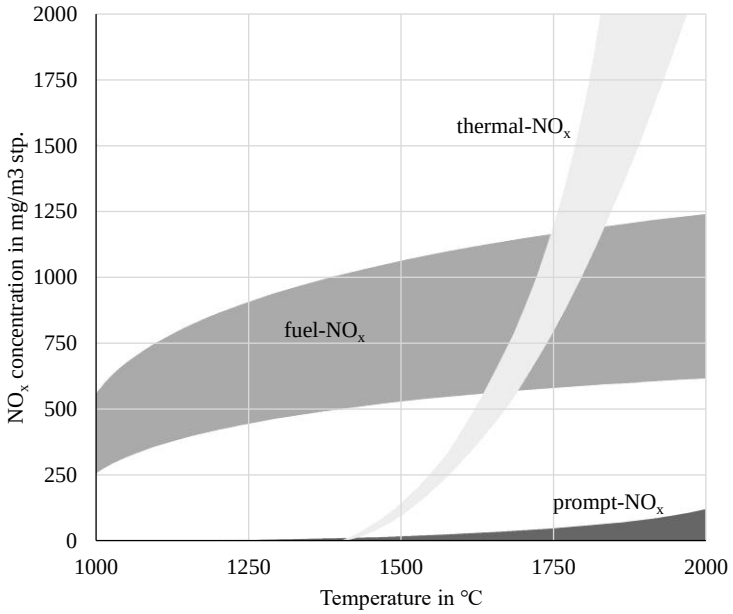

Figure 6 Temperature dependency of NO_x formation mechanisms in combustion processes – simplified presentation based on [45]

Combustion of solid biomass or wastes is usually carried out in smaller fixed bed boilers, grates or in fluidized bed combustors, where the combustion processes take place at a comparatively

low temperature. In such systems, the third mechanism – the *fuel-NO_x mechanism* mainly determines the final NO_x emissions [46]. Furthermore, in the case of LCVG that contain volatile N, where the flame temperatures usually do not exceed 1100–1300 °C, the fuel-NO_x formation mechanism determines the overall NO_x emissions.

1.2.2 Evolution of fuel-N during thermal conversion of solid biogenous fuels

The N chemistry in the solid fossil fuels such as coal, lignite, and peat has been an object of extensive studies for many decades. As the importance of biomass utilization for heat and energy production has increased over the last 30 years, biomass fuels also came into focus in research communities. Many studies on N in the solid biomass fuels, its release, partitioning, and finally, oxidation and reduction processes have been conducted over the last years.

The overview of the common knowledge on this topic is given in this chapter. This knowledge will further be necessary to understand the methodology applied, and the results achieved within the studies on the flameless combustion of N-containing gases presented in the publications within this doctoral thesis.

The N contained in solid fuels is usually the main factor determining NO_x emissions. As mentioned in Subsection 1.1.2, the N content in biomass fuels can vary widely. The lowest values are measured in a high-quality woody biomass. Many other biomass fuels, and mostly biomass residues, can contain up to a few percent, and the biomass of animal origin even more than $N_{daf} = 10$ %. The potential for NO_x formation during combustion of such fuels can therefore be very high. However, how much of the potential N will finally be emitted as NO_x depends not only on the fuel itself but also on various conditions (i.e., temperature, heating rates, pressure, oxidizer ratio and residence time) that the fuel is exposed to during the thermal conversion process [44]. Within such a process, the original fuel undergoes different conversion stages from the solid matter until it reaches a complete oxidation.

According to the common scientific concept, the first thermal decomposition step that follows the process of fuel drying is pyrolysis. Under primary pyrolysis, the early structure bond breaking leading to the evolution of volatiles and char is understood [47]. The volatiles consist of light gaseous species and tars [44]. The primary pyrolysis products continue to react further during secondary pyrolysis, where the reaction can either take place in the gaseous phase or heterogeneously. The pyrolysis can be treated as an autonomous technological step in a process of fuel upgrading or can be understood as the first step in the combustion of a solid fuel particle. Further, depending on the conditions and amount of oxidizer, the gaseous intermediate compounds and the solid char can be oxidized until complete combustion is achieved. Such a model approach of the fuel decomposition process can also be reflected on the evaluation of N compounds as shown in a simplified fashion in Figure 7.

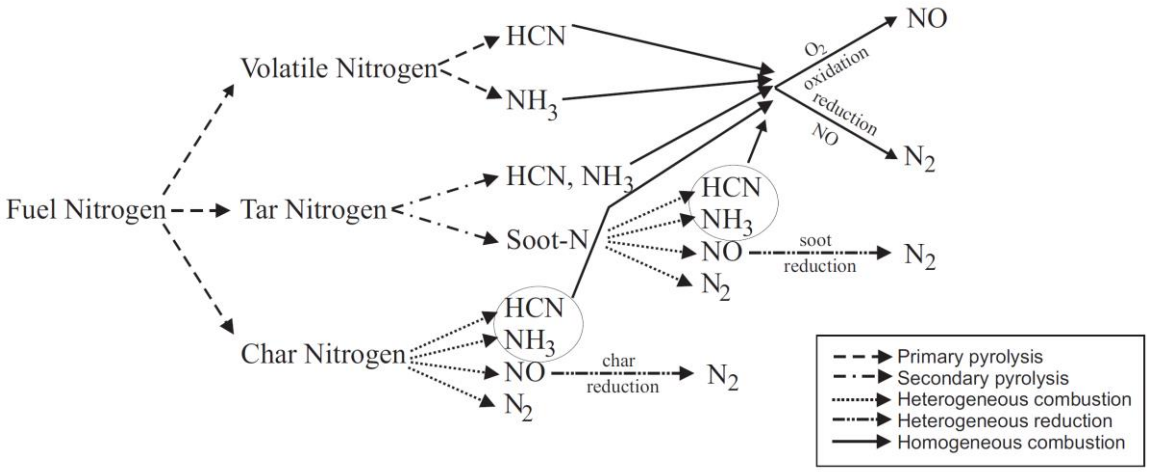

Figure 7 Evolution of fuel N during thermal conversion of solid fuels [48]

After the drying phase, the devolatilization distributes the initially bonded N among the volatile compounds, N contained in tars and N remaining in the solid char [48, 49]. The majority of the N in the biomass conversion is released with the volatiles [46, 50, 51]. The distribution of the nitrogen between the volatiles and the remaining char is roughly proportional to the volatile matter in the fuel [52].

The main gaseous compounds have been identified as NH_3 and HCN [46–51, 53–55]. HNCO, as a minor intermediate compound, has also been reported during the biomass pyrolysis in several studies [53, 56], and in higher amounts when animal biomass, such as chicken manure, was investigated [49]. Within the first step of thermal decomposition, there is also a significant amount of tar-N (N contained in large aromatic compounds) that further decomposes during the secondary pyrolysis to gaseous compounds, mostly to HCN and, in smaller amounts, to NH_3 [20, 49].

The exact distribution between HCN and NH_3 after the pyrolysis process varies widely depending on the type of biomass used, the experimental conditions, and even the measurement methodology. Sometimes the main compound from the pyrolysis is reported to be NH_3 [54], and sometimes it is HCN [46, 57]. Some experimental results found in the literature are collected in Table 2 to better illustrate this. Generally, it has been observed that the amount of light gaseous nitrogen containing compounds such as NH_3 and HCN and N_2 released from the solid fuel matter increases with the temperature during pyrolysis and that this phenomenon can further be accelerated when increasing the amount of oxidizer and changing from pyrolysis to gasification or a combustion regime. A systematic analysis of the N evolution during biomass pyrolysis is presented in [63]. The authors investigated the pyrolysis of switchgrass under the fluidized bed conditions in the inert atmosphere. With increasing temperature, the N fraction released as N_2 also increased and more light volatile compounds such as NH_3 and HCN were present in the product gas. At the same time, the fraction of N bound in char and in tars decreased as shown in Figure 8.

Table 2 NH_3 and HCN distribution under slow and fast pyrolysis conditions

Biomass Type	Reactor Type	HR	Fuel-N	CR N - NH3	CR N - HCN	CR N - HNCO	Reference
		°C/min	%-wt_{daf}	%	%	%	
Slow pyrolysis							
Wheat Straw	*TG-FTIR*	30	0.68	19	17	6	[58]
Wood pellets	*TG-FTIR*	30	0.33	5	14	2	[59]
Miscanthus	*TG-FTIR*	30	0.64	13	11	6	[59]
Chicken Litter	*TG-FTIR*	30	5.35	16	11	11	[60]
DDGS	*TG-FTIR*	10	4.84	24	16	3	[61]
Brewer spent grains	*QTB* + FTIR*	10	4.15	16	4	n.d	[54]
Coffee waste	*QTB*+ FTIR*	10	3.02	7	1	n.d	[54]
Pine Bark	*Tube Oven*	10	0.4	10	1	n.d	[54]
Fast pyrolysis							
DDGS	*Heated foil reactor*	900	4.84	1.2	6.4	n.d	[49]
Chicken Litter	*Heated grid reactor*	1000	4.35	15.1	20.3	n.d	[62]
Coffee waste	*QTB* + FTIR*	900	3.02	37.8	14.1	n.d	[54]
Fiberboard	*QTB* + FTIR*	900	3.62	36	9.1	n.d	[54]
Sewage sludge	*QTB* + FTIR*	900	5.47	50.7	8.6	n.d	[54]
Switchgrass	*Fluidized bed*	850	0.51	15	12	n.d	[63]

*- *Quartz Tube Furnace*

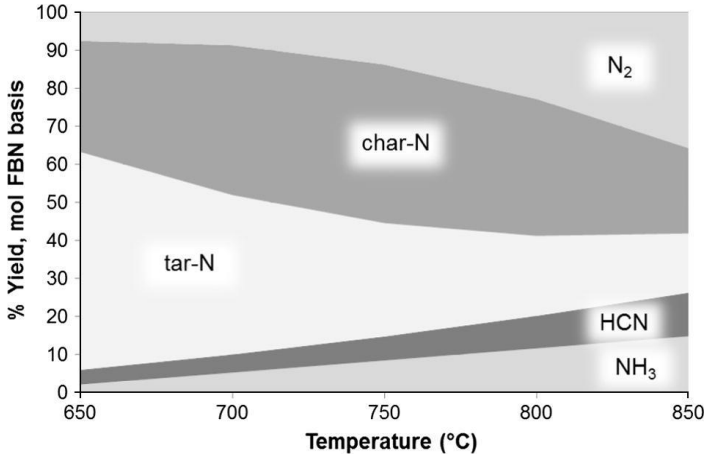

Figure 8 Yield of gaseous forms of nitrogen (N_2, HCN, and NH_3), char-N and tar-N. All results presented in the Figure 8 are related to the amount of nitrogen bond in the fuel (FBN). Reprinted from Publication [63]. Copyright (2021), with permission from Elsevier

In further steps, the decomposition of generated tars will proceed, releasing a part of N contained to the gaseous phase or, depending on the conditions, tars can be converted to soot particles with trapped N.

1.2.3 Fuel NO_x – homogeneous and heterogeneous NO_x formation

When the solid and gaseous products of the pyrolysis are exposed to any kind of oxidant under elevated temperatures, the process of decomposition and oxidation will proceed, and the fuel will undergo the gasification or, if enough oxidizer is available, the combustion process.
The remaining fraction of tars will completely decompose and release all the N as gaseous intermediate species. The N released to the gaseous phase will follow a series of diverse reactions leading to the formation of NO_x or reduction to molecular N_2. The selectivity of these reactions toward NO_x or N_2 is strongly dependent on the local reaction conditions and the availability of other compounds or radicals influencing the oxidation and reduction processes. The radical pool available for the conversion of N-species is strongly determined by combustion processes. The oxidation processes of light gaseous N-species are well described in the literature. A detailed description of such processes is complex and includes hundreds of elemental chemical reactions.

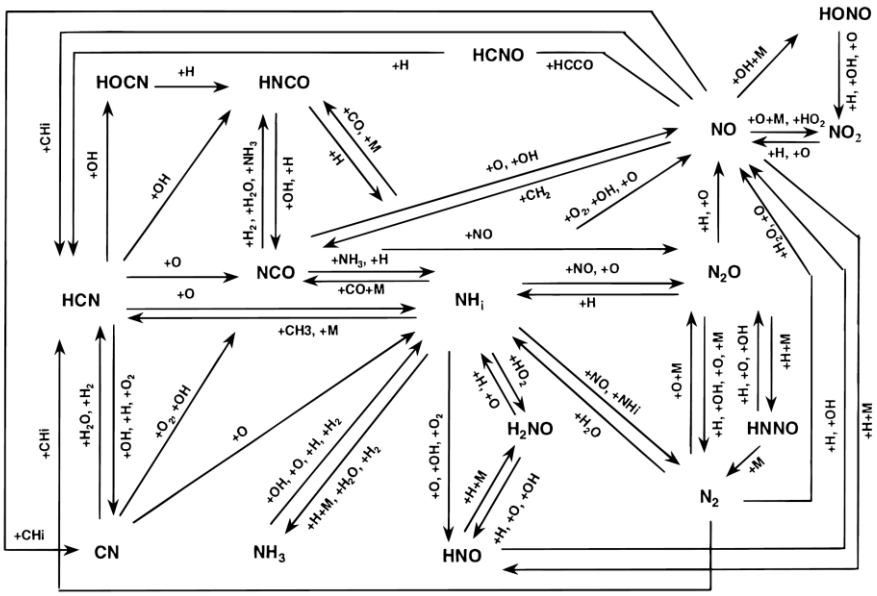

Figure 9 Simplified presentation of the kinetic scheme of the major gas-phase reactions for NOx formation and destruction in combustion. Reproduced with permission from [64]. Copyright (2021) American Chemical Society

Miller and Bowman reviewed the N oxidation chemistry and published a detailed reaction scheme in [42]. Over the years, this mechanism was further developed and was refined to various specific conditions [64]. However, the main structure and reactions did not change

significantly. Most of the relevant reactions for gas phase N-species leading to the formation of NO_x or to the reduction to molecular N are shown in Figure 9.

During the N-species oxidation, NH_i radicals are formed from the thermal decomposition of volatile NH_3 or, via a series of elemental reactions, also from HCN. These NH_i radicals can either be oxidized to NO in oxygen-rich conditions or can reduce the already existing NO to N_2. The major steps for the NO and N_2 formation via NH_i radicals formed from NH_3 and HCN are illustrated in Figure 10.
The NO reduction reactions using NH_i radicals are the basis of the SNCR (Selective Non-Catalytic Reduction) and SCR (Selective Catalytic Reduction) technology of NO_x removal from flue gases. The remaining nitrogen in the solid char in the presence of oxidizer undergoes heterogeneous reactions forming NO and some minor amounts of HCN and HNCO [44, 65, 66]. It has been shown in many studies that a big part of the NO released can directly be reduced to N_2. The NO reduction over – and in – the biomass char particles was studied in [66–68].

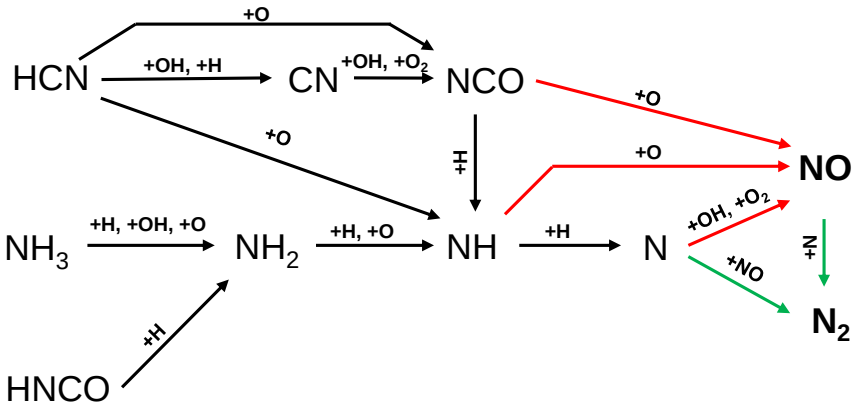

Figure 10 Major steps for NO and N_2 formation from NH_3, HCN and intermediate HCNO. Reactions selected from [64] based on the results presented in Section 2.5

It has also been proved that the biomass char can reduce the NO formed over its surface, and that the effect is catalyzed by inorganic elements included in the fuel [68]. In contrast to the nitrogen released with the volatiles, the char-N conversion into NO_x is more difficult to overcome [69]. It has also been shown that the char-N to NO_x conversion is highly dependent on the fuel particle size. The smaller the particle, the higher is the conversion to NO under fuel lean conditions [66].

1.2.4 Established NO_x reduction technologies

The extensive research on NO_x formation mechanisms led to the development of many strategies to limit the environmental impact of the combustion processes. The developed methods can be divided into the primary and secondary measures. Primary measures focus on the combustion process itself and prevent the formation of NO_x. The goal of secondary

measures is the denitrification of the combustion products gases and the removal of the already formed NO_x.
The primary measures are usually preferable, as they are generally much easier to implement, require less technological effort and are cheaper in terms of their operation. In bigger power station units, the secondary measures are usually used when primary measures have been applied and the firing systems are optimized for low-NO_x conditions.

The following strategies are well established in combustion technology:

Optimization of the excess air amount – for the solid fuel firing systems where the fuel-N is the main source of the nitrogen oxides emissions, the decrease in excess air is an effective and cheap method to reduce final NO_x. Due to a lower amount of flue gas being generated, the excess air reduction has also a positive effect on the steam or hot water generator. However, at the low excess oxygen levels there is always a trade-off between the minimum NO_x and the rapidly rising products of incomplete combustion (gaseous and solid) due to limitations in the mixing and kinetics at low oxygen levels. Therefore, modern combustion systems are optimized to ensure the best possible mixing and burn out at low excess air ratios. Moreover, all modern firing systems (besides the small ones) are equipped with O_2 or CO/O_2 control systems that ensure the correct amount of air is introduced into the combustion chamber.

Air staged combustion – when decreasing the air in the primary combustion zone further as described above, the NO_x will be further decreased, although the combustion will not be complete. A fuel rich zone is created that promotes the reduction of the already created NO and realized NH_i and HCN compounds to N_2. The fuel rich conditions are kept for a sufficiently long time to ensure high reaction progress towards N_2. The missing air to complete the combustion is introduced later in the process, ensuring sufficient burn-out of the fuel. Once the fuel nitrogen is trapped in the stable N_2 compounds, it is not available during the burn-out process to form any NO_x, as the temperatures in the zone are too low. Air staging technology is commonly used in the combustion systems and is applied in boilers with firing systems of various types in a wide range of the rated thermal input power.
In modern applications, the division of the combustion process into primary and secondary combustion zones became a common praxis. The air staging can be realized via divided air distribution into one combustion chamber or via separation into two independent gasification and combustion chambers, such as was investigated in [9].
The application results not only in significantly lower NO_x [70–76] but can also lead to smaller particle emissions [71, 77]. The reduction in fine particle emissions can be attributed to both a decrease in alkali metal emissions and to emissions of unburned carbonaceous particles. The reported NO_x reduction was in the range 30 % up to 90 % depending on the fuels, experimental conditions and equipment used.

Reburning (also known as fuel staging) – in this strategy, two combustion zones are created. In the first combustion zone, fuel is burned with the air under over-stoichiometric conditions, also forming NO_x. Downstream of this zone, additional fuel is injected, forming a second combustion zone with under-stoichiometric conditions. Under reducing conditions and under the presence of CH_i radicals, the NO formed is converted back to intermediates such as HCN [78]. From this point on, the reduction can proceed as shown in Figure 10. In the past, natural gas was used as a reburning agent due to favorable ignition and mixing behavior. Furthermore, reduction using biomass fuels was investigated and discussed in the literature [79–81]. The results confirmed that biofuels are an efficient reburning agent that is cheaper than natural gas. However, challenges regarding the introduction of problematic inorganic compounds such as alkali or chlorides are expected.

Flue gas recirculation – the goal of flue gas recirculation is the flame dilution, thus reducing the temperature peaks and the O_2 partial pressure. The efficiency of this method is high if thermal-NO_x should be reduced. The flue gas recirculation can be realized by external recirculation of the flue gases from the flue gas ducts or internally via burner flow pattern. Flue gas recirculation may negatively influence the flame stability and the burn out of the fuels. Moreover, when the flue gases contain sulphur or chloride, and are externally recirculated at colder temperatures, corrosion issues might also appear [82].
The extreme version of the internal flue gas recirculation application is the flameless combustion. This technology will be described in detail in Subchapter 1.3. Flue gas recirculation is also broadly used as NO_x reduction technology in modern diesel engines.

Flame cooling via water and steam spraying – this is sometimes used for thermal-NOx reduction in natural gas burners as a relatively cheap retrofit strategy to fulfil emission limits. Due to spraying the water directly in the combustion zone, temperature peaks are avoided. The direct injection of the cooling agent into the flame may also have a negative impact on the flame stability. However, when correctly applied, the injection might be an efficient strategy to reduce NO_x in boilers, process heaters, and gas turbines [83–85].

If the primary measures do not ensure the desired reduction, secondary measures must be applied. These are focused on the active reduction of the NO_x in the flue gases. There are two established technologies that are based on the SNCR and SCR reaction mechanisms, involving reduction of the NO to N_2 using liquid NH_3 or urea ($CO(NH_2)_2$) injection.

The ***SNCR technology*** involves an injection of a liquid solution of NH_3 or $CO(NH_2)_2$ in the hot post-combustion zone. As the solvent evaporates, it starts to release NH_i radicals, which can react with the already formed NO. The reactions can be described by the following global equations:

$$2NO + 2NH_3 + \frac{1}{2}O_2 \Leftrightarrow 2N_2 + 3H_2O \quad \text{(R 8)}$$

$$2NO_2 + 4NH_3 + O_2 \Leftrightarrow 3N_2 + 6H_2O \quad \text{(R 9)}$$

The $CO(NH_2)_2$ reaction equations for NO and NO_2 are:

$$2NO + CO(NH_2)_2 + \frac{1}{2}O_2 \Leftrightarrow 2N_2 + CO_2 + 2H_2O \quad \text{(R 10)}$$

$$2NO_2 + 2CO(NH_2)_2 + O_2 \Leftrightarrow 3N_2 + 2CO_2 + 4H_2O \quad \text{(R 11)}$$

The efficiency of this process is highly dependent on temperatures. The SNCR works in a rather narrow temperature window between approximately 850 °C and 1050 °C, as shown in **Fehler! Verweisquelle konnte nicht gefunden werden.**. The values found in the literature show that the SNCR temperature window is slightly higher for urea than for ammonia [86]. The optimum temperature window is limited by lower temperatures by rapidly decreasing removal efficiency and increasing non-reacted NH_3 concentration in the flue gas (NH_3 slip). At higher temperatures, the injected NH_3 starts to generate additional NO following oxidation reactions, as shown in Figure 11

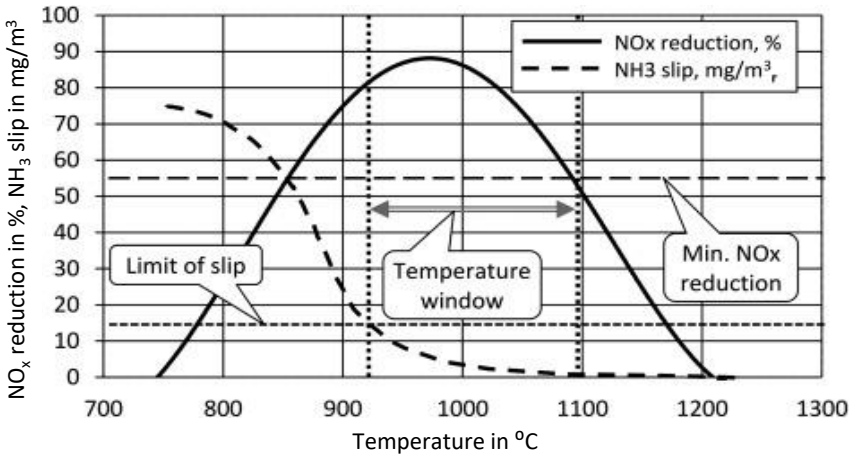

Figure 11 The SNCR system efficiency and the ammonia slip as a function of the flue gas temperature. Reprinted from [86], Copyright (2021), with permission from Elsevier

The SNCR is widely used in mid-sized combustion plants such as smaller utility boilers, industrial boilers, or waste incinerators. The main challenges for the application in the biggest utility boilers is usually related to the limited ability to penetrate the whole cross-section of the combustion chamber within the given temperature window.

In the plants combusting sulphur or chloride containing fuels, the unreacted NH_3 may react to ammonium sulphate, bisulfate, or ammonium chloride. The amount formed depends on the sulphur content of the fuel and the amount of NH_3 slip. Ammonia-sulphur salts can plug, foul, and corrode downstream equipment such as the air preheater, ducts, and fans.
If ammonium sulphates are present in the ash, the gaseous NH_3 can be released when mixing the ashes with alkali materials. This can also cause problems with the solid ash disposal.
To decrease the NH_3 slip, a layer of additional catalyst can be applied. Nevertheless, SNCR technology is much cheaper compared to SCR systems.

The SCR (Selective Catalytic Reduction) Technology – principally follows the same reaction paths as SNCR, however in SCR these reactions take place over a catalyst surface and, therefore, the SCR technology requires much lower temperature ranges. The optimum temperature is usually in the range between 300 and 400 °C [87]. SCR is the most efficient NO_x reduction technology and efficiencies of 80–90 % are commonly reported in the literature [88]. However, it is also the most expensive technology and is used in fossil fuel power plants, and by CHPs based on piston engines as well as in the automotive industry. Due to the high costs and technological effort, it is not used in smaller biomass power plants. Moreover, biomass derived fuels with high alkali content might have a negative impact on the catalyst's activity.

1.3 Fundamentals and state-of-the art of flameless combustion

The core of this work is the experimental and modelling combustion studies of low calorific value gases of biogenous origin using the so-called FLOX® technology, with a special focus on the flow design and fuel N chemistry. The biomass fuels and the fuel N evolution have been described in previous chapters. The third missing element is thus the combustion technology itself. The overview on the principles, and on the recent developments, is given in the following chapter.

1.3.1 Fundamentals of flameless combustion

The origin of flameless combustion technologies goes back to the 1970s. Weinberg [89, 90] studied the technical possibilities for combustion of LCVG. His idea was to stabilize the combustion process by means of additional heat transferred to the reactants, which was taken from the combustion products without mixing the streams. Due to the heat recirculation back to the combustion zone, the technology has been named "excess enthalpy combustion." The proposed developments were dedicated to the burning of poor-quality fuels and addressed the ignitability limits of mixtures that could not be utilized in conventional systems.
Heat regeneration and preheating reactants are also effective tools to increase the process efficiency and save fuel. The savings are both related to decreasing the losses in the flue gas enthalpy by lowering its temperature, and to decreasing the amount of the flue gas itself (due to less fuel being used). This saving is proportional to the preheat temperature. A simplified representation of heat recirculation in combustion systems in presented in Figure 12.

However, when increasing the preheat-temperature in conventional systems, the flame temperature automatically increases. This phenomenon has a strong negative impact on the NO_x emissions (also see Chapter 1.2.1). The disadvantage has been overcome in flameless combustion technology. This has been achieved by using a significant amount of flue gases to dilute the fuel and air prior to ignition, whereby the created combustion mixture has been brought over the temperature of self-ignition using either internal or external recirculation of the heat. Such combustion is characterized by uniform temperature distribution without the typical peaks observed in conventional flames. The highest temperatures observed in the combustor are much closer to the average combustion temperature.

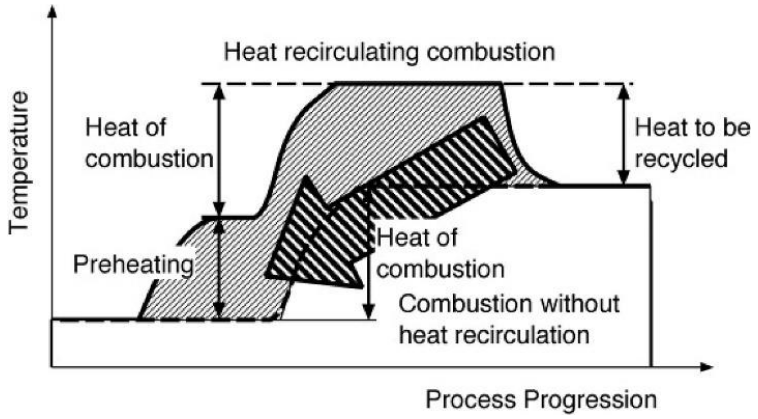

Figure 12 Simplified representation of heat recirculation in combustion systems. Reprinted from Publication [91] Copyright (2021), with permission from Elsevier. Originally based on [90]

In the literature, there are a few variants of this technology. The term "Flameless Oxidation" or its abbreviation "FLOX®" was introduced by Wünning and Wünning [92]. Other commonly used terms for this combustion mode are "Mild Combustion" [93] or "High-Temperature Air Combustion" [91, 94], where these three terms describe slightly varying combustion forms that are based on very similar principles. All the technological variations mentioned were originally developed to combust natural gas, and all three technologies can provide the highest combustion efficiencies with very low NO_x emissions.

The studies presented within this doctoral thesis are focused on the FLOX® technology and its application for the utilization of low calorific value gases. Wünning and Wünning define FLOX® as a stable combustion without a flame and with defined recirculation of hot combustion products [95]. This can be achieved with or without reactant pre-heating. Moreover, the process can be realized for lean, near stoichiometric or fuel rich combustion [95].

One of the main factors governing this process is the recirculation ratio, which is defined as follows [92]:

$$K = \frac{\dot{m}_{rec}}{\dot{m}_{fuel} + \dot{m}_{air}} \qquad \text{(Eq 1)}$$

where:
$\dot{m}_{rec}$ – mass flow of internally recirculated flue gas
$\dot{m}_{fuel}$ – mass flow of the fuel
$\dot{m}_{air}$ – mass flow of the air

The amount of recirculated hot flue gases has a significant influence on the combustion behavior. When utilizing natural gas, a stable flame could be maintained up to approximately K < 0.3 (area A – see Figure 13) for the whole range of the furnace temperature. A slight increase in the stability was observed at higher temperatures, thus, a slightly higher K was possible. The higher temperature increased the ignitability limits of the combustion mixture and equalized the effect of lower partial oxygen pressure at the flame front. Above the value K > 0.3, the combustion suffered and became unstable (area B). Due to the lower oxygen partial pressure, the flame speed decreased, causing lift off and finally blow out.
However, when further increasing the recirculation ratio to values K > 3, the hot flue gases bring the combustion mixture to above the self-ignition temperature (area C). From that point on, the combustion process is self-sustaining, and the ignition process is not dependent on the energy released in the conventional flame front. As a result, the flame front disappears, and the ignition process takes place volumetrically in the combustion chamber. If the combustion process reaches such conditions, one can describe it as being a flameless combustion.

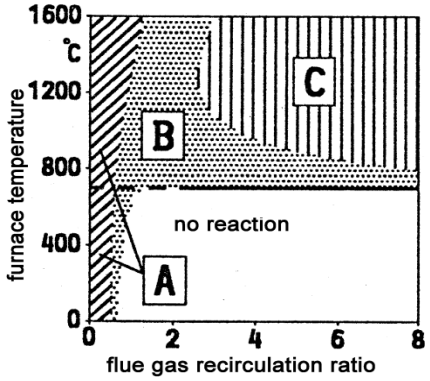

Figure 13 Flame stability limits as function of flue gas recirculation ratio (A - stable flame area A, B - unstable flame area and C - stable flameless oxidation area). Reprinted from [92] Copyright (2021), with permission from Elsevier

The suppression of flame formation under intensive mixing and dilution and the type of heat supply for the ignition process are the key characteristic factors. There are various strategies, which sometimes coexist, that are described in the literature to reach such conditions. The flame building suppression can be achieved by dilution of the combustion mixture, thus decreasing

the partial pressure of oxygen before ignition [95]. This effect can also be enhanced by spatial separation of the fuel and oxidizer flow, allowing them to first mix with the flue gases before mixing with each other [91, 96]. Another co-existing strategy is the elevated velocity of the reactants' injection, which is higher than the potential speed of the flame front. To maintain the combustion under suppressed flame building conditions, the heat necessary for the ignition must be supplied to the mixture. There are at least two strategies that can be used independently or in parallel. For example, in the HiTAC technology, the heat is recovered from the furnace flue gases to the air [94]. The temperature of air is high enough to bring the combustion mixture above the self-ignition point.

Another approach is the heat regeneration by hot flue gas recirculation and its mixing with the reactants before ignition. Independent of the heat recovery method used, namely regenerative or recuperative, in sum the recovery must be sufficient to bring the mixture above the self-ignition point for the given fuel and O_2 concentration.

Over the last three decades, natural gas fired flameless burners became state-of-the-art in various applications, saving fuels and radically reducing NO_x emissions. The success of this technology in industrial heating also pushed the development towards other fuels to enlarge the field of possible applications beyond the natural gas fired industrial furnaces.

The development of the flameless technology for solid fuels was mainly focused on the combustion of pulverized lignite and black coals. One of the first tests was performed at the International Flame Research Foundation (IFRF). During these tests, a coal burner with two coal jets and a centrally allocated air nozzle was applied. The experiments were conducted by firing high-volatile bituminous coal at a thermal load of 580 kW_{th}. The highly preheated combustion air was simulated with an O_2-enriched flue gas from the combustor. In these tests, the measured NO_x emissions in the exhaust gas were lower than expected from a modern conventional low-NO_x burner [91, 97].

Ristic [96] continued the development of the pulverized coal flameless burner. The tests using flameless small-scale burners (up to 300 kW_{th}), where a coal nozzle was arranged centrally and the air was injected via two separate nozzles, showed that the final NO_x emission can be reduced by 30 – 50 % in comparison to conventional flame burners. To achieve such reduction, the distance between the air and coal nozzles was maximized. The NO_x emission reduction was higher for coals with higher volatile content, as it is also observed for combustion in conventional burners. According to Ristic [96], the NO_x reduction potential is attributed mainly to the high oxygen dilution in the burner vicinity zone as well as to the reduction mechanism over the char particles that, in case of high recirculation, are well distributed within the combustion chamber.

The development of the flameless combustion for liquid fuels is also broadly reported in the literature.

In the experimental studies carried out by Weber et al. [91, 97], light and heavy oil was combusted under flameless conditions in the same IFRF furnace at similar conditions as those

used for pulverized coal. The authors reported that flameless conditions were easily achieved for light oil, whereas for heavy oil fuel, the visual existence of flame was observed. The combustion of heavy oil led also to excessive particulates and soot emissions. In the experiments, very low CO emissions were recorded. The NO_x for both fuels was also satisfactory, as low emissions were achieved without any specific NO_x reduction measures. However, during the tests, the combustion air already included a significant amount of NO_x, as the combustion air was simulated by oxygen enriched flue gases [97]. Therefore, the validity of the final NO_x assessment related to flameless combustion phenomena is limited.

Derudi and Rota [98] investigated liquid hydrocarbon fuels combustion under flameless conditions in laboratory-scale burners. The results showed that complete and stable combustion could be achieved, however the resulting NO_x was higher in comparison to CH_4 or LPG gaseous fuels. Azevedo et al. [99] tested bioethanol under flameless conditions with very low CO and NO_x emissions under laboratory conditions.

Further development towards the commercial application of a liquid flameless burner in a small-sized water cooled boiler was reported by Luhmann et al. [100]. In this study, the combustion of light fuel oil in a flameless oxidation mode was investigated. The focus was especially placed on low flue gas concentrations of NO_x and CO, thereby meeting European and German regulations, and on peak temperatures in the furnace. The result showed that the combustion system meets the strictest CO regulations (according to DIN EN 267 class 3 burners 60 mg/kWh$_{th}$) and the strictest NO_x regulations (according to 1. BImSchV, 110 mg/kWh$_{th}$).

1.3.2 Combustion of LCVG using flameless combustion

One of the major advantages of flameless combustion is its robustness, which is caused by high recirculation of the hot combustion gases that "borrow" the heat necessary for ignition via back-mixing of combustion products. In a flameless combustion mode, there is no flame to be supervised, and the combustion process is self-sustaining as long as the chamber temperature is maintained at a sufficiently high level. Internal heat recovery via recirculation overlapped with intensive mixing of fuel, oxidant, and flue gases results in an excellent burn-out as well as in suppressed thermal-NO_x formation.

Such properties predispose this technology for the utilization of LCVG, which are the primary focus of this thesis. The volumetric oxidation without a combustion initiating flame front resolves the biggest issue of LCVG burners, namely the flame stability.

The success of the R&D efforts of WS Wärmeprozesstechnik GmbH and the University of Stuttgart led to the foundation of the company e-flox GmbH. With more than fifteen years of experience, nowadays FLOX® is a very well established technology for the thermal oxidation of LCVG of various origins, such as biogas upgrading plants and landfill sites [101]. Such gases usually do not contain any meaningful quantities of organically bound nitrogen, so the NO_x emissions, similarly to natural gas flameless combustion, are low.

The biggest challenge when designing such burners is the geometry optimization that should promote the highest possible recirculation to obtain sufficient mixing and heating of the reactants, thereby ensuring a stable combustion process. Usually, the design is also supported by using appropriate CFD tools.

The testing of LCVG reported in the literature was usually performed in combustors originally designed for natural gas fired gas turbines. Lückerath et al. [102, 103] developed and demonstrated – for the first time – successful operation of the FLOX® combustor with low emissions at high pressure using natural gas. It was shown that the jet exit velocity of the fuel/air mixtures had a strong influence on the mixing process within the combustion chamber, and that the low emission operating range increased with this velocity. Addition of H_2 to the natural gas extended the range of stable operation. However, the NO_x emissions increased, probably due to inhomogeneities in the temperature distribution [102].

Based on a similar burner geometry, Rosendahl studied the potential application of the FLOX® combustor for low calorific value gases for micro gas turbines under atmospheric and middle pressure conditions [104]. In this application, the velocity of the jet was also crucial for the combustion conditions. Very low NOx (< 1 ppmv) was achieved at very low CO emissions. Other gases with high H_2 and CO contents were also successfully tested.

Furthermore, Danon et al. [105] successfully tested a flameless combustor originally designed for GT (gas turbine) application using LCVG. For the experiments, a catalytic AutoThermal Reforming (ATR) unit was used for the fuel gas production. In this unit, desulphurized Dutch natural gas (containing about 14 vol- % nitrogen) was reformed using steam and air, to a mixture of CH_4, CO, CO_2, N_2, and H_2 via catalytic partial oxidation and the water-gas shift reaction.

The composition of the product gas was similar to syngases produced during biomass gasification. The combustion air was preheated to 300 °C and injected into the prototype combustor with two different velocities. The cylindrical combustor was equipped with 12 fuel/air nozzles positioned in a circle in the front plate of the burner.

All CO and NO_x emissions measured were in a single digit range independent of the applied conditions. The NO_x rose slightly with the combustion temperature, while the CO emissions showed opposite trends. When increasing the calorific values, both CO and NO_x slightly increased.

Other authors tested various CH_4/CO_2 and H_2 mixtures as fuels that were representative of biogas or other synthetic fuels under flameless conditions [106–108]. All the tests resulted in very low NO_x emissions and a very good fuel burn-out.

However, all the above-mentioned studies did not treat fuel-N containing LCVG, so that the validity of the measured emission for fuel-NO_x formation is not given.

The focus of the work performed by Schuster in [9] was the development of a flameless burner for LCVG generated from the gasification of biomass residues. The results achieved in this work are the only qualitatively sound record in the literature of the experimental combustion of N-containing LCVG generated from the solid biomass under flameless conditions. This thesis

builds on these results, by supporting the burner development via CFD modelling, analysis of the results and continuing the study on the fate of N via experimental and modelling work. The experiments reported by Schuster et al. (see also Subchapters 2.1 and 2.2) were performed using a 116 kW solid biomass combustion system with integrated pre-gasifier as shown in Figure 14. The system was originally developed for wood pellets and wood chips only.

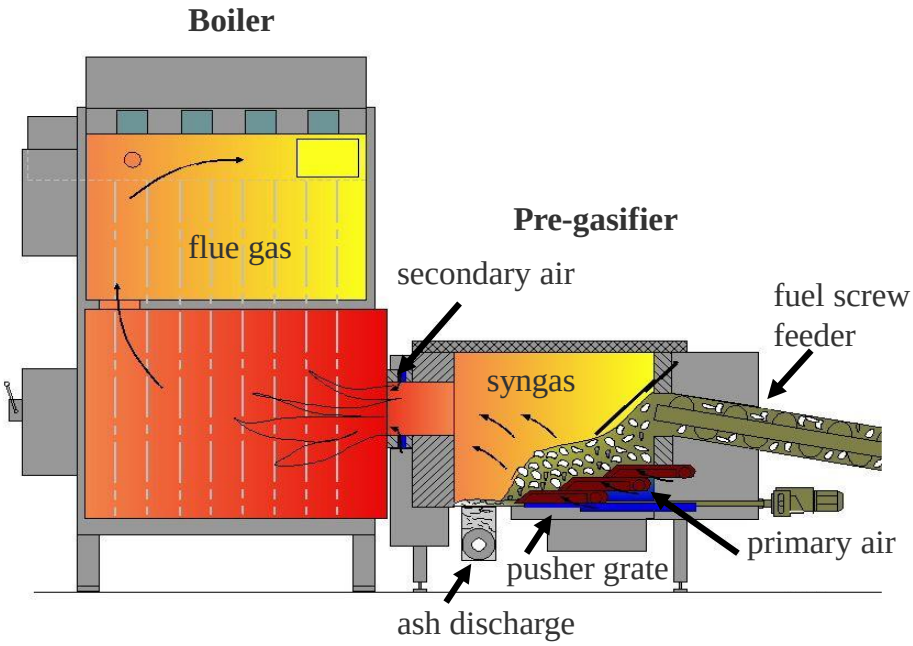

Figure 14 Solid biomass combustion system with integrated pre-gasifier [9]

The advantage of the original system is the spatial separation of the primary solid fuel gasification zone from the secondary burn-out chamber. The primary air is added under the pusher grate. The produced syngases leave the pre-gasifier, flowing through a narrow duct where secondary air is added. The created flame propagates within the first section of the burn-out chamber. The spatial separation of the solid fuel gasification and subsequent combustion should lead to better emissions of NO_x, CO and PM [71, 77, 109–113] in comparison to biomass combustion without air staging. Schuster designed and installed a new FLOX®-burner at the outlet of the pre-gasifier, replacing the secondary air injection [9]. After implementation of the new burner, the system could be operated at very low excess oxygen levels. This has been achieved even for fuels whose combustion in a system with a classic burner was not possible at all. While the NO_x levels could be decreased for wood chips, the emissions for fuels containing higher levels of fuel N were not satisfactory. The levels (e.g., for wheat husks) were even higher than in case of conventional combustion. Similar results can also be expected for the use of rapeseed cake pellets and wheat pellets, although no tests with these biomasses have been carried out on conventional pre-oven firing. Nevertheless, it can be assumed that by using the FLOX® burner, CO emissions can be reduced to a very low level. However, regarding NO_x emissions, no reduction can be expected for N-rich residues by integrating the FLOX® burner.

The operation of the furnace at much lower excess air levels is possible for all residues after the integration of a FLOX® burner. In summary, the combination of the spatially separated gasification and the subsequent combustion of the LCVG using flameless combustion successfully addressed many challenges when burning low-grade solid biomass fuels.

Table 3 Comparison of CO, NO_x emission and operation limits for tested bio-residues applying a conventional and a FLOX®-burner, based on papers presented in Subchapters 2.1 and 2.2.

Fuel	CO in mg/m³		NOx in mg/m³		Excess oxygen (lower limit) in vol-%	
	Flame	FLOX	Flame	FLOX	Flame	FLOX
wood chips	~ 200	< 30	~ 200	100 - 150	7	3
rape cake pellets	n.o.	< 30	n.o.	800 - 950	n.o.	3 - 4
wheat husks *	100 - 200	< 30	350	500 - 600	7	3 - 4
wheat pellets (2 % limestone)	n.t.	< 30	n.t.	600 - 800	n.t.	4

* slagging problems
n.o. operation not possible
n.t. not tested

Fuel flexibility, combustion stability and very low emissions of products of incomplete combustion are the most important advantages. However, the NO_x emission for biomasses with higher nitrogen content tends to be high.

1.4 Research objectives and outline of the work

This thesis builds on the experimental results achieved and reported by Schuster in [9], allowing further development and optimization of the flameless technology for the application of low-grade biofuels. The focus of the presented work is twofold. The first subject of the thesis is burner flow optimization using numerical tools such as CFD. One of the main aspects of the flameless combustion is the internal recirculation of the hot flue gases, which is crucial for the combustion stability and emissions. The recirculation is created by the momentum of the high velocity air injection. The main goal of the optimization is to achieve maximum recirculation for the given air jet momentum. Using 3-D numerical modelling, it is possible to quantify and compare the recirculation for various designs.

Nevertheless, the major objective of this thesis is related to the fuel-NO_x formation under flameless conditions. The experimental and numerical work presented addressed the main process parameters and mechanisms influencing the fuel-NO_x formation during combustion of biomass fuels, describe possible methodologies for the fuel-NO_x formation modelling and explain the main chemical mechanisms leading to the reduction and formation of NO_x under

flameless conditions. The results achieved in the papers presented are discussed alongside the most important results found in the literature.

The papers included in Chapters 2.1 and 2.2 address the subject of the proper tools and methods for flameless burners' geometry design and optimization. In these papers, it is shown that CFD analysis with a global chemistry model is a suitable tool for the proper geometry design to optimize the fluid flow in a flameless combustor. The methodology to calculate the desired recirculation is introduced to the software code for quantitative analysis of the flue gas flow pattern. However, the simplified chemistry models used in the CFD were not accurate enough to predict the proper gas composition patterns of the flameless combustion process.

The results obtained using the test rig showed that NO_x emission, which was expected to be low during flameless combustion, is in reality even higher than using a conventional burner system. Therefore, a new design of an air staged combustor using CFD analysis was proposed. Considering the limitations of the model applied, it was possible to analyze the flow patterns within the combustor, but the model was not accurate enough to analyze the chemistry of the combustion processes in detail and thus cannot correctly predict the NO_x and CO emissions.

To address the issue of elevated NO_x emissions during the flameless combustion of biogenous gases, further experimental tests were performed to investigate the influence of the gas composition and other combustion parameters on the emissions.

The experimental work and results described in the paper included in Chapter 2.3 build the basis for the understanding of the fuel gas composition on the NO_x emissions in flameless burners. The work was performed using synthetic mixed gases doped with NH_3. The gas composition chosen is similar to solid biofuel's gasification products. The results presented in this paper show that CH_4 concentration and the combustion stoichiometry have a major influence on fuel-NO_x creation (conversion rate of the NH_3 to NO_x) whereas the influence of the CO/H_2 ratio is very minor.

A further paper presented in Chapter 2.4 aligns the previously described experimental investigations with the results obtained using real product gas generated in a fluidized bed gasifier. The results show the dependencies between the gasifier operating parameters, product gas composition and final NO_x emissions. The concentrations of the NH_3 and hydrogen cyanide (HCN) in the product gas were measured to calculate the conversion ratios of these compounds to NO_x.

The last paper included in Chapter 2.5 analyzes the NO_x creation/reduction mechanisms in a flameless combustion to understand what kind of chemical processes occur in flameless combustors. With this work, a new approach of the NO_x modelling was proposed and validated using the data from previous papers. The proposed approach combines two methods of modelling – CFD with a simplified chemistry scheme for the proper modelling of the fluid flow (similar to what was presented in Chapters 2.1 and 2.2) and an idealized reactor network model with a detailed chemistry scheme for the modelling and deep analysis of the NO_x formation and reduction processes. In this paper, it is shown how to combine these two approaches to ensure

the necessary match between the experimental results and the results of the modelling. For the modelling, different types of detailed chemistry mechanisms were used, compared, and validated. The combustion processes were deeply analyzed and the best model was used for the explanation of the chemistry occurring in the flameless combustion. The chemical profiles of the flameless jets were visualized and discussed. The difference between the CH_4 containing combustion and the CH_4-free combustion process is shown and discussed. Based on the reaction rate analysis of the chemical reactors, the main fuel-NO_x creation/reduction mechanisms were identified, explained, and discussed.

1.5 Methods

In the framework of this doctoral thesis, various experimental and numerical modelling methods, and tools were used and combined to examine the different aspects of flameless combustion process. The experimental work was carried out using three different test rigs involving fixed bed and fluidized bed gasifiers, as well as two different types of flameless burners. The numerical part also includes two different numerical approaches. Although the applied methodologies are briefly explained in the presented papers themselves, this chapter provides a more comprehensive description of the experimental test rigs and modelling tools and methodologies.

1.5.1 Experimental setup

The first experimental rig presented in this thesis in Subchapter 2.3 is the combustion system combining the pre-gasifier with the subsequent flameless combustor. This combustion system and all measurement methods were described in detail by Schuster in [9].

The main experimental part presented in this thesis in Subchapters 2.3 and 2.4 was performed using a combustion chamber equipped with the recuperative 20 kW_{th} FLOX®-burner of REKUMAT® C-Za 150 Type produced by WS Wärmeprozesstechnik GmbH. This burner was originally developed for natural gas, however the robustness of the flameless combustion allows the application for LCVG gases as shown in Subchapters 2.3, 2.4 and in [101]. The REKUMAT® burner with the integrated ceramic recuperator is shown in Figure 15.

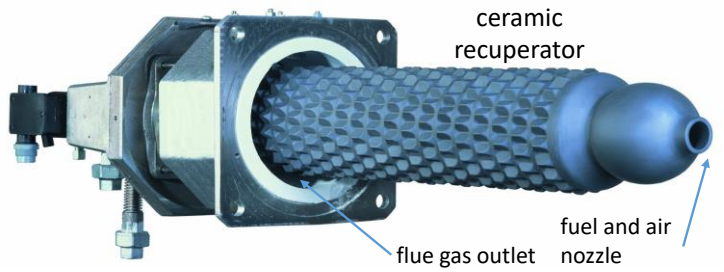

Figure 15 REKUMAT® C-Za 150 flameless burner. Source: www.e-flox.de

This burner is integrated in an insulated combustion chamber and coupled with various sources of different gaseous fuels, as shown in Figure 16.
The start-up fuel is natural gas. Using this fuel, the burner can operate in both flame and flameless mode. For this reason, the fuel is provided via two different inlets. The combustion chamber is heated to above 850 °C using a conventional stabilized flame. In the flame mode, the fuel is led via a standard fuel nozzle equipped with the flame stabilizer. Above 850 °C, the burner control system allows switching into flameless mode. In this mode, the fuel is internally led via an alternative centrally arranged fuel pipe without any stabilization. In the flameless mode, the combustion chamber can also be operated with other fuels, such as synthetically mixed LCVG or hot product gases generated in a fluidized bed gasifier.
The gas mixing station is a unit for the production of defined gas mixtures from different pure gases. To carry out the tests, the CH_4, CO_2, CO, H_2 and N_2 were combined in different mixing ratios to form an LCVG of desired composition. The flow of each gas was controlled via a mass flow controller and all the compounds were mixed in the common tank. Further, the mixture with the predetermined quantity and pressure was channeled to the flameless burner. Moreover, the fuel gas can be doped with NH_3. The flow of NH_3 is controlled by a high accuracy mass flow controller.

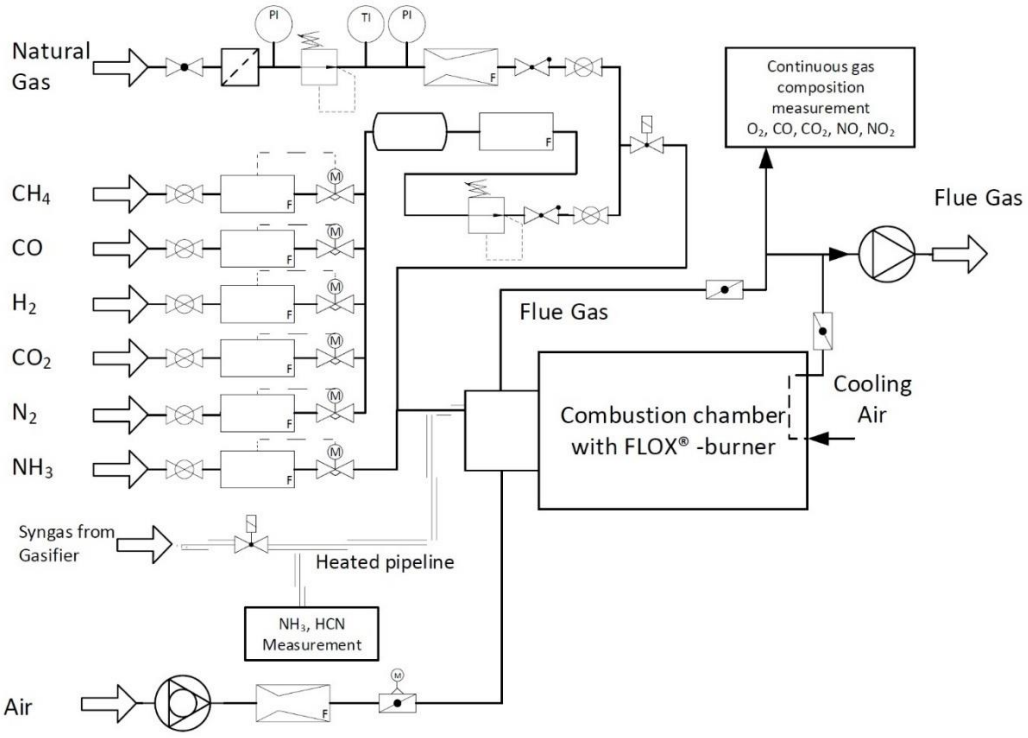

Figure 16 Simplified scheme of the combustion test rig

The additional coupling of the combustion test rig with a fluidized bed test rig gives the possibility to also test the flameless burner with real LCVG produced in a gasification process.

The electrically heated fluidized bed system shown in Figure 17 can be operated in both stationary (BFB-Bubbling Fluidized Bed) and circulating (CFB-Circulating Fluidized Bed) mode. The heating system allows the operation at temperatures up to a maximum of 1000 °C. The reactor has a height of 4.3 m and an internal diameter of 114 mm in the area of the fluidized bed. The diameter of the free board section is 135 mm. The dosing of the fuel is carried out by a dosing unit, which uses two dosing screws to transfer the fuel to the main conveyor screw, which introduces the fuels right above the nozzle bottom. As a fluidization medium, preheated air is passed into the reactor through the nozzles located at the reactor bottom. In a circulating operation mode, the solids separated in the first cyclone can be recirculated via a siphon into the reactor.

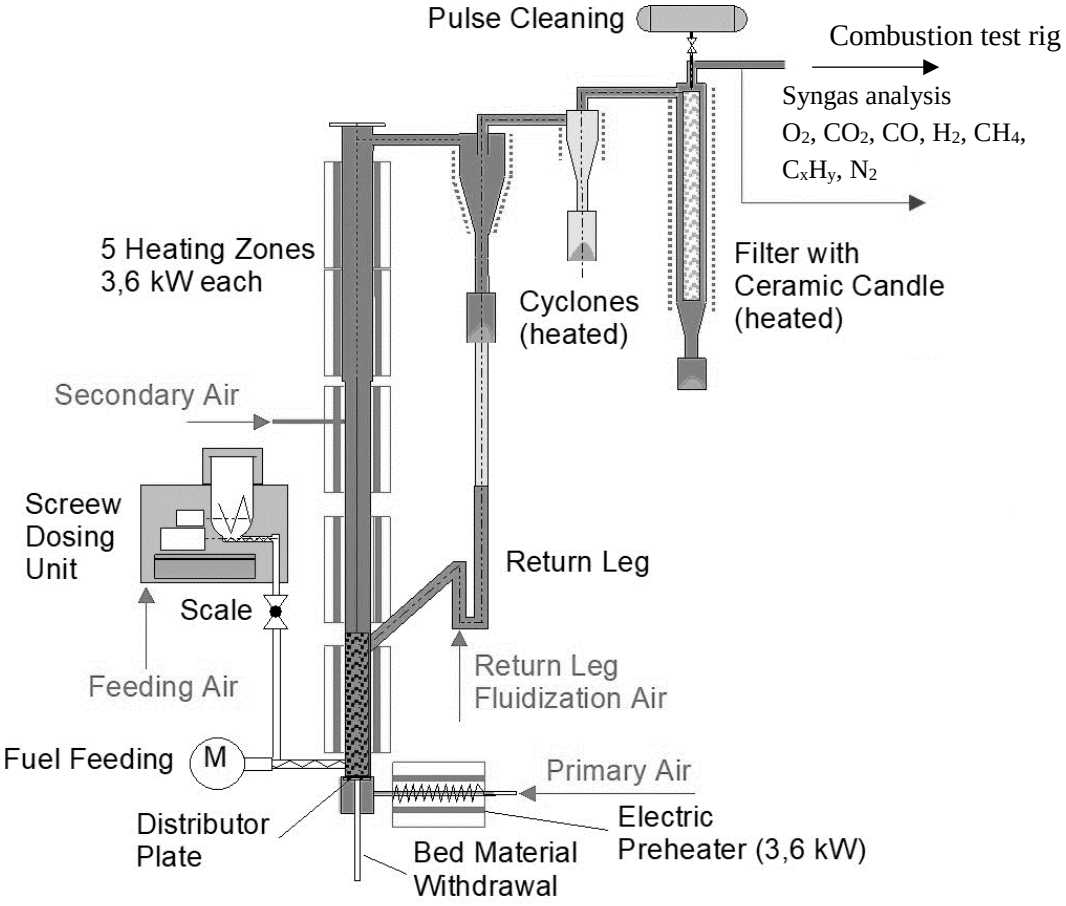

Figure 17 Fluidized bed test reactor

However, all tests described in this thesis were performed in the bubbling mode. The second cyclone was followed by a ceramic candle filter to remove fine solid particles from the product gas. After gas cleaning, the product gas either enters the torch, where it is completely oxidized, or it is fed to the combustion test rig via heated lines.

1.5.1 Sampling and gas analysis

The measuring instruments listed in Table 4 were used for the measurement of the combustion flue gas composition and for the characterization of the gasifier product gas composition. In addition to the measuring range of the devices, the measuring principle and the manufacturer are also specified.

Table 4 Equipment used for flue gas and syngas composition measurements

	Compound	Range	Principle	Manufacturer
Flue gas	CO	0–1000 ppmv	NDIR- absorption	Fisher-Rosemount
		0–1 Vol-%	NDIR- absorption	Fisher-Rosemount
	CO_2	0–20 Vol-%	NDIR- absorption	Fisher-Rosemount
	O_2	0–25 Vol-%	paramagnetic	Fisher-Rosemount
	NO, NO_2	0–1000 ppmv	chemiluminescence	Eco Physics
		0–10000 ppmv	chemiluminescence	Eco Physics
Product gas from Gasifier	CO	0–50 Vol-%	NDIR-absorption	ABB
	CO_2	0–30 Vol-%	NDIR-absorption	ABB
	CH_4	0–20 Vol-%	NDIR-absorption	ABB
	H_2	0–100 Vol-%	thermal conductivity	ABB
	O_2	0–25 Vol-%	paramagnetic	ABB
	C_xH_y	0–100 Vol-%	GC-PPQ and WLD	Varian Micro-GC

Flue gas composition – the sampling of the flue gas sample was carried out using a perforated probe over the entire cross-section of the exhaust pipe. The flue gas was sucked by a heated pump with an upstream heated filter and fed into the measuring gas cooler, where the water vapor was condensed. The emission measurements are therefore related to a dry volume. The measurements were carried out continuously.

Gasifier product gas composition – for the determination of the tar- and water-free composition of the gasifier product gases, the sample was continuously taken downstream of the candle filter. To prevent contamination and water ingress in the measuring instruments, the measuring gas streams were cooled to 0 °C and filtered in several stages. The measurement of all compounds beside C_xH_y took place continuously. The measurements using gas chromatography were taken four times over each 30 minutes of operation.

Since the measuring instruments used in both test rigs have a linear relationship between the measuring signal and the measured gas concentration, it was possible to check the displayed measured values through two-point calibration. Calibration was performed at the beginning and at the end of each test day. N_2 was used for zero-point calibration and test gas mixtures of N_2 and the respective gas components were used for spreading. The deviations were logged and later incorporated into the evaluation of the measurement data. From the two-point calibrations

at the beginning and end of the measurement session, the corresponding calibration functions were calculated and considered by the final data evaluation.

Product gas volume flow – The determination of the water- and tar-free product gas volume flow at the outlet of the gasifier consists of a condenser, filter, and an analogue gas meter. The condenser is a water-cooled tube bundle heat exchanger in which the water and tars condense. After the condenser, the product gas passes through a multi-layer filter unit consisting of activated carbon for tar separation and silica gel to remove the remaining moisture from the product gas flow. After the filter unit, the water- and tar-free product gas volume flow is measured discontinuously before and after each combustion test session. The simultaneous measurement of the product gas flow during combustion experiments is not possible.

NH_3 and HCN measurements – the concentrations of NH_3 and HCN were determined using wet chemistry methods. To collect the sample, a partial flow of the product gas was extracted via a sampling probe, which was installed directly at the entry to the burner. The sample flowed via a heated line and heated filter and passed via three washing bottles, each filled with the corresponding solvent. The washing bottles were located in an ice bath to condense the respective component. For the determination of NH_3, a 0.01 mol/l H_2SO_4 solution and for the determination of HCN, a 2.0 mol/l NaOH solution was used.
After leaving the three bottles with the solvents, the gas sample was led via a fourth impinger bottle filled with isopropanol and via silica gel to protect the pump and gas meter unit. The gas sample was further analyzed in an O_2 measurement device to monitor the tightness of the entire sampling line. The content of NH_3 and HCN was subsequently analyzed by the laboratory DEKRA Umwelt GmbH in accordance with VDI 2461/2 and DIN 38406 E5. The contents of the first two bottles was analyzed separately to the third bottle solution to assure the quality of the sampling.

1.5.2 Numerical modelling

The goal of the modelling work performed was twofold. On the one hand, the modelling was used to study and optimize the internal flow in the combustors. On the other hand, the formation and reduction mechanisms of NO_x were analyzed to explain the main differences between the reactions of NO_x precursors in different gaseous mixtures under flameless combustion conditions.
Considering the complexity of the phenomena, the ideal model covering both application fields would imply the use of computational fluid dynamic code (CFD) for the flow modelling including chemistry schemes of combustion and pollutants. To keep the numerical effort at a reliable level, the CFD models usually couple the flow modelling with a simplified description of combustion chemistry for the main species. Once the velocity, density, temperature, and

species concentration fields are calculated, the pollutant chemistry e.g., for NO_x is evaluated in an independent post-processing step.
However, some studies showed that, under flameless combustion conditions, the simplified combustion model is not sufficient to correctly predict the temperature and gas concentration fields well enough to build on it, and to calculate the pollutant fields on this basis [114]. On the other hand, there is a scientific consensus that such simplified models are accurate enough to study the geometrical design of flameless burners [113, 114]. Such studies were performed and are described in Chapters 2.1 and 2.2
For accurate pollutant predictions, it is necessary to use so-called detailed chemistry schemes, which include combustion reactions of the main gaseous species and the interrelated pollutant formation reactions [103, 114–116]. If such detailed schemes are implemented in a CFD, the determination of a numerical solution is very challenging and consumes a large amount of computing time. Therefore, in this thesis, an alternative two-step approach using simplified CFD and a network of idealized chemical reactors is proposed. In the first step, a CFD model was created to derive the main parameters of mixing processes. In the second step, these parameters were used as a boundary condition in the network of idealized chemical reactors where detailed chemistry schemes are applied. Such a two-step modelling approach is shown in Chapter 2.5. The tools used for the modelling work are described below.

1.5.2.1 Numerical modelling using CFD

For the CFD modelling presented in this thesis, two different applications were applied. The relatively simple simulations presented in Chapters 2.1 and 2.2 were calculated using the application AIOLOS, a code that was developed at the Institute of Combustion and Power Plant Technology (IFK), University of Stuttgart. For the boundary conditions generation used for the reactor network model in Subchapter 2.5, the commercially available software package FLUENT® was applied. Both applications allow numerical calculations of steady-state, three-dimensional, turbulent reacting flows. The basis of such modelling is the solving of the conservation equations for momentum, mass, species, and energy [114, 117–119]. In a generalized form, these can be presented for any mass-specific conservation variable ϕ in Cartesian coordinates, as follows:

$$\frac{\partial}{\partial t}(\rho\phi) + \frac{\partial}{\partial x_i}(\rho u_j \phi) = \frac{\partial}{\partial x_i}\left(\frac{\mu}{\sigma_\phi}\frac{\partial \phi}{\partial x_i}\right) + S_\phi \qquad \text{(Eq 2)}$$

The four terms describe the temporal change, the convective and diffusive transport, and the sources/sinks of the conservation variable ϕ for the considered volume. From these equations in stationary formulation follows a system of coupled differential equations. The discretization to solve the transport equations was performed in both applications with a conservative finite

volume method on coupled Cartesian and cylindrical in AIOLOS and body fitted grids in FLUENT®.

Turbulence modelling

Further modification of the equation system is necessary to consider the specific character of the modelled flow. The flow typically present in combustion chambers is highly turbulent and characterized by strong fluctuations of the considered variables in place and time. The turbulence could be modelled in detail by solving the momentum equation for instantaneous values, however such an approach is numerically very challenging. Therefore, in both applications used within this thesis the turbulence phenomenon is represented using the Reynolds and Favre averaging approach, which simplified the turbulence by time averaging of the calculated variables. The fluctuating parts are not directly represented by the numerical simulation and are included only through the turbulence model. This means that, after the simplification, the turbulence is not timely resolved and is represented by an additional stationary term in transport equations, which can be treated as a supplement to the convection term in this equation. A more detailed description of the Reynolds and Favre averaging approach is given in [114, 118, 119].

Through the additional description of the variable fluctuations in the transport equations, further unknowns are introduced in the equation system. To solve the equations and find the values of the fluctuations, an application of a further model is necessary that could close the equation system. The model applied in both application was the widely used k-ε model proposed by Jones and Launder [120]. The variable k is the term describing the kinetic energy of the turbulence, and ε describes its dissipation. Both variables are interconnected via so-called turbulent viscosity. For both k and ε two further conservation equations must be solved, closing the overall equation system. The detailed description of the derivation of the conservation equations can be found in the work of Schneider [119].

Global combustion chemistry mechanisms used in AIOLOS

The global chemistry scheme and the interaction between the turbulence and the chemistry were treated differently in the AIOLOS code (application used within Subchapters 2.1 and 2.2) and the FLUENT® software (application used in Subchapter 2.5).

In AIOLOS, a set of global reactions concerning the C_xH_y oxidation and breakdown, CO and H_2 oxidation is implemented [114, 121]. When CH_4 is considered as the highest hydrocarbon molecule, the reaction equations can be formulated as follows:

$$CH_4 + \left(\frac{1}{2} + \alpha\right) O_2 \longrightarrow CO + 2(1+\alpha)H_2 + 2\alpha H_2O \qquad \text{(R 12)}$$

$$CO + \frac{1}{2} O_2 \longrightarrow CO_2 \qquad \text{(R 13)}$$

$$H_2 + \frac{1}{2}O_2 \longrightarrow H_2O \quad \text{(R 14)}$$

The α parameter in reaction (R 12) is calculated under the assumption of a water-gas-shift reaction equilibrium. The global rate expression for the oxidation of CO was assumed according to kinetic parameters published by Howard et al. [122]. The H_2 oxidation is assumed to be infinitely fast and the reaction rates used can be found in [114]. The mechanism was optimized for the Eddy Dissipation Concept (EDC) coupling between the turbulence and the chemistry [114]. This concept, proposed by Magnussen [123], allows for the treatment of multi-step finite rate chemical reaction mechanisms of arbitrary complexity. Within this concept, the space of the fluid volume considered is divided into fine structures and the surrounding fluid. Combustion reactions take place when the reactant species are mixed on a molecular level at sufficiently high temperature. This molecular mixing occurs when the turbulent eddies break up and their kinetic energy dissipates into heat [118]. The mass fraction that represents such regions is calculated and treated as a perfectly stirred reactor where all the above reactions take place. The PSR reactor exchanges mass and heat with the surrounding fluid.

Global combustion chemistry mechanisms used in FLUENT®

The combustion of fuel was calculated according to a global, four-step simplified chemistry scheme for hydrocarbon oxidation proposed by Jones and Lindstedt [124]. In this work, fuels containing only CH_4, CO and H_2 were modelled, and therefore the global reaction scheme can be expressed as follows:

$$CH_4 + \frac{1}{2}O_2 \longrightarrow CO + 2H_2 \quad \text{(R 15)}$$

$$CH_4 + H_2O \longrightarrow CO + 3H_2 \quad \text{(R 16)}$$

$$H_2 + \frac{1}{2}O_2 \Leftrightarrow H_2O \quad \text{(R 17)}$$

$$CO + H_2O \Leftrightarrow CO_2 + H_2 \quad \text{(R 18)}$$

The first two reaction steps describe the hydrocarbon decomposition. The first one is dominant in fuel lean conditions, and the second one in fuel rich conditions. The third reaction describes the hydrogen oxidation and the last reaction describes the water-gas-shift reaction.

The interaction between the turbulence and the chemistry was modelled using the Eddy Dissipation Combustion Model (EDCM) proposed by Magnussen and Hjertager [125]. This model assumes that chemical reactions are fast, and that the rate of combustion is determined by the rate of mixing of reactants on the molecular scale. The reactions are limited either by the availability of the fuel or the oxidizer [126].

The overview of all applied numerical models in AIOLOS and FLUENT application is given in Table 5.

Table 5 Overview of the numerical models used for CFD calculations

	AIOLOS	**FLUENT®**
Grid	Cartesian	Body Fitted
Turbulence modelling	RANS	RANS
Turbulence closure model	k-ε	k-ε
Chemistry	Global (Standard)	Global (Jones and Lindstedt)
Chemistry coupling	EDC	EDCM
Radiation	Discrete Ordinates	Discrete Ordinates

1.5.2.2 Numerical modelling using reactor network models

The CFD modelling described in the previous subchapter focused on the correct representation of flow under highly turbulent conditions. The global chemistry mechanisms implemented in the CFD models are accurate enough to optimize the geometry of the burners by analyzing the recirculation of hot gases, which is essential for the flameless combustion stability. However, for the analysis of N chemistry, another approach was used in this work. To contain the computational demand for the flameless combustion modelling within reasonable limits, detailed chemical reaction mechanisms were applied while simplifying the description of the fluid dynamics using ideal chemical reactor models. Such modelling approach for pollutant emission calculations has already been used in the past. For example, Mancini has used a network of PSR reactors to model NO_x in mild combustion of natural gas [127].

The modelling described within this work was performed using the CHEMKIN PRO software package. Two different detailed chemistry schemes were used. These are closely described in the paper presented in Subchapter 2.5.

In this study, the use of plug flow reactors was identified as a suitable way to model the chosen combustion process. A PFR is an idealized flow reactor such that along the direction of the flow all the reaction mixture is moving along at the same speed and there is no mixing with the products of reactions. On the other hand, the reaction mixture is well mixed within each plug, or on the cross-section plane of the PFR. This idealization makes the flow reactor analysis simplified, as now one can treat the PFR as a one-dimensional flow reactor [128].

It is obvious that idealized flow representation using one single chemical reactor cannot be representative for any real combustion device. Nevertheless, many modelling and validation trials performed in preparation for the work presented in Subchapter 2.5 showed that, by using a network of PFR reactors, it is possible to significantly simplify the fluid flow description of a flameless combustor and still accurately describe all relevant chemical processes. This was not successful when using single PSRs or their networks, or single PFR reactors. The necessary

condition for the application of the reactor network model demands a basic knowledge about the distribution of reactants between the different reactors, which means the basic mixing process must be adequately represented in the reactor network. The necessary information was derived from the previously performed CFD calculations.

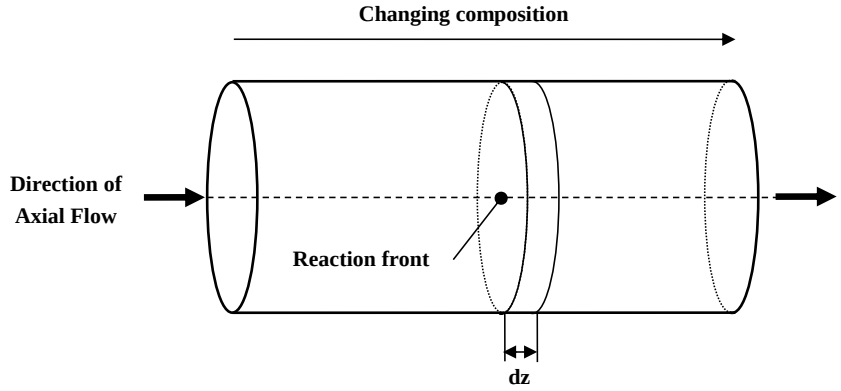

Figure 18 Conventional schematic representation of an ideal plug flow reactor (PFR)

To establish the reactor network model, parameters such as air/fuel distribution, distribution of the recirculated gases and the respective residence time for the PFRs need to be estimated based on the CFD results.

To transform the CFD results into values suitable for a 1-D reactor model, the entire combustion chamber was first divided into two main regions with positive and negative axial flow that represented the jet and recirculation regions, respectively. The positive flow was divided into discrete volumes. The positive flow consisted of fuel, air, and entrained recirculated gases. The distribution of each between the PFRs and their residence times were estimated based on the mass flow and velocity patterns of the CFD calculation. The simplified visualization of the model transformation is shown in Figure 19.

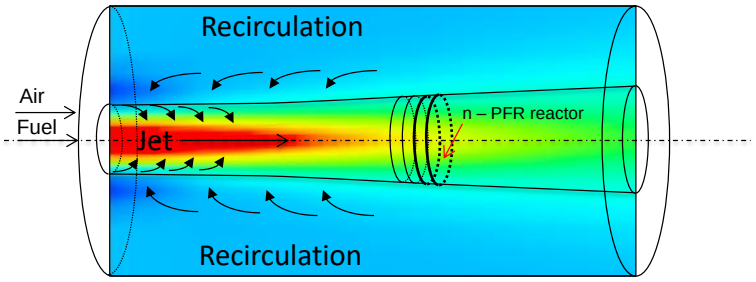

Figure 19 Transformation of the 3-D CFD result into 1-D reactor network model

Further, a proper mixing approach between air and fuel must be set. The mixing approach replaces the 3-D flow pattern of the combustion chamber resulting from CFD modelling. In this work, the influence of three different mixing approaches on the model predictions was tested.

Similar representations of mixing have already been reported in the literature when studying Selective Non-Catalytic Reduction (SNCR) and reburn processes [129, 130].
The simple mixing approach proposed by these authors is based on the maximum mixedness model of Zwietering [131]. This model assumed a continuous entrainment of the feed stream along the length of the PFR, at the appropriate rate, at various side entrances corresponding to different locations. Oliva et al. [129] proposed two types of implementation of the model of Zwietering. The first so-called "direct approach" implies the injection of the side stream continuously in the bulk stream (main flow). The second approach, the so-called "indirect approach" reverses the streams and considers the continuous introduction of the bulk flow into the side stream.

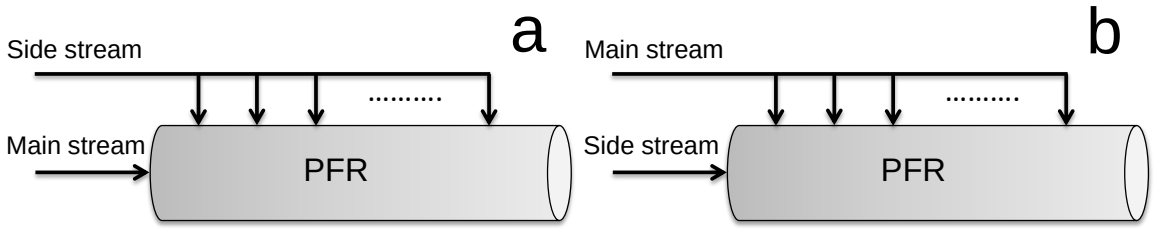

Figure 20 Direct (a) and indirect (b) mixing approach

In the combustion chamber modelled in this work, three different streams of air, fuel, and the recirculated gases were mixed along the jet. Therefore, it was necessary to extend the models proposed by Oliva et al. by adding another side stream. Another difference to the models proposed by Oliva et al. is the fact that, in this work, the side streams were discretized and therefore discontinuously mixed with the bulk. When establishing the model, it was not clear which stream should be treated as the bulk and which as the side stream. Therefore, both models were applied and validated against the experimental data. The first assumption was to treat the preheated air as the main stream, due to its very high inlet velocity and volume flow. In this approach, the fuel and recirculated flue gases were distributed along the main air jet. This approach is called the fuel-into-air mixing approach. The second approach, here called the air-into-fuel approach, considered the entrainment of the air and recirculated flue gases into a stream of fuel. The simplified schemes of the two mixing approaches are shown in Figure 21.
The fuel or the air was only distributed along a certain length of the jet. This length is called – in this work – the mixing length. To explain how the mixing length was estimated, a mixture fraction factor needs to be introduced. The mixture fraction measures the local ratio between the fuel and the oxidizer, and can be expressed using the following correlation:

$$\xi = \frac{Y_i - Y_{i,ox}}{Y_{i,fuel} - Y_{i,ox}} \quad \text{(Eq 3)}$$

where Y_i is the elemental mass fraction for element i.

The mixture fraction describes the local mixing conditions based on the relation between the local and initial concentration of certain compounds in fuel and oxidizer. Therefore, a non-reactive element needs to be chosen for the proper calculation of this factor. For the combustion calculation, the most convenient element is N_2 since all other species are consumed or formed while combustion proceeds.

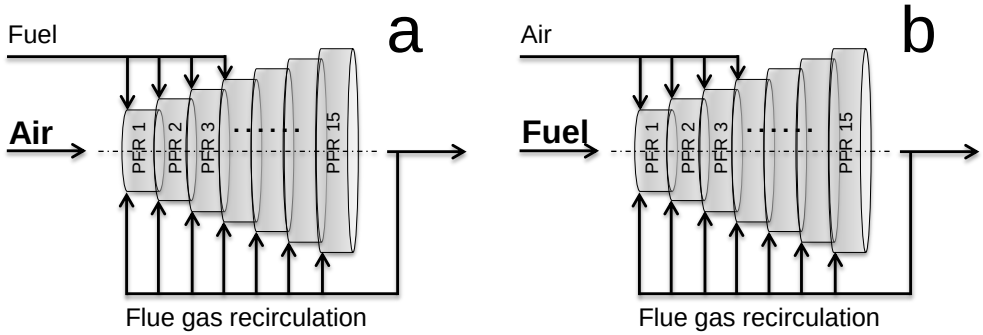

Figure 21 Fuel-into-air (a) and standard air-into-fuel (b) mixing approaches

The value of the mixture fraction determines the assumed length of mixing between the fuel and oxidizer. This value is estimated based on the detailed flow field results taken from the CFD modelling. The mixture fraction factor is calculated directly on the axis of the combustion chamber. For the fuel-into-air and the standard air-into-fuel mixing approach, the mixing length is defined as the length between the burner nozzle and the point when the mixture fraction reaches its stoichiometric value. In the case of fuel-into-air mixing, the fuel is distributed linearly in equal portions along the mixing length.

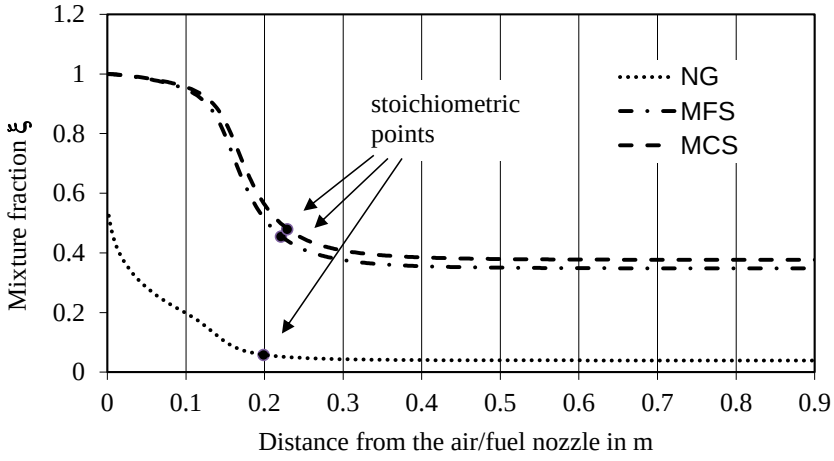

Figure 22 Visualization of the obtained mixture fraction curves for NG, MCS and MFS where NG – natural gas; MCS – methane containing syngas; MFS – methane-free syngas. Based on data obtained in Chapter 2.5

The amount of fuel introduced to the jet reaches its maximum value at the distance where the stoichiometric value of the mixture fraction was determined. From that point on, all the fuel is available for the combustion in the jet. In the standard air-into-fuel mixing approach, the distributed gas is the air and the definition of the mixing length stays the same. This means that the total amount of air is distributed linearly to the reactors, reaching the maximum value at the distance of the stoichiometric value of the mixture fraction. The mixture fraction curves obtained are based on the CFD results, and the inputs for the reactor network model are shown in Figure 22. For the NG the mixture fraction starts with much lower value than the mixture fraction calculated for the MFS and MCS. This means that for the natural gas the air started to penetrate the fuel jet already in the fuel nozzle.

The results of this model are described and discussed in the paper presented in Chapter 2.5 as well as in Subchapter 3.3.

2 Publications

2.1 Paper I: Early research – experimental study and design optimization using CFD

This paper was published in the proceedings of the 15th European Biomass Conference and Exhibition in Berlin, Germany, 2007.

Author's contribution to the paper:

- co-work in performing the experimental work related to combustion experiments using a flameless burner
- co-work on the evaluation of the experimental results
- independent performance of the modelling work – proposed methodology, evaluation of the boundary conditions, set-up of the model, and results evaluation
- co-authorship of the paper – co-writing, preparation of the data, data visualization and editorial work

APPLICATION OF FLOX TECHNOLOGY FOR THE UTILISATION OF LOW-GRADE BIOFUELS

A. Schuster, M. Zieba, G. Scheffknecht
Institute of Process Engineering and Power Plant Technology (IVD), University Stuttgart
Pfaffenwaldring 23, D-70569 Stuttgart, Gerrmany

J.G. Wünning
WS Prozesstechnik GmbH
Dornierstraße 14, D-71272 Renningen, Germany

ABSTRACT: The demand on biomass for heat and power production has intensively increased within the last years due to the rising gas and oil prices. Up to now mostly high-quality biomass (e.g. wood pellets, untreated wood) is used for heat production but also low-grade biomass becomes more and more of interest. For utilization of low-grade biomass an advanced combustion technology is required due to its high content on pollutants, e.g. nitrogen. Gasification of solid bio-residues to generate low calorific value (LCV) gases and their subsequent combustion is one of the possible conversion pathways. Within the presented work a multi-nozzle burner for LCV gases applying flameless oxidation (FLOX®) was developed that has several advantages compared to conventional flame burners. The FLOX®-burner was integrated in an existing dual-chamber furnace and four different residues from biorefinery processes were tested. Besides a more stable combustion with an improved burnout and thus a broader range of operation also a better performance due to the operation at lower excess oxygen were achieved. Furthermore the high power density of a FLOX®-burner reduces the volume of the combustion chamber by about 75 %. However, the investigations have also shown that the FLOX®-burner can only reduce thermal NO emissions but NO emissions related to fuel-bond nitrogen (e.g. in high contents in agricultural residues) are still on a high level or even increased by the flameless combustion.

Keywords: agricultural residues, combustion, emission reduction

1 INTRODUCTION

The utilization of low-grade bio-residues is becoming of big interest not only because of the increasing prices for high quality biomass (e.g. wood pellets) but also due to increasing demand on bio-residue recycling in biorefinery processes where still fossil fuels are used to cover their demand on energy. Facing these drawbacks the European Project BIO-PRO [1] focused on the development of new combustion technologies to convert residues of the biorefinery processes to energy, thus allowing them to self supply the required energy. The core activity of the project is to transfer new burner technologies, originally developed for natural gas, to burn LCV gases generated from biomass. One of these innovative burner technologies is the flameless oxidation [2, 3].

The FLOX® technology has several substantial benefits regarding their application for LCV gases. First, gases with changing composition can be burned without adjustments of the burner and problems related to flame instabilities can be prevented. Second, the absence of a flame leads to a uniform temperature distribution and thus thermal NOx emissions can be reduced. First investigations have shown that LCV gases can be burnt in flameless mode, even at heating values as low as 2.5 MJ/m^3 [4].

The following paper will give an overview of the development of a FLOX®-burner for LCV gas generated from bio-residues, the optimization of the burner design by CFD simulations and experimental results obtained with a combined system of fixed-bed pre-gasifier and subsequent FLOX®-burner using different bio-residues.

2 DEVELOPMENT OF FLOX-BURNER FOR LOW-GRADE BIOFUELS

The FLOX-burner that will be developed shall be able to burn hot and tar loaded LCV gases generated from bio-residues in a prior fixed-bed gasifier. An existing 120 kW dual-chamber furnace at the Institute of Process Engineering and Power Plant Technology (IVD) will be used for the pre-gasification of the solid bio-residues and the integrated conventional flame burner will be replaced by the developed FLOX®-burner.

2.1 Burner design

In order to develop a FLOX®-burner the boundary conditions like gas composition and gas temperature has to be determined. These results were previously presented [5]. The LCV gases generated from wood chips and pellets in the existing 120 kW fixed-bed pre-gasifier are of poor quality (1 - 1.5 MJ/m^3). However, the high temperature of the gases (950 - 1000 °C) will relieve the ignition in the burner. According to the dimensions predetermined by the flame pipe and the requirements for flameless oxidation a multi-nozzle FLOX®-burner for 100 kW was designed in co-operation with WS Wärmeprozesstechnik GmbH. The FLOX®-burner consists of a 12.5 l cylindrical combustion chamber and a gas nozzle plate at the burner top with eight gas nozzles each with their own air supply. The burner outlet is constricted to improve the recirculation zone that is elementary for the FLOX®-mode. The burner and its integration in the dual-chamber furnace are shown in Figure 1. The combustion air is provided through the former combustion chamber, passes the double jacket of the burner and is thus pre-heated.

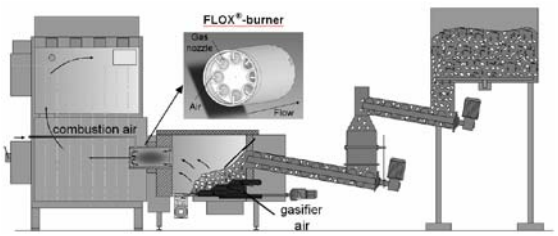

Figure 1: Fixed-bed pre-gasifier with subsequent FLOX®-burner

2.2 CFD simulations

To support the development process of the FLOX®-burner for LCV gases, CFD modeling was carried out. All presented numerical simulations were performed using the program 'AIOLOS' [6].The code is based on a conservative finite-volume formulation, using a standard k-ε model for turbulence. The interaction of turbulence and chemistry is modeled using Eddy Dissipation Concept (EDC). The chemistry used in AIOLOS is based on a set of global reaction mechanisms. The radiative heat transfer is calculated by the discrete-ordinates method. More detailed information about the program code is available in [6, 7].

It has to be noted that in the case of flameless combustion, usage of such simplified chemistry models lead to the local overestimation of temperature. The prediction of CO concentration is also not sufficient [8]. However, such numerical modeling can be used as a tool to solve the main technical problems concerning the flow and combustion-related stability problems.

At first, the original design (with constriction at the burner outlet and with gas nozzle plate) has been modelled. The influence of the LCV gas quantity and thus the load of the burner on the intensity of flue gas recirculation have been investigated. The combustion air flow was kept constant. The quantity of LCV gas generated in the gasifier has been varied from 70 to 130 % of nominal mass flow. The simulation results show that the main recirculation of flue gases is existing along the axis of the burner. In consequence, the hot exhaust gases are transported from the outlet of the burner to the vicinity of gas nozzles ensuring a stable combustion. The Figure 2 shows the axial velocity field for 70 and 100 % of nominal fuel flow.

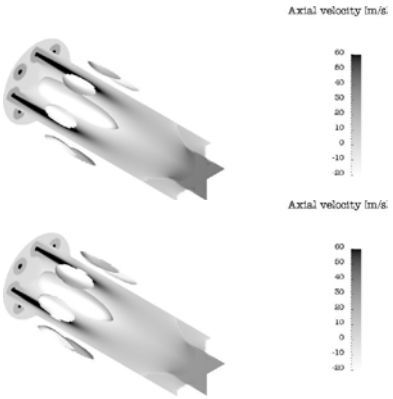

Figure 2: Velocity field, mass flow of LCV gas: 100 % (top) and 70 % (bottom)

The recirculation zone is presented with the help of iso-surface -8 m/s. The results show that the lower the fuel flow the bigger is the recirculation zone. However, in both cases recirculation is strong enough to ensure flameless oxidation regardless of variable fuel flow.

In the second step of CFD modeling different geometry simplifications have been investigated. The geometry combination without constriction and the geometry without gas nozzle plate have been modeled (Figure 3). In the first case, the results show that the constriction has no influence on the recirculation intensity compared to the basic construction. In the second case, the geometry without constriction has been further simplified by removing the gas nozzle plate. However, the recirculation has become very weak. The LCV gas flowing downstream counteracts the creation of the recirculation zone. The gas nozzle plate works as a protection for the gas backflow. Such low recirculation of flue gases might be insufficient to provide stable flameless combustion. Therefore, without this plate problems with combustion stability can occur.

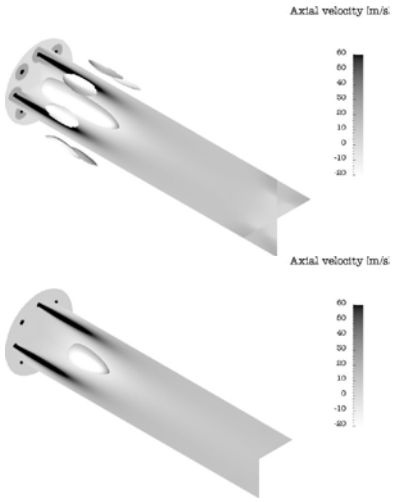

Figure 3: Velocity field, without constriction at burner outlet (top), without gas nozzle plate (bottom)

3 UTILISATION OF LOW-GRADE BIOFUELS

3.1 Experimental

Tests with the FLOX®-burner were carried out with four different bio-residues: wood chips, rape cake pellets, wheat husks and wheat pellets (2 % limestone added). The heating value varied between 13.6 MJ/m^3 for wood chips and 18.8 MJ/m^3 for rape cake pellets. The heating value of wheat husks and pellets were in between and about 15.6 and 16.2 MJ/m^3, respectively. Agricultural residues are characterized by a high nitrogen content in fuel, that is about 2.6 % for wheat husks (3.7 % for wheat pellets) and 5.4 % for rape cake pellets.

During the experimental tests with the different bio-residues either the amount of gasification air or the amount of combustion air was varied to investigate the operation range of the burner.

During the tests exhaust gas was continuously sampled and analysed at the exit of the boiler with respect to O_2, CO_2, CO, NO, NO_2 and NOx. For determination of LCV gas quality the produced gas from

the pre-gasifier was sampled at the end of the pre-gasifier; directly in front of the FLOX®-burner by a gas probe. The gas was then cooled and the condensed water and tars removed. The LCV gas was then analysed regarding the following components: CO, CO_2, CH_4, H_2 and O_2.

3.1 Influence of flameless combustion on emissions

Before the FLOX®-burner was integrated tests with the original dual-chamber furnace were carried out using wood chips, wood pellets, wheat husks and rape cake. As the dual-chamber furnace is designed for wood chips first tests were carried out with woody fuels. Both wood chips and wood pellets can easily be burnt and the measured CO emissions are below 200 mg/m^3 (@ 13 % O_2). NOx emissions varied between 100 mg/m^3 for wood pellets and 200 mg/m^3 for wood chips. As soon as the first chamber of the furnace is operated as pre-gasifier and thus the primary air is reduced, the secondary air has to be increased to keep the total air to fuel ratio. In that case the flame in the burner is more and more stretched and finally quenched at the backside of the combustion chamber, resulting in higher CO emissions.

Tests with wheat husks have shown similar trends regarding the CO emissions as in the previous tests. Very low CO emissions (below 30 mg/m^3) can only be obtained when the first chamber is operated under oxidizing conditions. Then the fuel is mostly converted in the pre-gasifier and the benefit of air-staging and thus NOx reduction is lost. NOx emissions are thus about 500 mg/m^3. At lower ER in the pre-gasifier the NOx emissions are reduced to about 325 to 350 mg/m^3, but in the same time the CO emissions increase to 100 to 200 mg/m^3 (see Figure 4). Furthermore, it has to be mentioned that enormous slagging problems on the grate occurred during the tests with wheat husks. Therefore, in further tests with the FLOX®-burner also wheat pellets with 2 wt-% limestone added will be used.

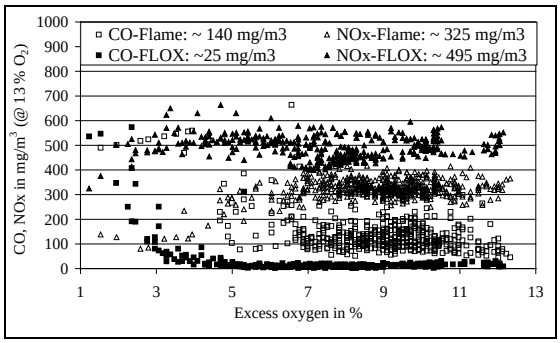

Figure 4: CO and NOx emissions for combustion of LCV gases generated from wheat husks with conventional and FLOX®-burner

A complete combustion of rape cake in the dual-chamber furnace could not be achieved in any test and the emissions of CO and hydrocarbons were always at a high level. Due to the small particle size the fuel bed on the grate was very dense and the air did not homogeneously pass the fuel bed. Thus, further tests with the FLOX®-burner will be implemented with rape cake pressed as pellets.

After integration of the FLOX®-burner in the test facility further tests with the bio-residues were carried out. The flameless combustion of LCV gases generated from wood chips is very stable over a broad operation range and very low CO levels (< 30 mg/m^3) can be achieved. Due to the very good mixing in the FLOX®-burner the burner can be operated at excess oxygen contents as low as 3 vol-%. Applying the original burner low CO emission can only be obtained for high ER in the pre-gasifier and for excess oxygen contents above 7 vol-%. NOx emissions are between 100 and 150 mg/m^3 and a bit lower than the ones applying the original burner.

Same results regarding the broad operation range up to minimum 3 to 4 vol-% excess oxygen and still very low CO emissions are observed for wheat husks, wheat pellets as well as rape cake pellets. However, a reduction of NOx emissions is not observed for the bio-residues with high fuel-nitrogen content. Even higher NOx emissions (~ 500 mg/m^3) are measured for combustion of LCV gases generated from wheat husks (Figure 4).

NOx emissions for tests with wheat pellets were in the range of 600 to 800 mg/m^3 and with rape cake pellets in the range of 800 to 950 mg/m^3. Slagging problems on the grate can be prevented when limestone is added to the wheat pellets as the ash melting point of the fuel is thus increased.

Table I gives an overview of the achieved CO and NOx emissions as well as the minimum excess oxygen content at that the burner can be operated with different bio-residues for both the original and the FLOX®-burner.

Table I: Comparison of CO, NOx emission and operation limits for tested bio-residues applying conventional and FLOX®-burner

Fuel	CO in mg/m^3		NOx in mg/m^3		Excess oxygen (lower limit) in vol-%	
	Flame	FLOX	Flame	FLOX	Flame	FLOX
wood chips	~ 200	< 30	~ 200	100 - 150	7	3
rape cake pellets	n.o.	< 30	n.o.	800 - 950	n.o.	3 - 4
wheat husks *	100 - 200	< 30	350	500 - 600	7	3 - 4
wheat pellets (2 % limestone)	n.t.	< 30	n.t.	600 - 800	n.t.	4

* slagging problems
n.o. operation not possible
n.t. not tested

3.2 Composition of generated LCV gas

A detailed characterisation of the LCV gas was carried out to evaluate the quality of generated LCV gas and thus the possibility of integrating an air staged FLOX®-burner for further NOx-reduction. In Table II the composition of LCV gases generated from different bio-residues in the fixed-bed pre-gasifier is presented. The gas analyses show that the produced gas in the pre-gasifier is of poor quality for all investigated fuels. The heating values of the LCV gases vary between 0.8 and 1.9 MJ/m^3 depending on fuel and operation conditions. The gas quality slightly improves while reducing ER in the pre-gasifier, but still significant amounts of oxygen are present in the produced gas. It can be assumed that the high oxygen content is a result of a poor mixing of fuel and gasification air in the pre-gasifier as well as the impact of air leakages that is increasing at low air flow rates. However, it has to be mentioned that the gas was

only sampled at a single point in the pre-gasifier and it can be assumed that the gas concentration vary in horizontal and vertical profiles due to the inhomogeneous distribution of air in the pre-gasifier.

During all tests the FLOX®-burner was able to burn the LCV gases that can change both in quality and quantity.

Table II: Composition of the LCV gases generated in the pre-gasifier

Gas		wood chips	rape cake pellets	wheat pellets
H_2	vol-%	1.4 - 2.4	1.2 - 3.4	1.7 - 3.2
CH_4	vol-%	0.4 - 0.6	0.6 - 1.5	0.5 - 1.2
O_2	vol-%	2.0 - 3.2	0.9 - 1.9	0.5 - 2.5
CO_2	vol-%	14.8 - 17.0	13.3 - 15.6	15.4 - 17.2
CO	vol-%	3.3 - 5.2	3.3 - 6.7	4.0 - 5.5
LCV	MJ/m^3	0.8 - 1.2	0.8 - 1.9	0.9 - 1.6

4 CONCLUSIONS

The development of a FLOX®-burner for LCV gases was of success. CFD simulations were used to support the optimization of the burner design. Several low-grade bio-residues can effectively be utilized. The combination of a fixed-bed pre-gasifier with a FLOX®-burner brings several advantages compared to the conventional firing system. A better burnout of the LCV gases is achieved due to a better mixing of the gases within the combustion zone. The burner can be operated at low excess oxygen contents that results in a higher efficiency compared to the original set-up. Furthermore, the combustion chamber of the FLOX®-burner is much smaller due to the better mixing and burn-out of the LCV gases that reduce investment costs.

Still one objective, the reduction of NOx emissions, is not achieved yet. High NOx emissions especially for fuels with high nitrogen content are observed. Although less experience exist with the combustion of residues of flour and oil mills NOx emissions are still on an unacceptable high level. Changes in burner operation did not have any influence on NOx emissions. Even higher NOx emissions were observed for the utilization of wheat husks compared to the conventional flame burner. Although reference tests with the original burner for wheat pellets and rape cake pellets are not carried out, it can be assumed that similar trends would have been observed. If the increase of the NOx emissions is related to the better burnout of the gases or even to a better conversion of fuel nitrogen under flameless oxidation conditions will be part of further investigations.

For the utilization of bio-residues with a high nitrogen content further NOx reduction measures has to be applied. Therefore, further investigations concentrate on the development of an air staged FLOX®-burner.

Gas quality measurements have shown that the LCV gases generated in the pre-gasifier have a very low heating value below 2 MJ/m^3. Still, the gases can be burned in the FLOX®-burner without problems due to the high gas temperature and the pre-heating of the combustion air. However, the high remaining oxygen content in the LCV gases does not allow testing an air staged burner in the existing test facility as a reducing zone cannot be establishing under these conditions.

As in larger gasifiers normally better gas qualities are obtained and the application of air staged FLOX®-burners can become of interest, first design investigations for an air staged FLOX®-burner will be done by further CFD simulations.

ACKNOWLEDGEMENT

The research activities were funded by the European Commission within the 6th framework programme under contract number SES6-CT-2003-502812. Sincere thanks are given.

REFERENCES

[1] www.eu-projects.de/bio-pro

[2] J. G. Wünning, Flammlose Oxidation von Brennstoff. Dissertation, Aachen, 1996

[3] J. A. Wünning, J. G. Wünning, Ten Years of Flameless Oxidation, Technical Applications and Potenials. 4th High Temperature Air Combustion, Rom, November 2001

[4] R. Berger, M. Schmid, J. G. Wünning, Low-NOx Schwachgasverbrennung mit flammloser Oxidation. Gaswärme International, 54 (2005), J. 6, p. 382-385

[5] A. Schuster, R. Berger, G. Scheffknecht, Utilisation of solid bio-residues in a new combustion system applying flameless oxidation. Proceedings of the 14th European Biomass Conference, Paris (France), 2005, p. 1298-1301

[6] U. Schnell, Progress in computational fluid dynamics, 1(4):208-218, 2001

[7] D. Foertsch, A Kinetic Model of Pulverised Coal Combustion for Computational Fluid Dynamics, Ph.D. thesis, IVD, Universität Stuttgart, 2002

[8] J.P. Kim, U. Schnell, Scheffknecht, G., Numerical Modelling of Flameless Combustion for Natural Gas. 7th European Conference on Industrial Furnaces Boilers (INFUB), Oporto (Portugal), 2006, paper #79

2.2 Paper II: Early research – experimental study and new design development using CFD

This paper was published in the proceedings of the 15th IFRF Members' Conference in Pisa, Italy, 2007.

Author's contribution to the paper:

- co-work in performing the experimental work related to combustion experiments using a flameless burner
- co-work on the evaluation of the experimental results
- independent performance of the modelling work – proposed methodology, evaluation of the boundary conditions, set-up of the model, and results evaluation
- co-authorship of the paper – co-writing, preparation of the data, data visualization and editorial work

OPTIMISATION OF CONVENTIONAL BIOMASS COMBUSTION SYSTEM BY APPLYING FLAMELESS OXIDATION

A. Schuster, M. Zieba and G. Scheffknecht

Institute of Process Engineering and Power Plant Technology
University Stuttgart
Pfaffenwaldring 23, 70569 Stuttgart
GERMANY
schuster@ivd.uni-stuttgart.de

J. G. Wünning

WS Wärmeprozesstechnik GmbH
Dornierstr. 14, 71272 Renningen
GERMANY
j.g.wuenning@flox.com

ABSTRACT

The utilisation of low-grade biomass requires an appropriate technology that meets the increased demands regarding emission reduction (e.g. NOx). Within this work a new burner for low calorific value (LCV) gas applying flameless oxidation (FLOX®) will be presented that replaces the conventional flame burner of a dual-chamber furnace. The integration of an adapted FLOX®-burner has shown several benefits. Different bio-residues were tested and a more stable combustion with enhanced burnout was achieved for all tested fuels. Furthermore, the burner can be operated in broader range of operation and closer to stoichiometric conditions. Due to the high power density of a FLOX®-burner the complete facility could be downsized in the future. Still, the tests have shown that the NOx reduction potential of a FLOX®-burner is limited for LCV gas combustion since the most NO emissions are related to fuel-bond nitrogen.

In the LCV gases generated from wheat pellets and rape cake pellets high concentrations of NO-precursors (NH_3 and HCN) are measured that are subsequently be oxidized to NO in the FLOX®-burner. Therefore, an air-staged burner for N-rich LCV gases based on flameless combustion is proposed where NO-precursors can be reduced to N_2 in a first substoichiometric region. CFD simulations were applied to investigate an appropriate design of an air-staged FLOX®-burner. Special emphasis is placed on the creation of a sufficient internal recirculation of flue gases required for flameless combustion. First results of CFD simulations are presented.

1 INTRODUCTION

The utilisation of biomass to produce bio-fuels and other bio-based materials in biorefineries is considered to grow steadily within the next years. These processes suffer oftentimes from the fact that the generated bio-residues can not furthermore be used internally due to their poor quality. The European project BIO-PRO [1] is aiming on overcoming this drawback by developing easy and robust technologies to convert the residues of the biorefinery processes to energy, thus allowing them to self-supply the required energy. The core activity of the project is to transfer new burner technologies, originally developed for natural gas, to burn LCV gas generated from biomass. One of these innovative burner technologies is the flameless oxidation.

At the Institute of Process Engineering and Power Plant technology a new combustion system for solid residues is under development. In a first step solid bio-residues are gasified in a

commercial fixed-bed gasifier and subsequent the hot LCV gases are directly burned in an adopted FLOX®-burner developed within the project.
The presentation will give an overview of the test results with the new combustion system using four different bio-residues. The emission behaviour depending on different fuel qualities will be shown with special emphasis on the NOx formation process. In order to get a better understanding of the NOx conversion within the combined gasifier-FLOX®-burner-system a detailed analysis of the produced LCV gas was carried out and will show the potential for NOx reduction. The applicability of an air-staged FLOX®-burner for nitrogen rich fuels was investigated by applying numerical simulations using a three-dimensional Computational Fluid Dynamics (CFD) program "AIOLOS". First simulation results of the air-staged burner will be presented.

2 EXPERIMENTAL

In the following section the test facility that was built-up for the experimental investigations is described. Different bio-residues are tested for the utilisation in the new combustion system.

2.1 Test facility

For the experimental investigations a 116 kW commercial dual-chamber furnace for wood chips was applied. For the utilisation of low-grade bio-residues the first chamber will be operated as a fixed-bed pre-gasifier and the subsequent combustion of the LCV gases shall be improved by the integration of a FLOX®-burner adapted to LCV gases. A detailed description of the originally test facility can be found in a previous publication [2]. According to the boundary conditions determined in preliminary tests a FLOX®-burner suitable for integration to the fixed-bed pre-gasifier was designed and the original burner was replaced (Figure 1). The FLOX®-burner was integrated in the flame pipe - the connection of pre-gasifier and boiler.

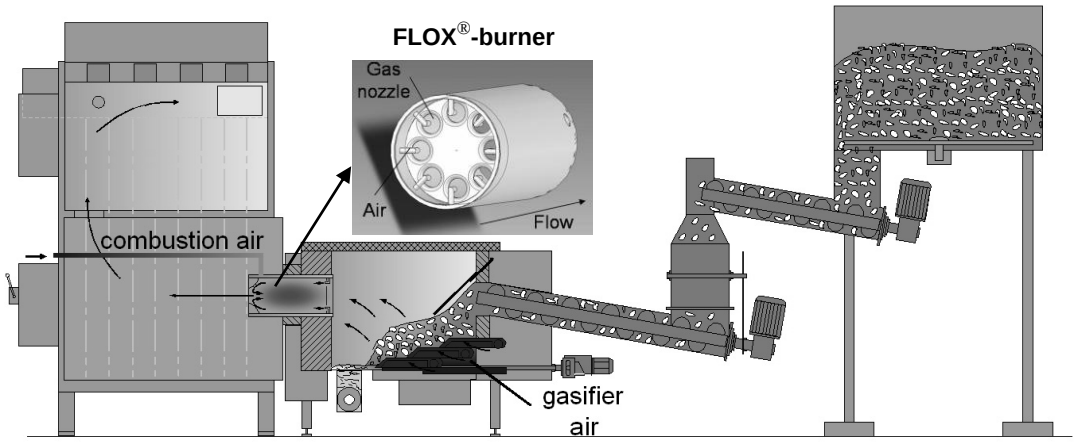

Figure 1. Fixed-bed pre-gasifier with subsequent FLOX®-burner

The developed FLOX®-burner is a multi-nozzle burner that consists of eight gas nozzles each with its own air supply. Due to limited accessibility the combustion air is supplied from the backside of the boiler. The air passes the double jacket of the burner and is thus pre-heated. The complete burn out of the LCV gas takes place in the cylindrical combustion chamber of the burner. The exhaust gases pass then both of the original combustion chambers before entering the water boiler system.

2.2 Fuels

Tests with the new developed FLOX®-burner were carried out with wood chips, rape cake pellets, wheat husks and wheat pellets (with 2 % limestone added). The characteristics of all

tested fuels are given in Table 1. The four fuels differ mostly by their moisture, ash and nitrogen content. Rape cake pellets have the highest ash and nitrogen content, but also the highest heating value. Wheat husks and pellets have also a considerable amount of fuel-bond nitrogen, but only half of the amount that rape cake pellets have. The addition of limestone to wheat pellets is increasing the ash content, but prevents the ash slagging problems observed in the tests with wheat husks.

Fuel		**Wood chips**	**Rape cake pellets**	**Wheat husks**	**Wheat pellets (+2 % limestone)**
Moisture	wt-% (ar)	21.1	8.7	12.4	14.4
Ash	wt-% (ar)	0.2	5.4	2.6	3.7
C	wt-% (ar)	38.3	45.8	38.1	38.0
H	wt-% (ar)	5.1	7.5	8.6	6.2
N	wt-% (ar)	< 0.3	4.7	2.0	2.1
S	wt-% (ar)	< 0.3	0.5	< 0.3	< 0.3
H_U (LCV)	MJ/kg (ar)	13.6	18.8	15.6	16.2

Table 1. Composition of tested bio-residues

2.3 Analyses

During the tests exhaust gas was continuously sampled and analysed at the exit of the boiler with respect to O_2, CO_2, CO, NO, NO_2 and NOx.

For determination of LCV gas quality the produced gas from the pre-gasifier was sampled at the end of the pre-gasifier; directly in front of the FLOX®-burner by a gas probe. The gas was then cooled and the condensed water and tars removed. The LCV gas was analysed with respect to CO, CO_2, CH_4, H_2 and O_2.

Furthermore the content of NH_3, HCN and NO in the produced gas was determined to evaluate the conversion of fuel-nitrogen to N-precursors (mainly NH_3 and HCN) and to NO that is formed already in the pre-gasifier. For NO determination the gas was sampled via gas probe at the end of the pre-gasifier. The gas was then cooled and the condensed water and tars removed before entering the NO analyser. For NH_3 and HCN determination the gas was again sampled via gas probe at the end of the pre-gasifier. The gas sampling pipe was as short as possible and insulated to prevent condensing of ammonia already in the sampling pipe. The gas was then lead to an ice bath with impinger bottles, where NH_3 and HCN are solved in the corresponding solvent. A 0.01 M H_2SO_4 solution was used for NH_3 determination and a 2.0 M NaOH solution for HCN determination. The gas flow was measured and controlled by a gas pump. The content of NH_3 and HCN in the solutions was afterwards analysed in laboratory according to VDI 2461/2 and DIN 38406 E5. For each setting two (wheat pellets) or three (rape cake pellets) gas samples were collected. The content of NH_3 and HCN is given as average value of the analysed samples.

3 OPERATION EXPERIENCE WITH DIFFERENT BIO-RESIDUES

3.1 State-of-art furnace

Preliminary tests with the conventional dual-chamber furnace were carried out to assess the fuel flexibility of the state-of-art technology. The tested fuels are wood chips (reference fuel), residues of flour mills (wheat husks) and residues of oil mills (rape cake). For the combustion of wood chips under conventional operation conditions CO emission between 100 and 150 mg/m^3 (@ 13 % O_2) and NOx emissions between 150 and 200 mg/m^3 were observed (Figure 2). As soon as the equivalence ratio (ER) in the pre-gasifier was reduced below 0.4 high CO emissions were observed. Changes of the primary air in the pre-gasifier were

counterbalanced with adjustments of the secondary air to keep a constant overall lambda. With increase of secondary air the flame is extended and then quenched at the backside of the combustion chamber that results in high CO emissions.
The tests with wheat husks have shown similar trends regarding CO emissions as in the previous tests with wood chips. At low ER in the pre-gasifier the secondary air flow is increased and thus the flame is stretched and finally quenched. In Figure 2 CO and NOx emissions are shown for an ER in the pre-gasifier of 0.7. Very low CO emissions (below 30 mg/m^3) can only be obtained at ER higher than 1.0 in the pre-gasifier. Then the fuel is mostly oxidised in the pre-gasifier and the benefit of air-staging, NOx reduction, is lost. At all, the NOx emissions are higher due to higher N-content in the fuel than for the tested woody fuel. The NOx emissions varied between 320 and 510 mg/m^3 depending on the CO level.
The rape cake was used as received from the oil mills. However due to the small particle size the fuel bed on the grate of the pre-gasifier was very dense and the air did not homogeneously pass the fuel bed. Thus, the emissions of CO and hydrocarbons were very high and even soot were observed. A complete burnout was not established. It can be concluded that the rape cake in this shape can not be used in a fixed-bed gasifier. Further tests will be implemented with rape cake pressed as pellets.

3.2 Combined system of pre-gasifier and FLOX®-burner

A FLOX®-burner suitable for integration to the fixed-bed pre-gasifier was designed based on gas quality measurements that will be presented in the next section. The integrated multi-nozzle is shown in Figure 1.
Tests with the integrated FLOX®-burner were carried out with woods chips, wheat husks, wheat pellets and rape cake pellets. In Figure 2 the relation between CO and NOx emissions and excess oxygen content in the flue gas for wood chips is presented at an ER in pre-gasifier of 0.4. The FLOX®-burner can be operated over a broad range of excess oxygen and down to 3 % excess oxygen (λ = 1.16) with very low CO emission before CO emissions increase significantly. This is a considerable improvement compared to the test results with the conventional dual-chamber furnace that is normally operated between 7 to 9 % excess oxygen and CO emissions in the range of 100 to 400 mg/m^3 (Figure 2). The influence of excess oxygen on NOx emissions is marginal. NOx emissions for the tests with the new system are slightly lower than the ones observed during the tests with the conventional dual-chamber furnace.

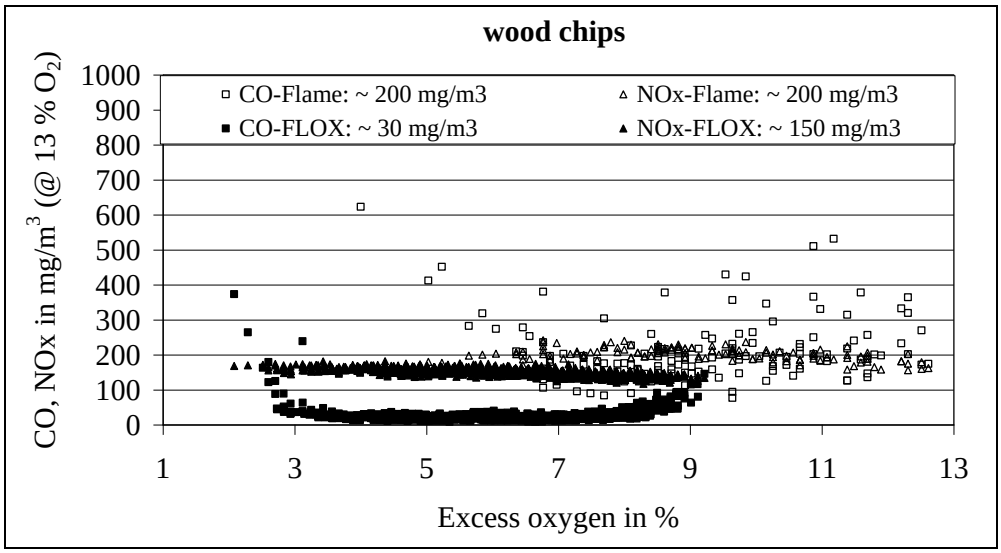

Figure 2. Comparison of CO and NOx emissions for conventional dual-chamber furnace and new system with integrated FLOX®-burner using wood chips

During the tests with wheat husks also a very good burnout was achieved and CO emissions were again at a low level (below 20 mg/m^3). NOx emissions depend on the ER in the pre-gasifier. At ER higher than 0.5 NOx emissions were at a low level, between 480 and 550 mg/m^3 (at 13 % O_2), considering the N-content of 2.0 % in the fuel. Higher NOx emissions (between 880 and 1000 mg/m^3) were measured when the pre-gasifier is operated at lower ER. In Figure 3 CO and NOx emissions for wheat husks combustion applying the conventional dual-chamber furnace and the new system with integrated FLOX®-burner are compared. Similar to the results with wood chips the new system can be operated over a broad range of excess oxygen and down to 4 vol.-% excess oxygen without a significant increase of CO emissions. CO emissions using the state-of-art technology are at a higher level over the entire operation range and increase at excess oxygen contents lower than 7 vol-%. Furthermore, it has to be mentioned that even at constant operation conditions the excess oxygen varied in a broad range (2.5 to 12 vol.-%). Still, the burner can handle the changing gas composition and the burn-out of the LCV gas can still be complete. The changing LCV gas composition is probably caused by fluctuations in the pre-gasification step. Reasons for that are both the small fuel particle sizes and generated ash slagging on the grate that creates a very dense fuel bed influencing the air penetration through the fuel. Further tests were conducted with wheat pellets that contain 2 wt.-% limestone to prevent ash slagging on the grate. While on one hand a broad operation range, a better burnout of the gases and thus lower CO emissions are achieved applying the new system the NOx emissions are on the other hand raised by about 50 %.

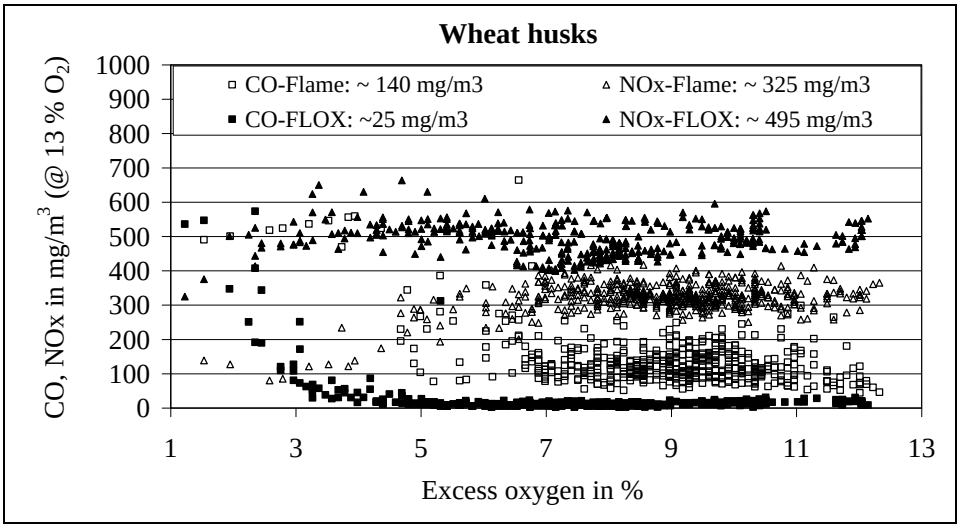

Figure 3. Comparison of CO and NOx emissions for conventional dual-chamber furnace and new system with integrated FLOX®-burner using wheat husks

Similar results are obtained for the tests with wheat pellets, but the ash slagging on the grate was prevented and thus a more stable operation was achieved. NOx emissions were at a slightly higher level (600 to 800 mg/m^3) obviously due to the higher nitrogen content in fuel.
The fourth tested fuel is rape cake, but now pressed to pellets. Remarkable again is the broad range of operation of the new system from 1.17 to 1.7 (3 to 9 % O_2) at very low CO emissions down to less than 10 mg/m^3 (at 13 % O_2). Higher NOx emissions were measured once more when the pre-gasifier is operated at lower ER. Obviously, the lower the ER in the pre-gasifier is the higher the NOx emission. Or in other words, the more the oxidation reactions are shifted to the FLOX®-burner the better the N-conversion to NOx due to the good mixing and oxidation conditions in the burner.
Table 2 summarises the emission levels and operation limits that can be achieved with the state-of-art technology and the new system with integrated FLOX®-burner for the tested bio-residues.

Fuel	CO in mg/m³		NOx in mg/m³		Excess oxygen (lower limit) in vol-%	
	Flame	FLOX	Flame	FLOX	Flame	FLOX
wood chips	~ 200	< 30	~ 200	100 - 150	7	3
rape cake pellets	n.o.	< 30	n.o.	800 - 950	n.o.	3 - 4
wheat husks *	100 - 200	< 30	350	500 - 600	7	3 - 4
wheat pellets (2 % limestone)	n.t.	< 30	n.t.	600 - 800	n.t.	4

* – slagging problems
n.o. – operation not possible
n.t. – not tested

Table 2. Overview of CO and NOx emissions for conventional dual-chamber furnace and new system with integrated FLOX®-burner

4 CHARACTERISATION OF LCV GAS

The experimental investigations with the new combustion system for low grade bio-residues have shown that due to the perfect mixing in the FLOX®-burner, CO emissions can be decreased significantly. Moreover, this can be achieved with very low oxygen concentrations in the flue gas. Still, higher emissions of NO_x were measured while burning nitrogen rich fuels in FLOX®-burners when compared to classical flame burners.

A detailed characterisation of the LCV gas was carried out to determine the quality of the generated gas and to evaluate the influence of the FLOX®-burner on the emission results. In a first step the LCV gases generated from wood chips, rape cake pellets and wheat pellets were analysed regarding to H_2, CH_4, O_2, CO_2 and CO at different ER in the pre-gasifier. Table 3 gives an overview of the measured gas composition and the thus calculated heating values of the LCV gases.

Fuel		woodchips			rape cake pellets			wheat pellets		
$ER_{pre\text{-}gasifier}$		0.5	0.7	0.9	0.7	0.9	1.2	0.8	0.9	1.1
H_2	vol-%	2.4	2.3	1.4	3.4	1.2	2.8	3.2	2.1	1.7
CH_4	vol-%	0.5	0.6	0.4	1.5	0.6	1.5	1.2	0.9	0.5
O_2	vol-%	3.1	3.2	2.0	1.9	1.1	0.9	2.1	0.5	2.5
CO_2	vol-%	14.8	15.1	17.0	13.3	15.6	14.5	15.4	17.2	15.5
CO	vol-%	5.2	5.0	3.3	6.7	3.3	6.2	5.5	4.5	4.0
H_U (LCV)	MJ/m³	1.2	1.1	0.8	1.9	0.8	1.7	1.6	1.2	0.9

Table 3. Gas concentrations and heating values of LCV gases generated from the test fuels

For all tested fuels the generated LCV gas is of poor quality and the heating value is below 2 MJ/m³. With decreasing ER in the pre-gasifier the gas quality is slightly improved except for the tests with rape cake pellets. Lowest heating values are measured for wood chips (0.8-1.2 MJ/m³) and the highest ones for rape cake pellets (0.8-1.9 MJ/m³). Oxygen concentrations are always on a high level even at substoichiometric conditions. On the other hand incomplete combustion was observed even in excess of stoichiometry and unburned compounds were measured. This indicates that the local conditions differ a lot from the

global ER due to insufficient mixing of air and fuel in the pre-gasifier. A better mixing of air and fuel will enhance the gas quality enormously.
Furthermore, it has to be mentioned that the gas composition is measured only at a single point in the pre-gasifier and it can be assumed that the gas composition also vary both in vertical as in horizontal profile. Still, the FLOX®-burner was able to burn the LCV gases despite its changing composition and low heating value during all tests.
Due to the high oxygen concentrations in the generated LCV gas it is likely that NO-precursors (mainly NH_3, HCN) formed during the gasification are already converted to NO in the pre-gasifier before entering the FLOX®-burner. Therefore, further analyses were carried out to assess the influence of the FLOX®-burner on the NO formation process for nitrogen rich bio-residues. Additional tests with wheat pellets and rape cake pellets were conducted in order to evaluate the degree of NO formation in the pre-gasifier. In Figure 4 the concentrations of NH_3, HCN and NO measured in the LCV gases generated in the pre-gasifier at different equivalence ratios are presented.

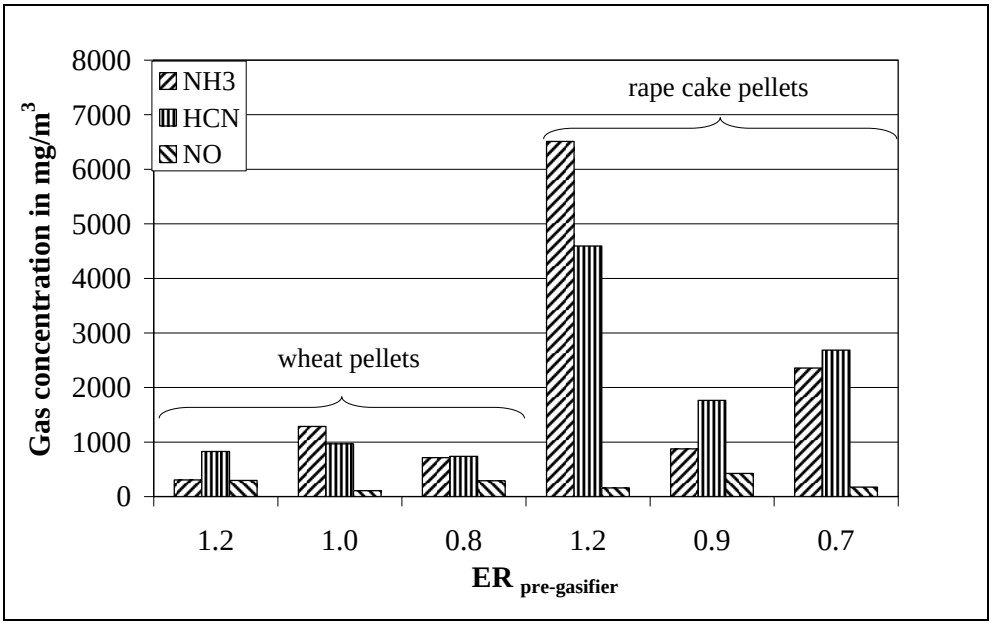

Figure 4. N-compounds in LCV gas generated in pre-gasifier using wheat husks and rape cake pellets

In the tests with wheat pellets concentrations of NH_3 and HCN up to 1280 and 970 mg/m^3 were measured, respectively. Due to the higher nitrogen content in rape cake pellets the concentrations of NO-precursors were higher and up to 6500 mg/m^3 (NH_3) and 4590 mg/m^3 (HCN). NO is already formed to some extend in the pre-gasifier and concentrations between 110 and 420 mg/m^3 were measured. It is obviously that the amount of NO-precursors is correlated to the amount of NO present in the gas. In gases with a high content of NO the concentration of NH_3 and HCN is low. Here, a higher rate of NO-precursors is already converted to NO. Normally higher NH_3 and HCN concentrations shall be found in gases generated in the pre-gasifier at low ER. Even though the highest N-precursor concentrations were detected in the LCV gas generated at ER = 1.0 (wheat pellets) and ER = 1.2 (rape cake pellets). Here, it is proven again, that the ER represents only the global conditions in the pre-gasifier, but local conditions in the pre-gasifier are of particular importance for the quality of the gas including the nitrogen conversion.

5 CFD-MODELING OF THE AIR - STAGED FLOX-FLOX BURNER

Detailed investigation of the product gas from the gasifier showed very high concentrations of NO_x precursors such as NH_3 and HCN as well as high concentrations of NO_x already

created in the gasifier. These compounds can be reduced to N_2 in substoichiometric regions created in the burner. Such regions can be generated through air staging. Therefore, the further development of FLOX®-burners for LCV gases is focused on staged burners. There are three types of staged burners which are feasible [3]. In the case of Flame-FLOX-type burners, a mixing chamber is installed before the FLOX-combustion chamber which shall ensure more defined reducing conditions. However, the FLOX-FLOX burner should result in the best operating conditions. This combination should not only ensure the best reducing conditions in the first substoichiometric zone but also excellent mixing and complete combustion in the second oxidation zone of the burner [3].
To support the development process of such two-stage burners, CFD modelling was carried out. All presented numerical simulations were performed using the program 'AIOLOS' [4].

5.1 Code description

The code is based on a conservative finite-volume formulation, using a standard k-ε model for turbulence. The interaction of turbulence and chemistry is modelled using Eddy Dissipation Concept (EDC). The chemistry used in AIOLOS is based on a set of global reaction mechanisms. The radiative heat transfer is calculated by the discrete-ordinates method. More detailed information about the program code is available in [4, 5].
It has to be noted that in the case of flameless combustion, usage of such simplified chemistry models lead to the local overestimation of temperature. The prediction of CO concentration is also not sufficient [6]. However, such numerical modelling can be use as a tool to solve the main technical problems concerning the flow and combustion-related stability problems.

5.2 Burner design and boundary conditions

As mentioned above, in the case of FLOX-FLOX air-staged burner, there are two zones working with internal flue gas recirculation. Nevertheless, such construction requires that enough air can be injected to generate sufficient mixing and flue gas recirculation in both zones. It has to be taken into account that this burner is designed for LCV gases combustion. It means that the required amount of air might exceed the amount needed to complete combustion. The better the quality of gas, the more air can be use to force the recirculation, and the better reduction and oxidation in the burner. Therefore, geometry of such burner has to be optimized to ensure good conditions in both mixing zones with a limited amount of air. Moreover, these zones have to be separated from each other in order to avoid sucking of the oxygen rich gaseous mixture from the oxidation zone to the reduction zone.
In the first modelling step, a simple air-staged burner design was modelled. The 3-D cross section of this burner in presented in Figure 5. This design is based on the original, multi-nozzle single staged construction.

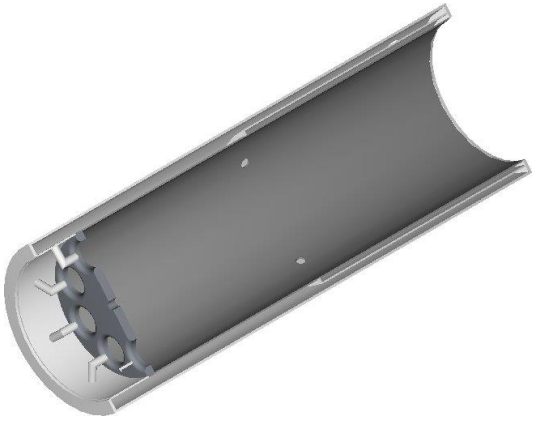

Figure 5. Air-staged FLOX-FLOX burner

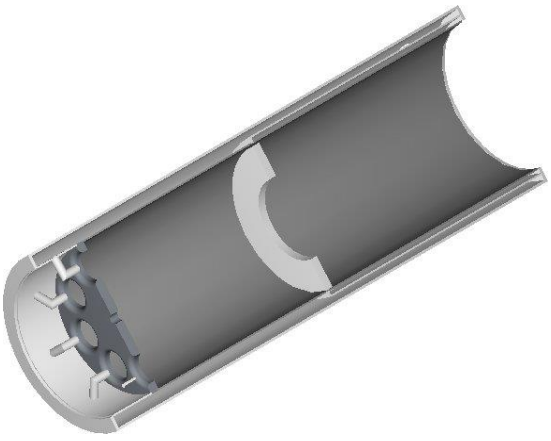

Figure 6. Air-staged FLOX-FLOX burner with orifice

The hot product gas generated in the gasifier is fed through the large circular nozzles. Air is injected in two stages: via eight nozzles in the front and via four in the middle of the burner. The boundary conditions are presented in the Table 4.

	Flow rate (kg/h)	Temperature (°C)	Composition (wt. %)
Product gas	86,3	900	CH_4 – 3,7 H_2 – 0,2 CO – 5,2 CO_2 – 24 H_2O – 9,2 O_2 – 1,5 N_2 – 56,2
Total air	106,5	Primary Air – 600 Secondary Air – 300	Dry Air

Table 4. Boundary conditions

The total flows of air and product gas as well as temperatures were assumed to be constant. The influence of equivalence ratio in the reduction zone on internal recirculation was investigated (ER_{red}=0,6, ER_{red}=0,8, ER_{red}=1).
In the second step of modelling, different geometry variations were modelled. All cases were calculated assuming ER_{red}=0,8 in the reduction zone. At first, the angle of secondary air injection was changed. After that, the design with the orifice between the first and second zone was modelled. The orifice is placed directly before the secondary air nozzles (Figure 6).
Finally, modelling of the burner without secondary air was carried out with the assumption of ER_{red}=ER_{tot}=0,8 in the burner. The last modelling result provides information about flue gas recirculation in the first zone without disturbance caused through the secondary air injection.

5.3 Modelling results and discussion

Influence of equivalence ratio on recirculation. Three different cases with ER = 0,6, 0,8 and 1 in the reduction zone were modelled. The total amount of air has been assumed to be constant. This results in an oxygen level of about 5 vol-% in dry flue gas.
It means, the more air injected in the first section of the burner, the less amount of air is injected in the second section. In order to better describe the recirculation the parameter Local Recirculation rate (LR) has been introduced. This rate is calculated as a ratio between the mass flowing through the specified cross-section in the opposite direction to the main stream ($\dot{m}_{rec}$) and the total mass flow of fuel ($\dot{m}_{fuel}$) and primary air ($\dot{m}_{PA}$) introduced into the burner.

$$LR = \frac{\dot{m}_{rec}}{\dot{m}_{fuel} + \dot{m}_{PA}} \qquad (1)$$

Figure 7 shows the local recirculation rate in the substoichiometric zone for the first four modelled cases. The results show that the recirculation strongly depends on air distribution between primary and secondary stage. Decreasing the ER in the first part of the burner to ensure good reducing conditions forces the recirculation zone to move to the vicinity of the secondary air injection. This causes sucking of the secondary air into the region where substoichiometric conditions should be achieved. On the other hand, increasing ER in the first zone forces the recirculation zone in the direction of the gas nozzles, decreasing the amount of the secondary air transferred to the reduction zone. However, the effect of reduction decreases also because of the larger amount of injected primary air. In the Figure 9 and Figure 11 the velocity field has been presented with the help of two perpendicular

surfaces. To better show the recirculation isosurface with an isovalue of -8 m/s has been used.

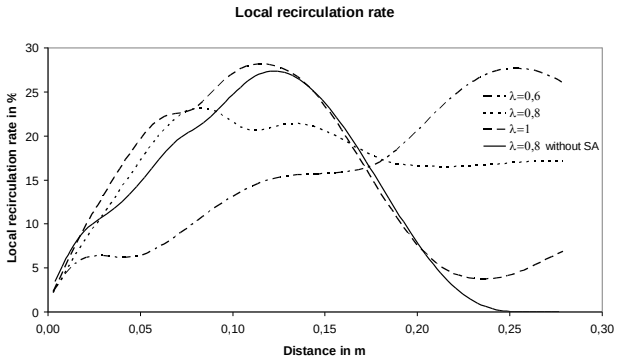

Figure 7. Local recirculation rate along the burner – ER variation

It has to be noted, that using the proposed design, problems with mixing and cold areas (Figure 8 and Figure 10) in the secondary part of the burner can occur. With this geometry, sufficient recirculation in the second zone cannot be achieved.

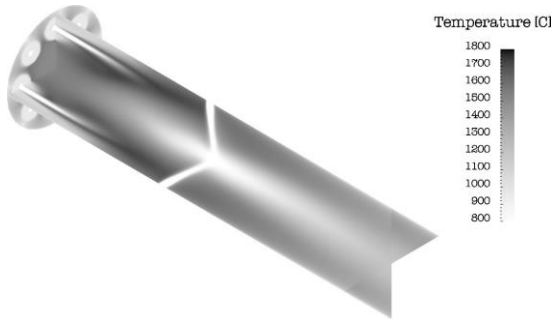

Figure 8. Temperature field; λ_{red}=0,8

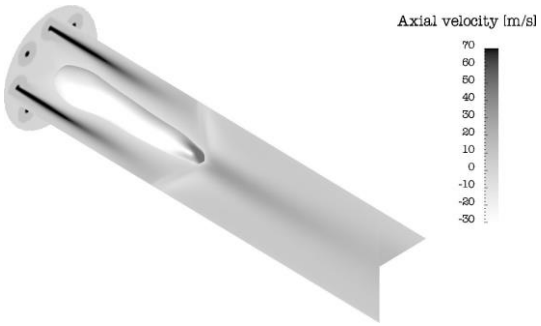

Figure 9. Velocity field; λ_{red}=0,8; Isosurface -8 m/s

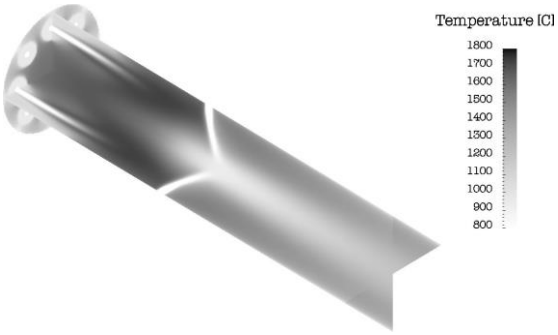

Figure 10. Temperature field; λ_{red}=1

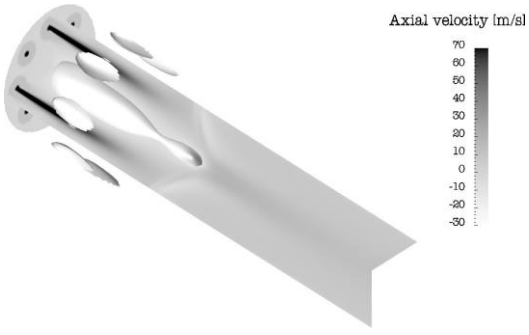

Figure 11. Velocity field; λred=1; Isosurface -8 m/s

Geometry variation. In order to obtain better separation of first and second zone as well as to minimize mixing problems, two other geometry settings have been modelled. Equivalence ratio in the first stage of the burner has been assumed to be 0,8. In the first case, the angle of secondary air injection has been changed from 90º to 45º. This results in good separation between the two stages. In Figure 12, local recirculation rate as a function of distance has been presented. It shows that for air injection with 45º, there is no recirculation in the vicinity

of secondary air injection. Figure 9 shows that the recirculation zone has been moved in the direction of the gas nozzles. Unfortunately, the change of the angle has not minimized problems with the mixing in the second stage of the burner. To achieve stronger recirculation in the second stage, the geometry with an orifice has been designed (Figure 6). The results of numerical modelling show that in this case the recirculation generated in the first stage is a little bit weaker then in the other modelled cases. However, it is possible to achieve much better mixing conditions in the second stage. This geometry seems to be the best of those that have been tested.

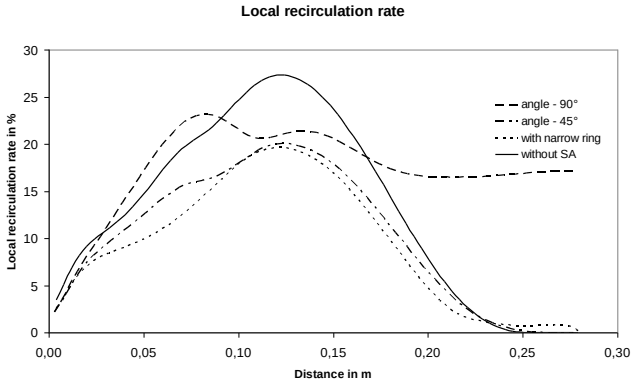

Figure 12. Local recirculation rate along the burner – geometry variation

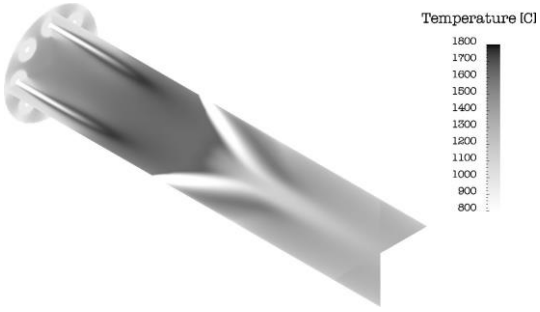

Figure 13. Temperature field; Geometry with the secondary air injection of 45°; λ_{red}=0,8

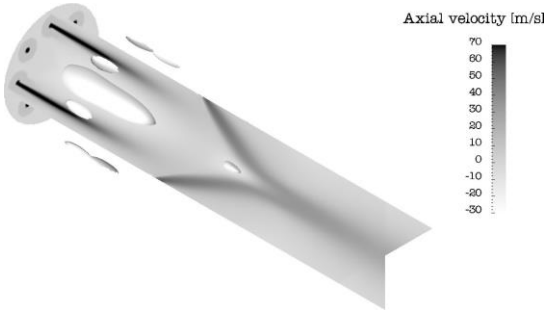

Figure 14. Velocity field; Geometry with the secondary air injection of 45°; λ_{red}=0,8; Isosurface -8 m/s

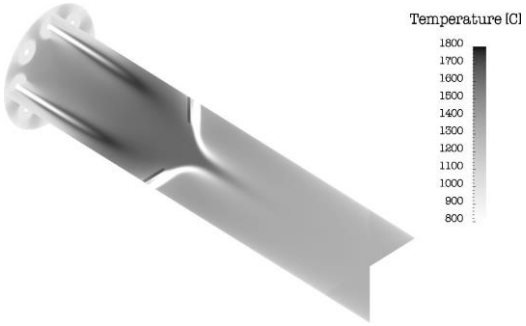

Figure 15. Temperature field; Geometry with orifice;λ_{red}=0,8

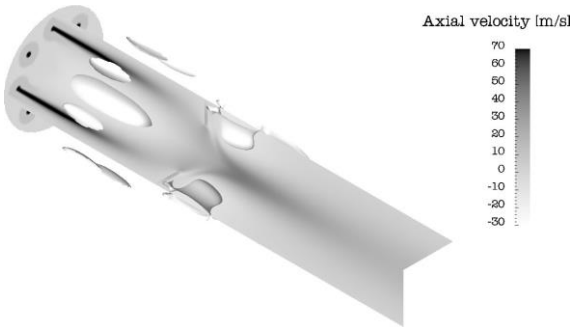

Figure 16. Velocity field; Geometry with orifice;λ_{red}=0,8; Isosurface -8 m/s

6 CONCLUSIONS

The integration of the FLOX®-burner brings several advantages compared to the configuration without the burner:

- A better burnout of the LCV gases is reached by a better mixing of the gases within the combustion zone.
- The burner can be operated at a low excess oxygen content that results in a higher efficiency compared to the original set-up.
- The combustion chamber of the FLOX®-burner is much smaller due to the better mixing and burn-out of the LCV gases that reduce investment costs.

Still one objective, the reduction of NOx emissions, is not achieved yet. Although there is less experience with the combustion of residues of flour and oil mills NOx emissions are still on an unacceptable high level. The tests have shown that an unstaged FLOX-burner indeed reduces thermal NOx emissions but the conversion of fuel nitrogen is even enhanced by the conditions within the FLOX-burner. For that a further NOx reduction technology has to be applied when fuel-N rich fuels are burned. The analysis of the LCV gas showed very high concentrations of NO-precursors such as NH_3 and HCN as well as high concentrations of NO already created in the gasifier. These compounds can be reduced to N_2 in substoichiometric regions created in the burner. Such regions can be generated by air staging. Therefore, the further development of FLOX®-burners for LCV gases is focused on staged burners. An air-staged FLOX-FLOX burner is proposed and numerical simulations using the code "AIOLOS" were carried out to investigate the design of such a staged burner. A staged FLOX®-burner should not only ensure the best reducing conditions in the first substoichiometric zone, but also excellent mixing and complete combustion in the second oxidation zone of the burner. The influence of equivalence ratio on recirculation within the burner was investigated. To optimize the recirculation, modelling of two other geometry variations was conducted. The results show that recirculation strongly depends on air distribution between the two stages in the burner. Sucking of secondary air into the primary zone can occur when decreasing equivalence ratio in the first stage of the burner, Moreover, using the design without an orifice between the stages, mixing in the second stage is not sufficient. To minimize these problems other geometry designs were proposed. The geometry with the orifice between the two stages provides the best stability, mixing conditions as well as good recirculation in both stages.

ACKNOWLEDGMENTS

The research activities were funded by the European Commission within the 6th framework programme under contract number SES6-CT-2003-502812. Sincere thanks are given.

REFERENCES

[1] www.eu-projects.de

[2] Schuster A., Berger R., Scheffknecht G., Utilisation of Solid Bio-Residues in a New Combustion System Applying Flameless Oxidation, 14th European Biomass Conference & Exhibition, Paris (France), 2005

[3] Berger R., Golec T., Schuster A., New Burner Systems for Low Calorific Value Gases Integrated with Pre-Gasifiers, 10th International Conference on Boiler Technology, Prace IMiUE Politechniki Slaskiej, 2006

[4] Schnell U., Progress in computational fluid dynamics, 1(4):208-218, 2001

[5] Foertsch D., A Kinetic Model of Pulverised Coal Combustion for Computational Fluid Dynamics, Ph.D. thesis, IVD, Universität Stuttgart, 2002

[6] Kim, J.P.; Schnell, U.; Scheffknecht, G.: Numerical Modelling of Flameless Combustion for Natural Gas. 7th European Conference on Industrial Furnaces Boilers (INFUB), Oporto (Portugal), 2006, paper #79

2.3 Paper III: Experimental study on fuel-NO_x using synthetic gases

This paper was published in the proceedings of the 16th IFRF Members' Conference in Boston, United States of America, 2009.

Author's contribution to the paper:

- performance of the experimental work, interpretation of the results
- main author of the paper –writing, preparation of the data, data visualization and editorial work

16th IFRF Members' Conference

THE INFLUENCE OF THE GAS COMPOSITION ON AMMONIA-TO-NO_X CONVERSION DURING FLAMELESS COMBUSTION OF LOW CALORIFIC VALUE GASES

M. Zieba, A. Schuster, G. Scheffknecht

Institute of Process Engineering and Power Plant Technology
University Stuttgart

Pfaffenwaldring 23, 70569 Stuttgart
GERMANY
zieba@ivd.uni-stuttgart.de

ABSTRACT

Flameless oxidation (FLOX®) technology has already demonstrated great potential in reducing thermal NO_x while burning natural gas [1-3]. However, the tests with biogenous fuels have shown a limited ability to reduce NO_x, where most of the NO_x emissions are related to the fuel-bond nitrogen [4,5].

During the gasification process, the nitrogen contained in the solid fuel is partly released to the product gases as ammonia (NH_3) or hydrogen cyanide (HCN). These compounds are partly converted to NO_x in the combustion processes. In this paper, the influence of the gas composition on the fuel nitrogen conversion (simulated by ammonia addition) to nitric oxide was investigated. Synthetic gases with different methane concentrations and CO/H_2 concentration ratios were doped with ammonia and burned in flameless mode. The concentration of ammonia, related to the total pre-combustion mixture (fuel gas and air), was the same for all experiments.

The NO_x emissions were measured and conversion ratios of ammonia to NO_x were determined. The results showed that the gas composition has a significant influence on the conversion of ammonia to NO_x. In particular, the methane content influences the ammonia-to-NO_x conversion. The lowest NO_x emissions and therefore the lowest conversion ratios were measured while burning methane-free gas. An increase of methane concentration in the gas corresponded to a rapid increase in the conversion ratios. The CO/H_2 content ratio had a minor influence on the conversion of ammonia to NO_x.

1 INTRODUCTION

Flameless oxidation (FLOX®) is a one of the most rapidly developing technologies in the last twenty years. This technology is based on the strong flue gas recirculation in the combustion zone created by the high momentum of the injected air. The stability of the combustion process without any flame stabilisation and the very good mixing conditions are big advantages of this technology. Flameless oxidation technology has already demonstrated great potential in reducing thermal nitrogen oxides (NO_x) while burning natural gas. The high internal recirculation of the hot flue gases dilutes the pre-combustion mixture and therefore reduces the high temperature peaks in combustion zone. This fact leads to significant reduction of thermal NO_x. Therefore, this technology can also be easily combined with the heat recovery (air preheating) which leads to significant reduction of fuel consumption and thus CO_2 emissions with very low thermal NO_x emission.

FLOX® technology has also been adapted to burn Low Calorific Value gases (LCV) generated by the biomass gasification [4,5]. Due to the high stability of the combustion process, LCV gaseous fuel even with a varying composition can be burned without adjustments of the burner and problems related to the flame instabilities. However, the tests

with different syngases generated by the biomass gasification, shows a limited ability to reduce NO_x emissions [4] while burning nitrogen-rich biofuels in FLOX® mode.
During gasification of biomass, the nitrogen contained in the solid fuel is partly released to the product gases as ammonia (NH_3) or hydrogen cyanide (HCN) [6,7]. During combustion of such gases, the nitrogen containing species may be oxidized to NO_x or reduced to N_2. The selectivity of this process depends on the gas composition, temperature and mixing of the reactants. Therefore, the final fuel NO_x emission depends on the nitrogen content in the biogenous fuel, gasification process and finally on the subsequent combustion process parameters.
Schuster et al. [8] investigated the formation of fuel nitrogen oxides during flameless combustion. The tested synthetic gas mixtures were supplied by mixing station that allows mixing CO, CO_2, CH_4, H_2 and N_2. In order to investigate the fuel nitrogen conversion, ammonia at different concentrations were added to the fuel stream. The compositions of the selected fuels are presented in Table 1.

		NG	MFG	MCG
CH_4	*vol-%*	95.6	-	6.5
C_2H_6	*vol-%*	2.4	-	-
H_2	*vol-%*	-	25.0	8.6
CO	*vol-%*	-	18.0	8.8
CO_2	*vol-%*	0.4	15.0	15.6
N_2	*vol-%*	1.6	42.0	60.5
LCV	*MJ/m^3stp*	36.1	5.0	4.4

Table 1 Composition of the selected gases

A compilation of the results are shown in Figure 1. The results of Schuster et al. showed that for all tests an increase of nitrogen oxides emissions were observed with increasing content of ammonia. Moreover, in the cases of natural gas (NG) and methane-containing syngas (MCG) the conversion of NH_3 to NO_x was found to be similar and relatively high. In contrast, the NO_x emission while burning methane-free gas (MFG) was significantly lower. It is an indication that the ammonia chemistry in flameless combustion is strongly influenced by the composition of the fuel gas, particularly with respect to the hydrocarbon content in the fuel.

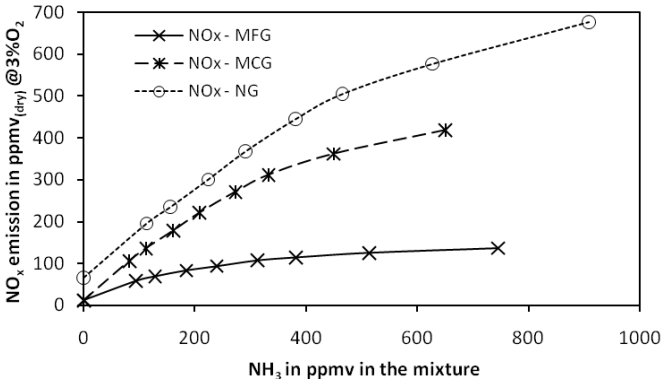

Figure 1 NO_x concentration in the flue gas for three different gases as a function of ammonia concentration in the pre-combustion mixture (fuel and combustion air)

Therefore, the main goal of this paper is the detailed investigation of the influence of gas composition (CO, H_2 and CH_4) and combustion process parameters on ammonia-to-NO_x conversion.

2 EXPERIMENTAL FACILITY AND TEST CONDITIONS

In the following chapter the burner test rig for the experimental investigations, the methodology of the investigation including the characterization of the tested fuels as well as the applied analysis methods are described.

2.1 Experimental facility – 20 kW FLOX®- burner

The experiments were performed using a 20 kW FLOX®- burner. The burner had been originally developed for natural gas and was subsequently modified to combust low calorific value gases. The test rig is shown in Figure 2

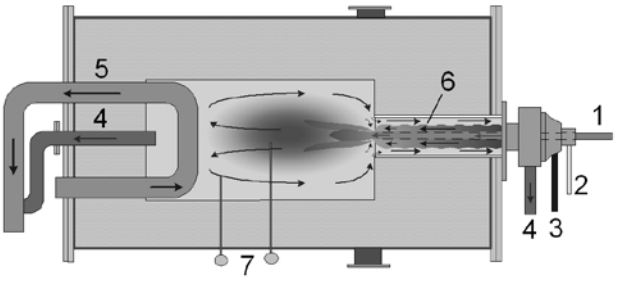

Figure 2 Scheme of FLOX®-burner test rig (1 – LCV gas with ammonia, 2 – natural gas, 3 – combustion air, 4 – flue gas, 5 – cooling, 6 – recuperator pipe, 7 – thermocouples)

The combustion chamber is heated up in flame mode up to 850ºC using natural gas (2). Above this temperature the burner can be switched to flameless mode and fired with ammonia doped LCV gas (1). The combustion air is preheated while flowing through the ceramic recuperator pipe (6). The temperature of the combustion chamber can be controlled using the air-cooled pipe (5).

The low calorific value fuels used in these experiments were prepared using a mixing station which allows mixing of CH_4, CO_2, CO, H_2 and N_2. Each component of the reactant gases was controlled by digital mass flow controllers, mixed evenly by a mixer and supplied to the reactor at room temperature. Additionally ammonia/argon mixture was introduced to the fuel stream to simulate the fuel related nitrogen oxides precursors. The amount of the NH_3/Ar mixture was controlled by a digital mass flow controller as well.

2.2 Fuel characterisation

As indicated by the fuel compositions summarized in Table 2 [9-12], CO and H_2 are the main combustible components in the biomass-gasified fuels produced in air blown and oxygen-blown gasifiers. The amount of CH_4 was relatively small. The lower heating values varied from 4 MJ/m^3 stp by the air-blown gasifiers, up to ca 9 MJ/m^3 stp by the oxygen- blown gasifiers.

Gasifier type		**Air-blown gasifier**				**Oxygen blown gasifier**
		2-stage gasifier (Viking)	Fluidised bed (Umsicht)	Circulating fluidised bed (Termiska)	Fluidised- bed (CFB-ECN)	Entrained flow (Carbo-V)
Composition						
H_2	*vol-%*	30.5	15.5	7.0 – 9.0	7.0	40.2
CO	*vol-%*	19.6	20.0	9.0 – 13.0	12.0	39.2
CH_4	*vol-%*	1.2	3.3	6.0 – 9.0	3.2	0.1
CO_2	*vol-%*	15.4	17.8	12.0-14.0	15.5	20.4
LHV	*MJ/m^{3}stp*	5.6	4.0 – 4.5	4.0 – 7.0	5.5	9.3

Table 2 Typical gas composition produced from biomass gasification

In the present studies CO and H_2 were also the main combustible components in the tested synthetic fuels. To cover the whole range of different gas compositions presented in Table 2, three synthetic gases with CO/H_2 ratios of 0.5, 0.7 and 1.5 were investigated. For each of the CO/H_2 ratio, methane content was varied between 0 and 10 vol-% to examine the effect of CH_4 in low concentration on the ammonia-to-NO_x conversion during flameless combustion. The CO_2 concentration was assumed to be 15 vol-% for all experiments. The ammonia was introduced to the fuel using 9.15 vol-% NH_3/Ar gaseous mixture. All the experiments input data are presented in Table 3.

	CO/H_2 Ratio	**CO**	**H_2**	**CO_2**	**CH_4**	**LHV**	**NH_3 in fuel**	**NH_3 in pre-combustion mixture**
	[-]	*vol-%*	*vol-%*	*vol-%*	*vol-%*	*MJ/m^{3}stp.*	*[ppmv]*	*[ppmv]*
Gas 1	0.5	18	36	15	0-10	6.16-9.74	2020-2974	700
Gas 2	0.7	18	25	15	0-10	4.97-8.55	1754-2713	700
Gas 3	1.5	27	18	15	0-10	5.35-8.93	1803-2761	700

Table 3 Composition of the synthetic gas mixtures used in the experiments

The experiments were carried out at the same power input of 18 kW. The CO and H_2 concentration was kept constant. Therefore, increasing the methane content, the lower heating value of the gas was also increasing. The concentration of ammonia was assumed to be 700 ppmv for all tested gases. The concentration of ammonia was related to the pre-combustion mixture of the fuel and the combustion air to ensure the same partial pressure of ammonia for every CO/H_2 ratio and methane concentration.

2.3 Analysis methods

Each flue gas component, such as NO, NO_2, NO_x, O_2, CO, CO_2 was continuously measured by the gas analyzer at the reactor exit. The ammonia-to-NO_x conversion ratio was calculated according to the following equation:

$$CR_{NH3\rightarrow NOx} = \frac{[NO_x]_{fluegas} \cdot \frac{\dot{V}_{N,fluegas}}{V_M}}{[NH_3]_{fuel} \cdot \frac{\dot{V}_{N,fuel}}{V_M}} \qquad (1)$$

where $[NO_x]_{fluegas}$ is the concentration of the total NO_x measured in flue gas, $[NH_3]_{fuel}$ is the calculated concentration of ammonia in the fuel, $\dot{V}_{N,fluegas}$ is the calculated amount of the flue gas, V_M is the molar volume of the substance at normal conditions.

It has to be mentioned that the total NO_x measured in the flue gas originates not only from the ammonia added to the fuel stream. A part of the total NO_x in the flue gas can be formed from atmospheric nitrogen. However, by flameless combustion of low calorific value gases the part of the NO_x coming from other sources then ammonia is relatively small and therefore, neglected in this paper.

3 RESULTS AND DISSCUSION

The development and adaptation of the FLOX® technology for low calorific value gases allow ammonia behaviour comparison in gases varied significantly in the composition. The lower heating value of the fuels varies from 5 to 10 MJ/m^3 stp in this studies. Due to the burner flexibility and combustion stability, the comparison of ammonia conversion can be done under very similar conditions for all tested fuels. The high dilution of the reaction zone caused by the recirculation of hot flue gases significantly decreases the temperature peaks in the combustion chamber. Therefore, the combustion for all fuels used in these studies occurs at

very similar intermediate temperature conditions. Moreover, the hot recirculated gases include nitrogen oxides that influence the nitrogen chemistry in the flameless jet.
In the following chapter the influences of methane in low concentrations, CO/H_2 ratio, excess oxygen and process temperature on ammonia-to-NO_x conversion are presented. Moreover, the results were discussed in order to indicate the possible explanations for the observed phenomena.

3.1 Influence of methane content on NH_3-to-NO_x conversion by different CO/H_2 ratios

In order to examine the influence of CH_4 content in the fuel on the ammonia-to-NO_x conversion, experiments with varying methane content were conducted. All experiments were carried out at power input of 18 kW. The air ratio (λ) was assumed to be 1.5. Therefore, the amount of combustion air was adjusted for every tested CO/H_2 ratio and methane concentration. The temperature of the combustion chamber was approximately the same for all experiments. However, when increasing the methane content the temperature was slightly changing in the range of 960 °C to 980 °C.
Figure 3 shows the NO_x concentration in the flue gas for three different CO/H_2 ratios as a function of methane concentration in the fuel.

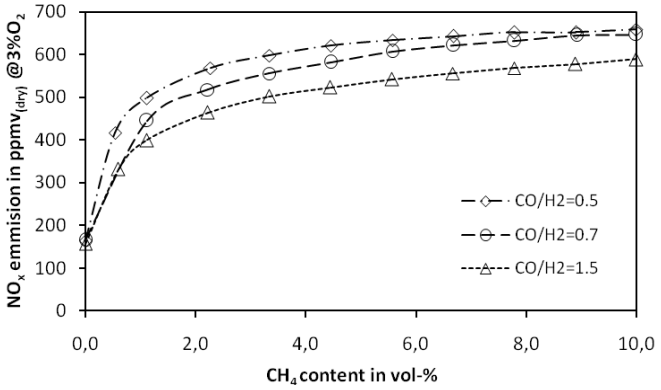

Figure 3 NO_x concentration in the flue gas for three different CO/H_2 as a function of methane concentration in the fuel; (T=970 °C, λ=1.5, P=18 kW)

For all tested CO/H_2 ratios the NO_x emissions were about 150 $ppmv_{(dry),}$ when no methane was added to the fuel . Increasing the methane content from 0 to ca. 6 vol-%, the concentration of NO_x in the flue gas was rising rapidly. Further increase above 6 vol-% of methane content had only minor influence on the NO_x emissions. At concentration of 10 vol-% the emissions reached the maximum observed values. Moreover, the emission of NO_x was increasing with decreasing CO/H_2 ratio. However, this effect was observed rather due to changing content of water vapour when varying CO/H_2 ratio. The dry flue gas volume gets lower due to increasing H_2 content in the fuel.

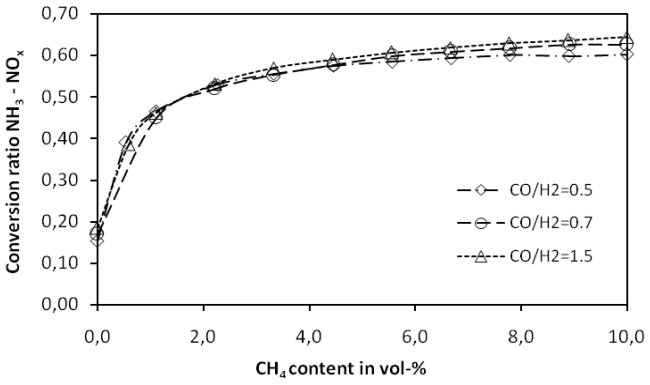

Figure 4 Ammonia-to-NO_x conversion ratio for three ratios as a function of methane concentration in the fuel; (T=970 °C, λ=1.5, P=18 kW)

Figure 4 shows the ammonia-to-NO_x conversion ratio as a function of methane concentration in the fuel. The conversion ratio was similar in all cases. The investigated CO/H_2 ratios had no significant influence on ammonia-to-NO_x conversion ratio. Varying the methane concentration, the conversion ratios were increasing from ca. 0.16 for methane-free mixtures to above 0.6, when 10 vol-% of methane was present in the fuel.
There are a few possible explanations reported in the literature for the observed phenomena.
Choudhuri et al. [13] have studied the combustion characteristics of hydrogen-hydrocarbon hybrid fuels. They reported that the presence of hydrocarbons in the fuel causes significant decrease of the mixture reactivity, which ultimately increases the ignition time.
Since the ignition delay depends on the fuel composition, the high velocity of the jet and the strong recirculation, characteristic for flameless combustion, can lead to crucial change of local air ratio at which the mixture ignites and the ammonia decompose. The longer ignition delay the higher amount of air and recirculated gases are mixed with the fuel in the jet when igniting. Since the ignition zone is not stabilized in the flameless combustor, it can significantly influence the ammonia-to-NO_x conversion. Moreover, the recirculated flue gas contains a significant amount of nitrogen oxides. Frassoldati et al. [14] have studied the combustion of carbon monoxide/hydrogen mixtures. They reported that the addition of NO can inhibits the reactivity of the system under stoichiometric and particular under fuel rich conditions, as a consequence of the growing importance of chain-termination reactions involving NO.
In the case of methane-free gas, due to the high reactivity of the fuel, the ammonia can decompose directly after the burner nozzle under fuel reach conditions. The hydrogen present in the fuel in high concentration oxidizes releasing high amounts of radicals such as H, OH and O. A part of these radicals reacts with the CO. Skreiberg et al. [15] investigated the ammonia chemistry below 1400 K under fuel-rich conditions in a flow reactor. They reported that the ammonia can decompose even at very high CO concentration. They observed that the carbon monoxide is oxidized almost exclusively through the reaction with OH radicals.
The hydrogen and oxygen radicals, formed during the H_2 and CO oxidation reactions, are than available for oxidation of ammonia. In the same work [15] it was observed that methane in relatively low concentrations, comparing to ammonia, can strongly inhibit the ammonia conversion under fuel-rich conditions.
Increasing the methane content in the fuel, ammonia and methane can start to compete for the same radicals occurring in the flameless jet. Therefore, the decomposition of ammonia can be delayed and shifted toward the fuel lean-side of the jet, thus increasing the conversion of ammonia to NO_x.

3.2 Influence of the air ratio and temperature on NH_3-to-NO_x conversion by varying methane content

In order to investigate the influence of the air ratio on the NO_x emissions, ammonia doped fuel with CO/H_2 ratio of 0.7 and varying methane concentration was burned with two different air ratios (λ) of 1.3 and 1.6. The methane content was varied between 0 and 4.5 vol-%. Figure 5 shows the NO_x emissions obtained in these experiments. The tests were carried out at 970 °C and the power input of 18 kW. Similar to the previous experiments the NO_x emissions were increasing with methane content in the fuel for both investigated air ratios. However, for methane-free mixtures the air ratio had a minor influence on the NO_x emissions. The ammonia-to-NO_x conversion ratio, presented in Figure 6, was similar for both air ratios for methane-free gas. Increasing the methane content in the fuel, the influence of air ratio was slightly growing.
The same experiments were additionally carried out at 900 °C to investigate the influence of the operating temperature on the NO_x emissions. The results are shown in Fugure 7. Both of the measurements for λ=1.3 and 1.6 shows similar results for the tested temperatures. The temperature difference was too small to observe any major differences in ammonia-to-NO_x conversion. However, the investigation under higher operating temperature was limited by the low calorific values of the tested fuels. The lower operating temperature was limited by the minimal required temperature of the combustion chamber for flameless combustion.

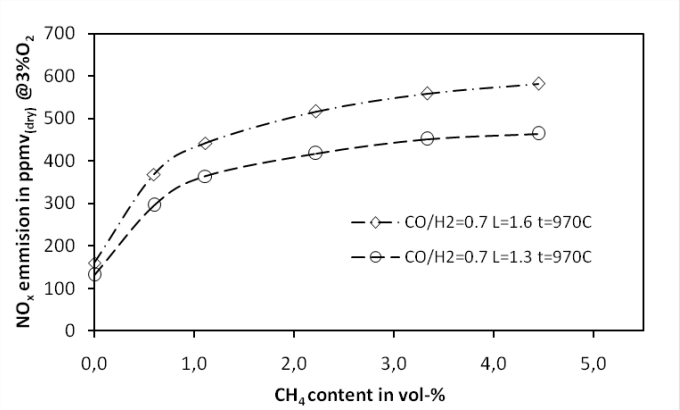

Figure 5 NO_x concentration in the flue gas for CO/H_2=0.7 and λ=1.3 and 1.6 as a function of methane concentration in the fuel; (T=970 ºC, P=18 kW)

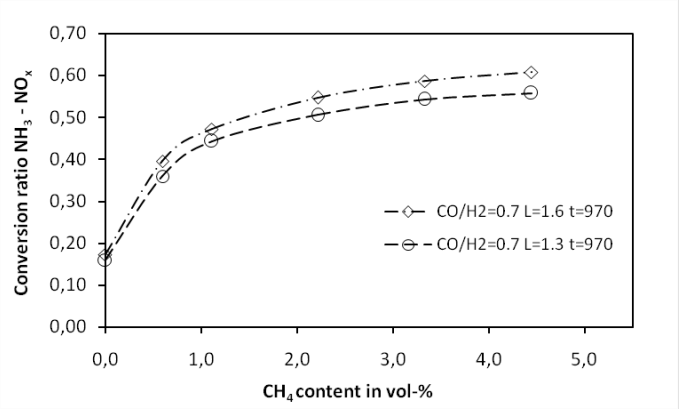

Figure 6 Ammonia-to-NO_x conversion ratio for CO/H_2=0.7 and λ=1.3 and 1.6 as a function of methane concentration in the fuel; (T=970 ºC, P=18 kW)

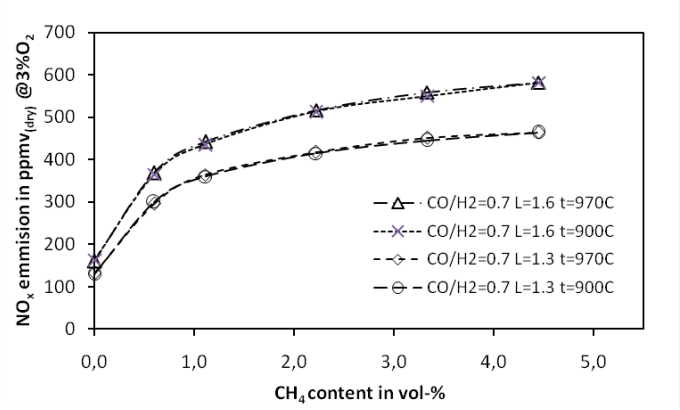

Figure 7 NO_x concentration in the flue gas for CO/H_2=0.7 and λ=1.3 and 1.6 as a function of methane concentration in the fuel; (T=970 ºC and 900 ºC, P=18 kW)

4 CONCLUSIONS

The present studies show the influence of the fuel composition on ammonia-to-NO_x conversion during flameless combustion of low calorific value gases. Depending on the gas composition, there can be a large difference in the conversion of NH_3 to NO_x. In particular, the methane content influences the ammonia-to-NO_x conversion. The lowest NO_x emissions and therefore the lowest conversion ratios were measured while burning methane-free gas. Increasing the methane content from 0 to ca. 6 vol-%, the concentration of NO_x in the flue gas was rising rapidly. Further increase above 6 vol-% of methane content had smaller influence

on the NO_x emissions. The tested CO/H_2 ratios in fuel had a minor influence on the conversion of ammonia to NO_x. Higher air ratio enhanced the emission of NO_x. The influence of the stoichiometry was growing with the methane content in the fuel.

5 REFERENCES

[1] J.A. Wünning and J.G. Wünning, Prog. Energy Combust. Sci. 23, p.81–94, (1997)

[2] C. Galletti, A. Parente, L. Tognotti, Combust. Flame 151, p. 649-664, (2007)

[3] A. Cavaliere, M. de Joannon, Prog. Energy Combust. Sci. 30, p. 329-366, (2004)

[4] A. Schuster, M. Zieba, J. G. Wünning, G. Scheffknecht, "Optimisation of conventional biomass combustion system by applying flameless oxidation", 15th IFRF Members' Conference, Pisa, 2007

[5] A. Schuster, M. Zieba, G. Scheffknecht, J. G. Wünning, "Application of FLOX® Technology for the utilisation of low-grade biofuels", Proceedings of 15th European Biomass Conference, Berlin, Germany, p. 1703-1706, 2007

[6] J. Leppälahti, T. Koljonen, Fuel Proc. Tech. 43, p. 1-45, (1995)

[7] M. Becidan, Ø. Skreiberg, J.E. Hustad, Energy and Fuels 21, p. 1173-1180, (2007)

[8] A. Schuster, S. Erhardt, G. Scheffknecht, J. G. Wünning, "Conversion of Amonnia to NO_x for flameless oxidation of low calorific value gas", 7th High Temperature Air Combustion and Gasification International Symposium, 13-16 January 2008, Phuket, Thailand

[9] A. van der Drift, J. Van Doorn, J. W. Vermeulen, Biomass Energy 20, p. 43-56, (2001)

[10] J. P. Ciferno, J. J. Marano, "Benchmarking Biomass Gasification Technologies for Fuels, Chemicals and Hydrogen Production", Final Report, DOE Contract No. DE-AM26-99FT40575, June 2002

[11] M. Bolhar-Nordenkampf, R. Berger, "Analyse und Evaluirung der Thermo-Chemischen Vergasung von Biomasse", Landwirtschaftsverlag, Münster, 2006

[12] www.bgg.mek.dtu.dk

[13] A. R. Choudhuri, S. R. Gollahalli, Int. J. Hydrogen Energy 28, p 445 - 454, (2003)

[14] A. Frassoldati, T. Faravelli, E. Ranzi, Int. J. Hydrogen Energy 32, p. 3471-3485 (2007)

[15] Ø. Skreiberg, P. Kilpinen, P. Glarborg, Combust. Flame 136 p. 501-518 (2004)

2.4 Paper IV: Experimental study on NO_x using gasifier product gases

Title: The Fate of Ammonia and Hydrogen Cyanide during Flameless Combustion of Low Calorific Value Gases

This paper was reviewed and subsequently published in 2012 in:
International Journal of Thermodynamics (IJoT)
doi: 10.5541/ijot.313

Author's contribution to the paper:

- performance of the experimental work, interpretation of the results
- main author of the paper –writing, preparation of the data, data visualization and editorial work

International Journal of Thermodynamics (IJoT)
ISSN 1301-9724 / e-ISSN 2146-1511
www.ijoticat.com

Vol. 15 (No. 1), pp. 35-41, 2012
doi: 10.5541/ijot.313
Published online: Feb. 10, 2012

The Fate of Ammonia and Hydrogen Cyanide During Flameless Combustion of Low Calorific Value Gases*

Mariusz Zieba[a**], Mathias Fink[a], Anja Schuster[a], Günter Scheffknecht[a] and Roland Berger[b]

[a]Institute of Combustion and Power Plant Technology (IFK), University of Stuttgart, Germany
[b]e-flox GmbH, Renningen, Germany
E-mail: mariusz.zieba@ifk.uni-stuttgart.de

Abstract

In this paper, a review of the experimental investigations on the fuel-NO_x formation during flameless combustion is presented. The first series of experiments described in the paper were conducted using ammonia doped synthetic gases with different compositions. During these experiments, the influence of gas composition on the conversion of ammonia (NH_3) to NO_x is investigated. The second series of experiments were conducted using product gas generated in a fluidized bed gasifier. These results show the dependencies between the gasifier operating parameters, product gas composition and final NO_x emissions. Moreover, the concentrations of the ammonia and hydrogen cyanide (HCN) in the product gas were measured in order to calculate the conversion ratios of these compounds to NO_x. The results show the significant influence of the gas composition and the gasifier process parameters on the final NO_x emissions. In particular, the hydrocarbon content influences the ammonia to NO_x conversion. The lowest NO_x emissions and therefore the lowest conversion ratios were measured while burning gases with a low hydrocarbon content. An increase of the hydrocarbon concentration in the gas corresponded to a rapid increase in the conversion ratios.

Keywords: *Fuel-NO_x; Flameless Combustion*.

1. Introduction

The wide-ranging applicability of the Flameless oxidation (FLOX®) technology for the utilization of natural and low calorific value gases has already been proven and reported in the literature (Wünning at al.,1997; Galleti et al., 2007; Cavaliere et al., 2004). This technology became of interest due to its great potential in reducing thermal nitrogen oxides (thermal-NO_x) while burning natural gas. In addition to excellent burnout, the fact that fluctuations in the fuel composition do not lead to combustion instabilities is a reason for the high interest in combusting low calorific value gases (LCV) in flameless burners. However, the tests with biogenous gaseous fuels have shown a limited ability to reduce NO_x, where most of the NO_x emissions originate from the fuel-bound nitrogen (Schuster et al., 2007a, Schuster et al., 2007b). During the gasification processes, the nitrogen contained in the solid fuel is partly released to the product gases as ammonia (NH_3) or hydrogen cyanide (HCN). These compounds are formed as a result of thermal destruction of proteins and amino acids contained in the biomass (Leppälahti et al., 1995; Becidan et al., 2007). The NH_3 and HCN compounds are either converted to NO_x or reduced to neutral N_2 in the combustion process. The selectivity of this process depends on the gas composition, temperature and mixing of the reactants during combustion. In this paper, a review of the experimental investigations on the fuel-NO_x formation during flameless combustion is presented. The first series of experiments described in the paper were conducted using synthetic gases with different compositions. During these experiments, ammonia was added to the fuel stream in order to investigate the fuel nitrogen conversion. The aim of these experiments was to investigate the influence of the gas composition on the conversion of ammonia to NO_x. Moreover, experiments in which product gas generated in a bubbling fluidized bed (BFB) gasifier is subsequently combusted in a FLOX®-Burner are presented. Since the gasifier product gas composition depends on the gasification process parameters such as air ratio (AR) and temperature, the final NO_x concentration is also influenced by these factors. The aim of these experiments was to investigate the dependences between gasifier operating parameters, the product gas composition (combustibles, NH_3 and HCN concentration) and final NO_x emissions during flameless combustion of these gases.

2. Experimental

In this section the test rigs, the tested fuels as well as the analysis and measurement methods are presented.

2.1. Burner test rig

The experimental facility consists of a 20 kW FLOX®-Burner coupled either with the gas mixing unit during experiments with synthetic gases or with the fluidized bed gasifier during experiments with solid fuels. The burner shown in Figure 1 has been originally developed for natural gas and was subsequently modified to combust low calorific value gases. During start-up the combustion chamber is heated in flame mode up to 850 °C using natural gas. Above this temperature the burner can be switched to flameless mode and fired either with low calorific value gas prepared in the gas mixing unit or with product gas generated in the gasifier. The combustion air is preheated while passing through a ceramic recuperator pipe. The temperature of the combustion chamber is controlled using an air-cooled pipe. In flameless burners the preheated

This paper is an updated version of a paper published in the ECOS'10 proceedings. It is printed here with permission of the authors and organizers.
**Corresponding Author

combustion air is introduced separately to the fuel into the combustion chamber. The air velocity of about 70 to 100 m/s causes high internal recirculation of the hot flue gases. These hot products are partially mixed with the fuel and oxidizer before the mixture ignites. As a result, there is no identifiable flame front. The reactants are strongly diluted and the temperature field is homogeneous without high peaks (Wünning at al.,1997).

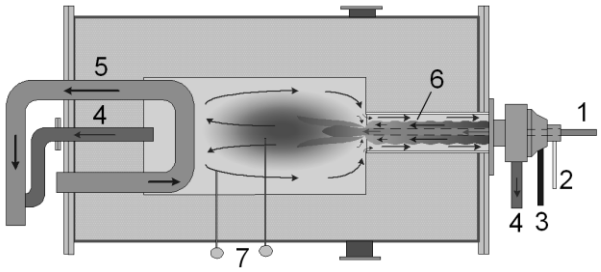

Figure 1. Scheme of FLOX®-Burner test rig (1 – natural gas or LCV gas with ammonia, 2 – natural gas, 3 – combustion air, 4 – flue gas, 5 – cooling pipe, 6 – recuperator pipe, 7 – thermocouples).

2.2. Gas mixing unit

The gas mixing unit, where the fuel gas is prepared, allows mixing of CH_4, CO, CO_2, H_2 and N_2. The flow of each gas is controlled by a digital mass flow controller. The gases were mixed and supplied to the burner at room temperature. Additionally, ammonia was introduced to the fuel stream to simulate the fuel nitrogen oxides precursors.

2.3. Bubbling Fluidised Bed (BFB) gasifier

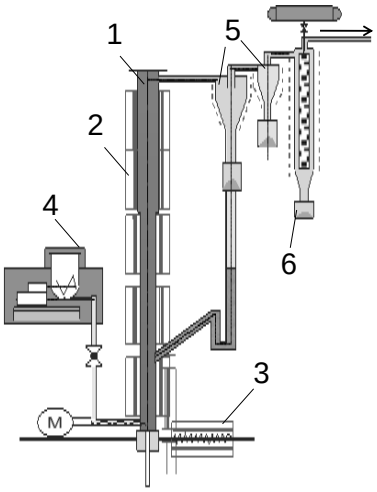

Figure 2. Scheme of BFB gasifier (1 –reactor tube, 2 – electrical heaters, 3 – air preheater, 4– fuel feeding unit, 5 – cyclones, 6 –candle filter).

The reactor shown in Figure 2 is made of high-temperature steel and is heated by five electrical heating zones which can be controlled separately. The heating zone at the bottom of the reactor vessel, where the bed material is fluidized and the biomass is fed has a heating capacity of 11 kW_{el}. Every other heating zone above has a heating capacity of 4 kW_{el}. The maximum heating zone temperature is 1000 °C, while the resulting maximum process temperature can be 950 °C. The fluidization air can be preheated up to 900 °C in a two zone electrical gas preheater. The absolute pressure in the BFB is controlled by a pressure control valve in the range of 0-100 mbar. The fuel feeding system is a screw feeder system where the fuel volume flow rate is controlled. The fuel rate can be set between 1 and maximum 7 kg/h depending on the type of fuel used. The product gas exits the reactor vessel and proceeds to two electrically heated cyclones connected in series, followed by a candle filter. As a result, dragged particles like ashes, char and bed material are removed. After the candle filter, a part of the product gas is led through a suction point to gas analysis. The main part of the product gas is led via a stainless steel pipe heated to 350 °C to the FLOX®-Burner.

2.4. Fuel composition – experiments with synthetic gases

During typical air gasification the main combustible components in the product gas are carbon monoxide and hydrogen. The amount of methane and higher hydrocarbons is usually relatively small. However, the composition of the gasification product gas depends on the solid fuel used, gasifier operating parameters and gasifier type. During the experiments with synthetic gases the composition of the investigated fuels is similar to the product gases from the gasification processes. In order to cover such a wide range of different gas compositions three synthetic gases with CO/H_2 ratios of 0.5, 0.7 and 1.5 were investigated. For each of the CO/H_2 ratios, the methane content was varied between 0 and 10 vol-% to investigate the influence of hydrocarbons on the ammonia to NO_x conversion. The concentration of CO and H_2 was kept constant for each CO/H_2 ratio. Therefore, increasing the methane content in the mixture led to a decrease in nitrogen (N_2) concentration and an increase in lower heating value of the fuel. The ammonia concentration of 700 ppmv was constant for all experiments. This concentration is related to the total mixture of fuel and combustion air to ensure the same ammonia partial pressure for each mixture. All of the mentioned experiments were carried out at the same power input of 18 kW. The compositions of the tested synthetic fuels are summarized in Table 1.

Table 1. Composition and lower heating value (LHV) of the synthetic fuels.

		Gas 1	Gas 2	Gas 3
CO	(vol-%)	18	18	27
H_2	(vol-%)	16	25	18
CO_2	(vol-%)	15	15	15
CH_4	(vol-%)	0-10	0-10	0-10
CO/H_2	(-)	0.5	0.7	1.5
LHV	(MJ/m^3_{stp})	6.2-9.7	5.0-8.5	5.4-8.9
NH_3	(ppmv)	700	700	700

2.5. Solid fuel composition and gasifier settings – experiments using BFB gasifier

In the second series of experiments the flameless burner was fired using product gas from the gasifier. Wood pellets and rape cake pellets were used as a fuel for the tests. During the experiments air was used as a gasification agent. The characteristics of the solid fuels are given in Table 2.

The rape cake pellets were chosen due to the high nitrogen content in the fuel. Both of the presented fuels were gasified under two different temperatures and gasifier air ratios. All experimental conditions are presented in Table 3.

Table 2. Characteristics of the tested biomass.

		Wood pellets	Rape cake pellets
Moisture	(wt-% ar)	7.36	8.10
Ash	(wt-% ar)	0.54	5.94
C	(wt-% ar)	46.43	45.00
H	(wt-% ar)	5.77	6.67
N	(wt-% ar)	<0.3	4.98
S	(wt-% ar)	<0.3	0.48
LHV	(MJ/kg dm)	20.20	17.76

Table 3. Gasifier operating parameters.

Fuel	Gasification parameters	
	T (°C)	Air Ratio
Wood pellets	750	0.15
		0.22
	875	0.15
		0.22
Rape cake pellets	750	0.22
	875	0.22

2.6. Analysis and measurement methods

In order to evaluate the fuel-N conversion ratios to NO_x the following equation was applied

$$CR_{N\rightarrow NOx} = \frac{[NO_x]_{fluegas} \cdot \dot{V}_{fluegas}}{[N]_{fuel} \cdot \dot{V}_{fuel}}, \quad (1)$$

where: $[NO_x]_{fluegas}$ - NO_x concentration in the flue gas in $ppmv_{dry}$, $[N]_{fuel}$ - concentration of NH_3 and HCN in the fuel in $ppmv_{dry}$, $\dot{V}_{fluegas}$ - flue gas flow in m^3_{stp}/h, $\dot{V}_{fuel}$ - fuel flow in m^3_{stp}/h. During all tests the exhaust gas was continuously sampled and analysed at the combustion chamber exit with respect to O_2, CO_2, CO, NO, NO_2 and NO_x. During the experiments in which the burner was coupled with the gasifier the product gas was analyzed continuously with respect to CO, CO_2, CH_4, H_2 and O_2. Moreover, a gas chromatograph was used to determine the content of ethene (C_2H_4), ethane (C_2H_6) and propene (C_3H_6). The ammonia and hydrogen cyanide concentrations in the product gas were measured in order to investigate the dependencies between gasifier operating parameters, product gas composition (combustibles, NH_3 and HCN concentration) and final NO_x emission during flameless combustion of these gases. The concentration of ammonia and hydrogen cyanide was measured using the wet chemistry method. The product gas was sampled in the vicinity of the burner inlet. The gas sampling pipe was heated up to 350 °C to avoid ammonia and tar condensation. The gas was flowing through a heated filter and was led to three impinger bottles placed in an ice bath. A 0.01 M H_2SO_4 solution was used for ammonia and a 2 M NaOH solution was used for hydrogen cyanide absorption. The gas flow, temperature, pressure and oxygen concentration in the gas was measured to ensure high quality of the sampling. The content of NH_3 and HCN in the solutions was afterwards analysed according to DIN38406, (1983) and DIN38405, (1981). For each gasifier setting two gas samples were collected. The content of NH_3 and HCN is given as an average value of the analysed samples.

3. Results

In this section the experimental results achieved using ammonia doped synthetic gases and product gases generated in the BFB gasifier are presented.

3.1. NOx emission during NH3 doped synthetic gas combustion

In order to investigate the dependencies between hydrocarbon concentrations in the fuel and fuel nitrogen to NO_x conversion, experiments with a varying methane content were conducted. The air ratio was set to 1.5. Since the high dilution of the reaction zone caused by the internal recirculation of the hot flue gases significantly decreases the temperature peaks in the chamber, the combustion of all tested fuel mixtures occurs at a very similar and homogeneous temperature. When increasing the methane content the temperature was slightly changing in the range of 960 to 980 ºC. However, such small temperature differences do not have a considerable influence on ammonia to NO_x conversion ratios (Zieba et al., 2009b). Figure 3 shows the NO_x concentration in the flue gas for three different CO/H_2 ratios as a function of methane concentration in the fuel. A rapid increase of NO_x emissions can already be observed at the lowest investigated methane concentrations of about 1vol-%. At the methane concentration of approx. 2 vol-% the slope of the trend curve decreases. However, the NO_x emissions increase with increasing methane concentration across the whole investigated range. The measured NO_x emissions are higher in gases with a lower CO/H_2 ratio.

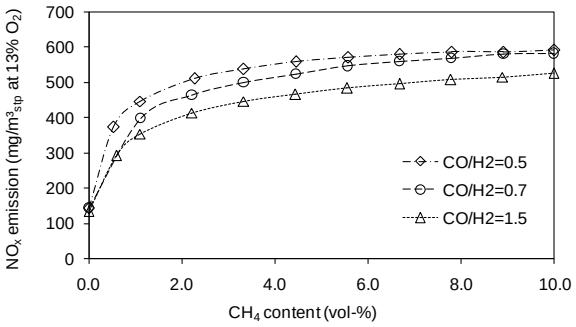

Figure 3. NO_x concentration in the flue gas as a function of methane concentration in the fuel; (t_{comb}=970 °C, AR=1.5).

Figure 4 presents the calculated ammonia to NO_x conversion ratios. The results show that the investigated CO/H_2 ratios had no significant influence on the conversion ratios. The higher NO_x emissions by lower CO/H_2 ratios were observed due to the changing content of water vapour in the flue gas resulting from the hydrogen oxidation. Varying the methane concentration, the conversion ratios increase from about 0.16 for methane-free mixtures to above 0.6, when 10 vol-% of methane was present in the fuel.

In order to investigate the influence of the burner air ratio on the NO_x emissions, ammonia doped fuel with a CO/H_2 ratio of 0.7 and varying methane concentration was burned at two different air ratios of 1.3 and 1.6. The methane content was varied between 0 and 4.5 vol-%. Figure 5 shows the NO_x emissions obtained in these experiments. The tests were carried out at 970 °C, with a

power input of 18 kW. Similar to the previous experiments the NO_x emissions increased with increasing methane content in the fuel for both investigated air ratios. However, for methane-free mixtures the air ratio had a minor influence on the NO_x emissions. Increasing the methane content in the fuel saw the influence of burner air ratio slightly increase.

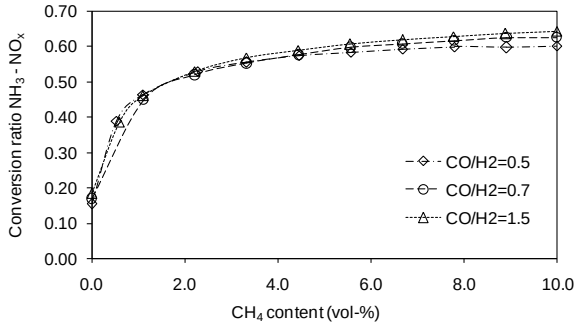

Figure 4. Ammonia to NO_x conversion ratio as a function of methane concentration in the fuel; (t_{comb}=970 °C, AR=1.5).

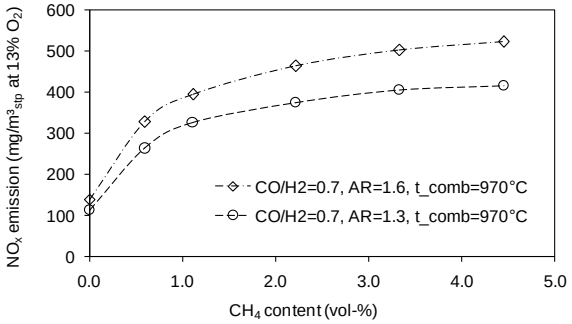

Figure 5. NO_x concentration in the flue gas as a function of methane concentration in the fuel; (t_{comb}=970 °C,).

3.2. NO_x emission during flameless combustion of product gases generated in the BFB gasifier

In order to investigate if similar dependencies described in Section 3.1 can also be observed using product gases generated from biomass gasification, a series of experiments using wood pellets and rape cake pellets as a gasifier feedstock were conducted. The product gas generated in the gasifier was subsequently combusted using the flameless burner. During the experiments the product gas composition, including NH_3, HCN and the flue gas composition were measured simultaneously. The composition of the product gas from gasification process can not be as precisely controlled as synthetic gas from a mixing unit. Therefore, to influence the product gas composition the solid bio-fuels were gasified at 750 °C and 875 °C with an air ratio of 0.15 and 0.22 in the case of wood pellets and 0.22 in the case of rape cake pellets.

Figure 6 shows the measured hydrocarbon concentrations for both fuels for all tested operating gasifier parameters. With a rising temperature and air ratio the total amount of hydrocarbons was similar and decreased slightly for both fuels. During the gasification of rape cake pellets much higher amounts of C_2H_4 were present in the product gas in comparison to wood pellets product gas. Higher gaseous hydrocarbons than C_3H_6 and tar were not measured.

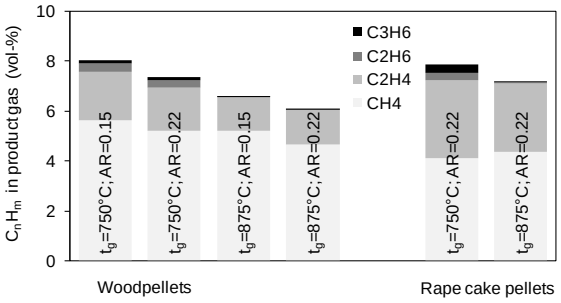

Figure 6. Hydrocarbon concentrations in the product gas during wood and rape cake pellets gasification.

3.2.1 Fuel-NO_x precursors and NO_x emission -wood pellets

The measurement results of fuel NO_x precursors obtained during wood pellets gasification are presented in Figure 7. Ammonia was the main nitrogen containing compound present in the gas. Its concentration increased with the gasifier temperature. The concentration of HCN behaves in a quite opposite manner as it decreases with increasing temperature. The influence of the gasifier air ratio was minor. However, the concentration of both of the fuel-NO_x precursors shows a tendency to increase with higher gasifier air ratio and temperature.

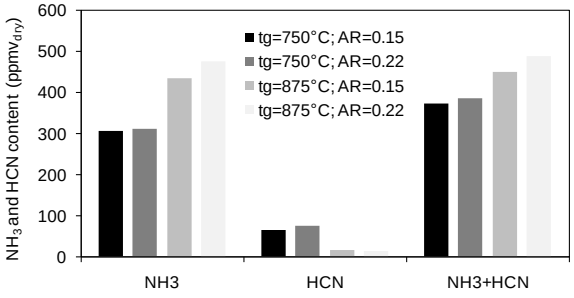

Figure 7. NH_3 and HCN concentrations in the wood pellets gasification product gas.

The product gases were combusted in the flameless burner at the average combustion chamber temperature of 1050 °C. Although the quality and quantity of the product gas was changing due to gasification process instabilities the combustion process was very stable. The amount of combustion air was varied, resulting in flue gas excess oxygen in the range between 1 to 8 vol-%. Complete combustion was first observed at 1.5 vol-% O_2 in the flue gas, much earlier than expected. By further decreasing excess oxygen, particularly below 1 vol-%, a rapid increase in CO emissions was measured. Figure 8a shows the NO_x emissions observed during the experiments. The black crosses represent NO_x emissions while burning product gas generated at a gasifier temperature of 750 °C, whereas the grey crosses show the emissions achieved at a gasifier temperature of 875 °C. The gasifier air ratio in both cases was 0.15. The NO_x emissions are plotted against the excess oxygen in the flue gas.

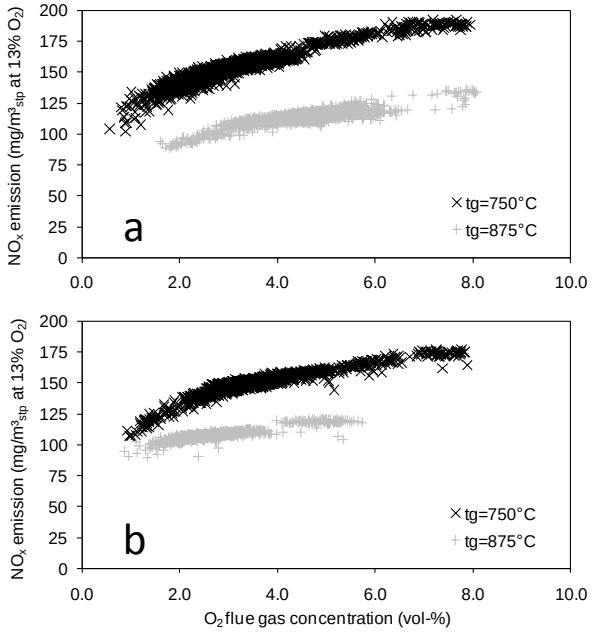

Figure 8. NO_x emission during product gas combustion from wood pellets gasification; a – gasification air ratio 0.15, b – gasification air ratio 0.22

Although, the NH_3 and HCN content in the product gas generated at 875 °C was higher, the emissions of NO_x are significantly lower. Due to lower hydrocarbon concentrations much less of nitrogen containing compounds in the product gas are converted to NO_x. Very similar results were observed for a higher gasifier air ratio. The results are presented in Figure 8b. Also in this case a higher NO_x emission level was measured during the combustion of product gases generated at a lower gasifier temperature, thus containing more hydrocarbons. Higher excess oxygen during combustion slightly enhanced the NO_x formation. The influence of the gasifier air ratio was minor. However with a higher amount of gasification air the emissions were slightly lower. The results also confirm that during combustion of gasifier product gases the content of hydrocarbons is crucial for the ammonia and hydrogen cyanide conversion ratios. The calculated conversion ratios for combustion of wood pellets are presented in Figure 9. The conversion ratio values higher than one indicate that a certain percentage of NO_x emissions are not originating from the fuel nitrogen. It can be assumed that this part of NO_x emissions is a thermal-NO_x which mostly depends on the temperature and its contribution to the total NO_x emissions is the same for all tested conditions and fuels. Since the exact amount of the thermal part of NO_x is unknown it could not be extracted from the total NO_x emissions.

3.2.2 Fuel-NO_x precursors and NO_x emission –rape cake pellets

Contrary to wood pellets the rape cake pellets contain a high amount of fuel-bound nitrogen. Therefore, high concentrations of fuel-NO_x precursors in the gasifier product gas and accordingly high NO_x concentrations in the flue gas were expected. The results are presented in Figure 10.

The concentrations of ammonia and hydrogen cyanide measured in the product gas were much higher than in the case of wood pellets gasification. Concentrations up to 35000 $ppmv_{dry}$ were observed. Contrary to results obtained with wood pellets, a higher NH_3 concentration and a lower HCN concentration were measured in the product gas generated at a lower gasifier temperature. The total concentration of both fuel-NO_x precursors was lower at higher gasifier temperatures. The product gas was subsequently combusted using the flameless burner. The average combustion chamber temperature of 1050 °C was the same as that during the combustion of the wood pellets product gas. The amount of combustion air was varied in order to investigate the influence of the burner air ratio on NO_x emissions. In the case of the rape cake pellets product gas, complete combustion was possible beginning at an excess oxygen level of 2 vol-%. The NO_x emissions were about one order of magnitude higher in comparison to wood pellets product gas combustion. The results are presented in Figure 11. Similarly to the wood pellets case higher NO_x emissions were measured at a lower gasifier temperature. The difference was growing with the excess oxygen in the flue gas. A higher combustion air ratio significantly enhanced the NO_x formation.

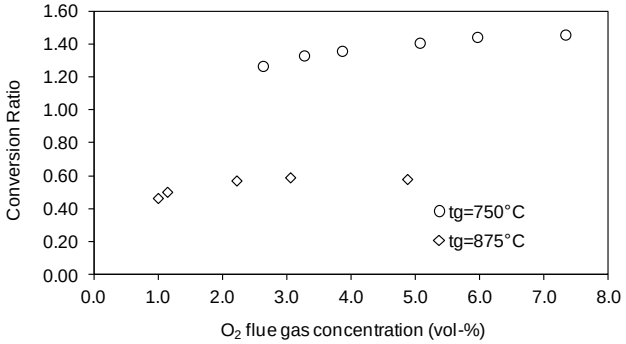

Figure 9. NH_3 and HCN to NOx conversion ratios during product gas combustion from wood pellets gasification (AR=0.22).

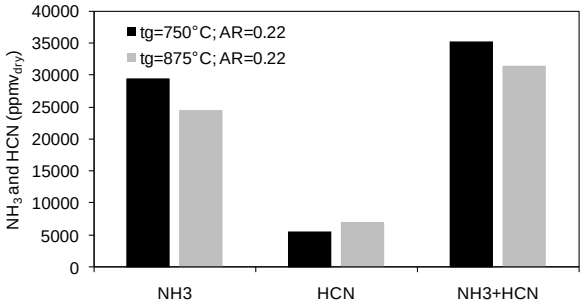

Figure 10. NH_3 and HCN concentrations in the rape cake pellets gasification product gas.

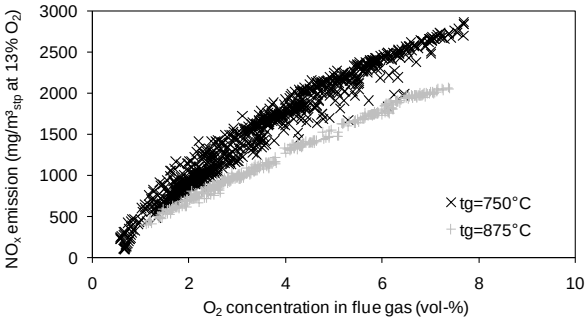

Figure 11. NO_x emission during product gas combustion from rape cake pellets gasification (AR=0.22)

The lower NO_x emissions at a higher gasifier temperature were not only observed because of the lower concentration of NO_x precursors in the product gas. Similar to the wood pellets experiments this case also saw lower hydrocarbon concentrations lead to lower conversion ratios of fuel-nitrogen. Figure 12 shows the calculated conversion ratios for product gas from rape cake pellets gasification.

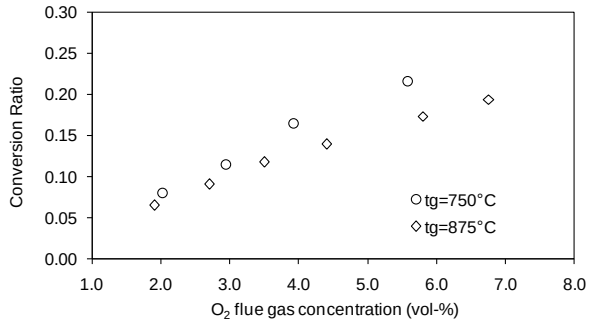

Figure 12. NH_3 and HCN to NOx conversion ratios during product gas combustion from rape cake pellets gasification (AR=0.22)

The conversion ratios were calculated using Eq. (1). The conversion ratios calculated for combustion of product gases generated at the gasifier temperature of 875 °C are lower than those at 750 °C in the whole investigated range of excess oxygen. The difference between the values for the two temperatures increases with increasing excess oxygen in the flue gas.

4. Discussion

Presented results show that during flameless combustion of N-containing gases, the fuel-N to NO_x conversion ratio strongly depends on the hydrocarbon concentrations. This phenomenon can be explained by the results obtained in previous modeling studies of the authors (Zieba et al, 2009a). They examined the ammonia behavior during flameless combustion of methane-free and methane-containing ammonia doped gases using detailed chemistry. It has been found that the presence of methane strongly influences the ignition behavior and thus the location and the stoichiometry under which the ammonia reacts. In the presence of methane, due to the longer ignition time, ammonia contained in the fuel is reacting with delay in the fuel-lean. Whereas during combustion of methane-free gases, reactions occur rapidly and ammonia decomposes in a substoichiometric region of the reaction zone. In Choudhuri et al., (2003) an investigation of the combustion characteristics of hydrogen-hydrocarbon hybrid fuels is presented. This study confirms that the ignition delay can be significantly influenced by hydrocarbons. Moreover, (Skreiberg et al., 2004) investigated the ammonia chemistry below 1400 K. They also reported that methane in relatively low concentrations can strongly inhibit the ammonia conversion under fuel-rich conditions. Increasing the methane or hydrocarbon content in the fuel can see ammonia and hydrocarbons start to compete for the same radicals occurring in the combustion process. Therefore, the decomposition of ammonia can be shifted toward the fuel-lean side of the combustion, thus enhancing the conversion to NO_x.

5. Conclusions

The presented experimental studies show the fate of ammonia and hydrogen cyanide during flameless combustion of different low calorific value gases. The first series of experiments in which ammonia doped synthetic gases were burned under flameless conditions showed that depending on the gas composition, large differences in the conversion of NH_3 to NO_x can occur. In particular, the methane in low concentrations influences the ammonia to NO_x conversion. The lowest NO_x emissions and therefore the lowest conversion ratios were measured while burning methane-free gas. A rapid increase of NOx emissions could already be observed at the lowest investigated methane concentrations. The NOx emissions increased with increasing methane concentrations in the whole investigated range. The tested CO/H_2 ratios in the fuel had a minor influence on the conversion of ammonia to NO_x. During the second series of experiments, product gases generated from two different solid bio-fuels in a BFB gasifier were burned in the flameless burner. The goal of these studies was to show the dependencies between gasifier operating parameters and thus the composition of the product gas and final NO_x emissions during subsequent flameless combustion. The results shows the same tendencies observed during tests with ammonia doped synthetic gases. Also in this case the fuel nitrogen conversion was influenced by the product gas composition. According to investigated gasifier parameters the amount of hydrocarbons and fuel-NO_x precursors was changing. In the case of wood pellets product gas combustion, much higher NO_x emissions were observed with lower gasifier temperatures and thus with higher hydrocarbons concentrations in the product gas. This was observed even when the concentration of NH_3 and HCN was lower at a lower gasifier temperature. In the case of nitrogen-rich rape cake pellets, much higher concentrations of NH_3 and HCN were measured in comparison to wood pellets. This case also saw higher hydrocarbon concentrations lead to higher conversion rates of NH_3 and HCN to NO_x. In all cases a higher combustion air ratio enhanced the NO_x emissions. This was observed particularly during the combustion of the nitrogen-rich rape cake pellets product gas.

References

Wünning J.A. and Wünning J.G., 1997, Flameless oxidation to reduce thermal-NO formation, Prog. *Energy Combust. Sci.* 23, pp.81–94.

Becidan M., Skreiberg Ø., Hustad J.E., 2007, NO_x and N_2O Precursors (NH_3 and HCN) in Pyrolysis of Biomass Residues, *Energy Fuels 21*, p. 1173-1180, (2007).

Cavaliere A., De Joannon M., 2004, Mild Combustion, *Prog. Energy Combust. Sci. 30*, pp. 329-366.

Choudhuri A.R., Gollahalli S.R., 2003, Characteristics of hydrogen-hydrocarbon composite fuel turbulent jet flames, *Int. J. Hydrogen Energy 28*, pp 445 – 454.

Galletti C., Parente A., Tognotti L., 2007, Numerical and experimental investigation of a mild combustion burner, *Combust. Flame 151*, pp. 649-664.

German Standard DIN 38406-E5, 1983, Methods for the examination of water, waste water and sludge; determination of ammonia-nitrogen (E5).

German Standard DIN 38405-D13, 1981, Methods for the examination of water, waste water and sludge; determination of cyanides (D13).

Leppälahti J., Koljonen T., 1995, Nitrogen evolution from coal, peat and wood during gasification: Literature review, *Fuel Proc. Tech. 43*, pp. 1-45.

Schuster A., Zieba M., Wünning J.G., Scheffknecht G., 2007, "Optimisation of conventional biomass combustion system by applying flameless oxidation", *Proceedings of 15th IFRF Members' Conference,* Pisa.

Schuster A., Zieba M., Scheffknecht G., Wünning J.G., 2007, "Application of FLOX® Technology for the utilisation of low-grade biofuels", *Proceedings of 15th European Biomass Conference*, Berlin, Germany, pp. 1703-1706.

Skreiberg Ø., Kilpinen P., Glarborg P., 2004, Ammonia chemistry below 1400 K, *Combust. Flame 136*, pp. 501-518.

Zieba. M, Schuster A., Scheffknecht G., 2009a, Influence of gas composition on ammonia to NO_x conversion during flameless combustion of low calorific value gases, *Proceedings of 16th IFRF Members' Conference*, Boston.

Zieba. M. Brink. A., Schuster A., Hupa M., Scheffknecht G., 2009b, Ammonia chemistry in a flameless jet, *Combust. Flame 156*, pp. 1950-1956.

2.5 Paper V: NOx modelling using combined CFD and reactor network models

Title: Ammonia chemistry in a flameless jet

This paper was reviewed and subsequently published in 2009 in:
Combustion and Flame
doi: 10.1016/j.combustflame.2009.07.002

Author's contribution to the paper:

- performance of the experimental work, interpretation of the results
- main author of the paper – writing, preparation of the data, data visualization, and editorial work

Combustion and Flame 156 (2009) 1950–1956

Contents lists available at ScienceDirect

Combustion and Flame

journal homepage: www.elsevier.com/locate/combustflame

Ammonia chemistry in a flameless jet

Mariusz Zieba [a,*], Anders Brink [b], Anja Schuster [a], Mikko Hupa [b], Günter Scheffknecht [a]

[a] Institute of Process Engineering and Power Plant Technology, University of Stuttgart, Pfaffenwaldring 23, D-70569 Stuttgart, Germany
[b] Process Chemistry Centre, Åbo Akademi University, Biskopsgatan 8, 20500 Åbo, Finland

ARTICLE INFO

Article history:
Received 7 January 2009
Received in revised form 1 March 2009
Accepted 6 July 2009
Available online 5 August 2009

Keywords:
Flameless combustion
Fuel-NO_x
Ammonia conversion

ABSTRACT

In this paper, the nitrogen chemistry in an ammonia (NH_3) doped flameless jet is investigated using a kinetic reactor network model. The reactor network model is used to explain the main differences in ammonia chemistry for methane (CH_4) containing fuels and methane-free fuels. The chemical pathways of nitrogen oxides (NO_x) formation and destruction are identified using rate-of-production analysis. The results show that in the case of natural gas, ammonia reacts relatively late at fuel lean condition leading to high NO_x emissions. In the pre-ignition zone, the ammonia chemistry is blocked due to the absence of free radicals which are consumed by methane–methyl radical (CH_3) conversion. In the case of methane-free gas, the ammonia reacted very rapidly and complete decomposition was reached in the fuel rich region of the jet. In this case the necessary radicals for the ammonia conversion are generated from hydrogen (H_2) oxidation.

1. Introduction

Flameless oxidation technology (FLOX®), has already demonstrated great potential in reducing thermal NO_x formation [1–3] while burning natural gas. In contrast to combustion within classical flames, temperature peaks are avoided due to the high internal recirculation of combustion products. Recent works on FLOX® technology are focussed on its adaptation to combust low calorific value gases generated from the biomass [4]. During air gasification of biofuels, the fuel nitrogen is released mainly as ammonia or hydrogen cyanide (HCN) in concentration up to thousands ppm. These compounds are formed as a result of thermal destruction of proteins and amino acids contained in the biomass [5,6]. During combustion of such gases, the nitrogen-containing species may be oxidised to NO_x or they may be reduced to N_2. The selectivity of this process depends on the gas composition, temperature and mixing of the reactants. The main chemical routes of NO_x formation from fuel nitrogen were established by Miller and Bowman [7]. There are several publications in literature dealing with the ammonia chemistry related to high temperature conditions in flames [7–12], as well as related to moderate temperatures which can occur in fluidized bed combustion [13] or in post-combustion processes [14].

The conditions in flameless combustion are different from those mentioned above. Due to the high momentum of the oxidizer jet, internal recirculation of the hot combustion products occurs. These hot products are partially mixed with the fuel and oxidizer before the mixture ignites. As a result, there is no identifiable flame front. The reactants are strongly diluted and the temperature field is homogeneous without high peaks. Schuster et al. [15] observed that the ammonia conversion in such jets depend strongly on the gas composition: the conversion of ammonia to NO_x in gases containing only carbon monoxide (CO) and H_2 is very small compared to gases containing hydrocarbons. According to the authors knowledge no one has yet modelled NH_3 conversion in ammonia-doped flameless jets.

The goal of this paper is to explain the main differences in nitrogen chemistry between methane-containing and methane-free ammonia-doped gases in flameless jets. A reactor network models with detailed reaction mechanisms are used for the modelling. In order to establish the main reactor model parameters such as residence time, oxidizer/fuel mixing and recirculation ratio of the hot product gases, computational fluid dynamics (CFD) modelling of the combustion chamber was performed. Three different ammonia-doped gaseous mixtures have been simulated and compared against previously published experimental data [15].

2. Experimental background

All experimental data used in this paper to validate the modelling results were taken from Schuster et al. [15]. The objective of the experiments was to investigate the ammonia oxidation and thus the conversion of volatile fuel nitrogen to NO_x under flameless conditions. The experiments were performed using a 20 kW FLOX®-burner. The burner had been originally developed for natu-

* Corresponding author. Fax: +49 711 685 63491.
E-mail address: zieba@ivd.uni-stuttgart.de (M. Zieba).

0010-2180/$ - see front matter © 2009 The Combustion Institute. Published by Elsevier Inc. All rights reserved.
doi:10.1016/j.combustflame.2009.07.002

ral gas (NG) and was subsequently modified to combust low calorific value gases. The test rig is shown in Fig. 1.

Different gas mixtures were used in the experiments of Schuster et al. Three of them have been selected for the model validation. The composition of all selected gases and their calorific values are summarised in Table 1. The first fuel is a natural gas (NG) with a lower heating value of 36 MJ/m^3 i.N. The natural gas contains mainly methane and very small amounts of ethane (C_2H_6), carbon dioxide (CO_2) and nitrogen (N_2). The amount of higher hydrocarbons can be assumed to be negligible. The next two gases are synthetic low calorific value (LCV) mixtures provided by a mixing station. Methane-containing syngas (MCS) represents a gas generated from biomass air blown gasification. The third tested gas is a methane-free syngas (MFS). Ammonia and hydrogen cyanide are the main NO_x precursors created during the gasification of biomass [5,6]. In order to investigate the fuel nitrogen conversion, ammonia at different concentrations were added to the fuel stream [15]. The concentration of NH_3 was varied between 0 and 900 ppmv$_{(dry)}$ for NG, 0–750 ppmv$_{(dry)}$ for methane-free syngas, and 0–650 ppmv$_{(dry)}$ for methane-containing syngas. The value is related to the ammonia concentration in the gas and the combustion air mixture. All experiments were carried out at a firing capacity of 18 kW, a temperature of approximately 1000 °C and with 50% excess air.

With no ammonia added to the fuel stream, the emitted NO concentration was 50 ppmv$_{(dry)}$ when natural gas was the fuel, whereas for other tested LCV gases the value of NO in flue gas was about 10 ppmv$_{(dry)}$. For all of the tested gases, the NO emission increases with increasing ammonia concentration. In the cases of natural gas and methane-containing syngas the conversion of NH_3 to NO was found to be similar and relatively high. In contrast, the NO emission while burning methane-free gas was significantly lower. It is an indication that the ammonia chemistry in flameless combustion is strongly influenced by the composition of the fuel gas, particularly with respect to the hydrocarbon content in the fuel. A compilation of the selected results of Schuster et al. are shown in Fig. 2.

3. Numerical modelling

The numerical modelling of the combustion process was performed using the commercial Chemkin 4.1 software package. The Åbo Akademi (*ÅA*) [16] kinetic reaction scheme was used to simulate the chemistry occurring in the combustion chamber. The *ÅA* mechanism was created for the simulation of the gas phase combustion of biomass-derived gases under moderate temperature conditions. The scheme is based on the mechanism of Glarborg et al. [17,18] and Miller and Glarborg [19]. The mechanism has been validated in the past and applied to a number of conditions giving satisfactory predictions of nitrogen and hydrocarbon combustion kinetics over a wide range of temperatures and air–fuel ratios [20–25]. Since the flameless combustion of ammonia-doped low calorific value gases occurs at moderate temperatures and

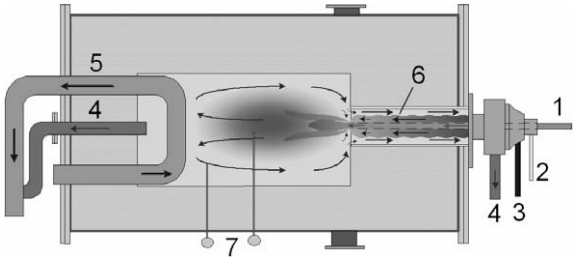

Fig. 1. Scheme of FLOX®-burner test rig (1 – LCV gas, 2 – natural gas, 3 – combustion air, 4 – flue gas, 5 – cooling, 6 – recuperator pipe, 7 – thermocouples).

Table 1
Composition of the selected gases.

	NG	MFS	MCS
CH_4 (vol%)	95.6	–	6.5
C_2H_6 (vol%)	2.4	–	–
H_2 (vol%)	–	25.0	8.6
CO (vol%)	–	18.0	8.8
CO_2 (vol%)	0.4	15.0	15.6
N_2 (vol%)	1.6	42.0	60.5
LCV (MJ/m^3 i.N.)	36.1	5.0	4.4

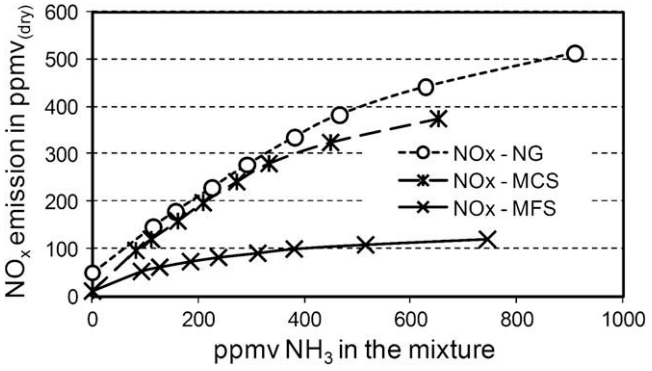

Fig. 2. NO_x concentration in the flue gas for three different gases as a function of ammonia concentration in the combustion mixture (fuel and combustion air).

the composition of the MFS and MCS fuels are similar to bio-derived fuels, the *ÅA* mechanism was considered a suitable scheme. The *ÅA* kinetic scheme involves 371 elementary gas phase reactions for the oxidation of H_2, CO, light hydrocarbons (C_1 and C_2) and methanol (CH_3OH). The mechanism also takes into account the reaction subsets of nitrogen pollutants such as the oxidation of NH_3 and HCN as well as sub-mechanisms describing the interactions between hydrocarbons and nitrogen-containing species.

To see to what extent the conclusions of this work depend on the chosen reaction scheme, the results obtained using *ÅA* mechanism were compared with results from the well established GRI-Mech 3.0 kinetic mechanism [26]. Although GRI-Mech 3.0 mechanism is not well suited for NH_3 oxidation, satisfactory results of ammonia-doped methane/air flames modelling using this mechanism have been reported in the past [8]. Moreover, the GRI-Mech 3.0 has already been used for the modelling of nitrogen pollutants during flameless combustion of methane [27]. The GRI-Mech 3.0 has been specifically designed to describe methane and ethane combustion at high temperatures [28].

3.1. Modelling approach

Fig. 3a illustrates the flow field (axial velocity) inside the modelled combustion process. The fuel and preheated air are introduced with high velocity forming a jet. The jet develops taking the product gases from its environment back into the stream. The mixing between the air, fuel and combustion products occurs continuously along the jet.

The model described in this work considers detailed reaction mechanisms implemented in a network of plug flow reactors (PFR). Fig. 3b shows the isothermal PFR's connected in series, which represent the jet propagation in the combustion chamber. In order to simulate the mixing processes two different approaches for the mixing of fuel with air have been used. Similar approaches have been successfully employed in different Selective Non-Catalytic Reduction (SNCR) and reburn modelling studies [29,30].

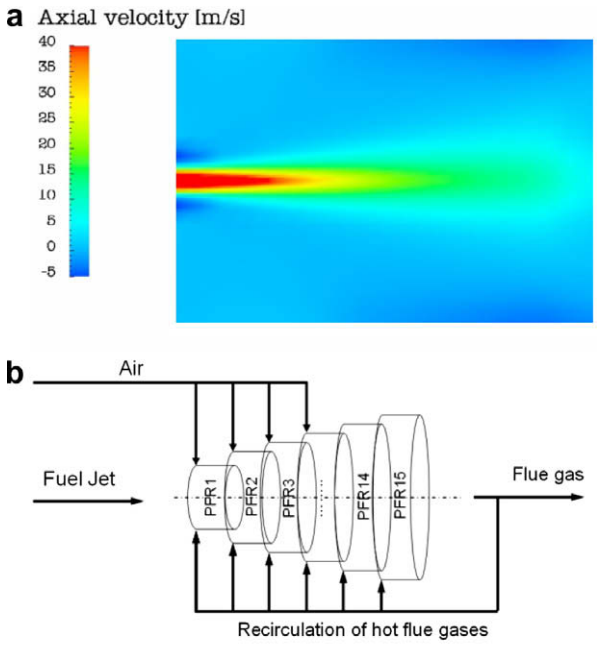

Fig. 3. Principle of the flameless jet model; (a) flow field in the combustion chamber and (b) reactor model air-into-fuel mixing approach.

Because of the high velocity and volume flow of the preheated air, the first assumption was to treat the air as the main stream and therefore to introduce the ammonia-doped fuel stepwise into the air jet. This approach will be called here the fuel-into-air mixing approach.

The second approach, the air-into-fuel mixing approach, assumes the entrainment of the oxidizer into the fuel stream. The amounts of entrained oxidizer mass flows into the PFR's were discretely distributed in equal amounts.

It has to be mentioned that the mixing between oxidizer and fuel occurs only along a part of the jet, which means the fuel or oxidizer is entrained only to some of PFR's in the model. The method of estimating the mixing length will be described in Section 3.2.

The recirculation of product gases is essential for flameless oxidation, whereby the combustion products are entrained into the jet, diluting the combustion environment and influencing the chemical reactions taking place and thus changing the end-flue gas composition. The calculations were carried out iteratively by using the end-flue gas composition from the preceding iteration as the input value for the composition of recirculated gases. This procedure was repeated until the system reached a steady state solution. The part of the jet where the oxidizer is still mixing with the fuel is discretized using 2 cm long reactors, whereas the remaining length is discretized using 10 cm long reactors. Additionally, the length of the last reactor has been set up in such a way that the complete residence time in the system is 2 s. This should ensure enough time to complete the combustion and decrease the pool of free radicals in the recirculated product gas. The stream of recirculated gases was assumed to be non-reactive.

3.2. Parameters estimation – CFD modelling

In order to estimate the main parameters of the reactor network model, such as the residence time for the PFR's, the mixing distance and the distribution of the recirculated gases, CFD modelling using the commercial code FLUENT was carried out. The simple modelling of the combustion chamber was done using the 4-step global hydrocarbon chemistry model of Jones and Lindstedt [31]. The turbulence–chemistry interaction was modelled applying the Eddy-Dissipation–Combustion Model of Magnussen and Hjertager [32]. The standard k–ε model has been used for the turbulence modelling.

The modelling results are shown in Fig. 4. In the reactor network model, every PFR represents a certain part of the propagating jet (1-D model). Therefore the residence time for each reactor could be estimated based on the average velocity of the propagating jet at a certain position. The velocity is presented in Fig. 4a. The velocity decreases with increasing mass flow of the jet. Fig. 4b shows the mass flow of the jet. The difference between the input mass flow and the local mass flow of the jet indicate the local dilution caused by the internal recirculation of the combustion products. The recirculation mass flow was calculated as the difference between the average mass flow for a certain reactor, taken from the CFD results, and the mass flow transported from the preceding reactor. The mixing between fuel and oxidizer takes place only along a part of the jet. The location where mixing is considered to be complete was estimated using the mixture fraction factor. The mixture fraction measures the fuel/oxidizer ratio and can be written in terms of the mass fraction as

$$\xi = \frac{Y_i - Y_{i,ox}}{Y_{i,fuel} - Y_{i,ox}} \tag{1}$$

where Y_i is the elemental mass fraction for element i. The subscript *ox* and *fuel* denotes the value at the oxidizer or fuel stream inlet, respectively. The values of stoichiometric mixture fractions for NG, MCS and MFS were 0.058, 0.48 and 0.45, respectively.

It was assumed that the mixing process is complete when the mixture fraction factor on the axis of the simulated combustion chamber (using CFD code) has reached the value of the stoichiometric mixture fraction.

4. Results and discussion

The development and adaptation of the flameless technology for low calorific value gases creates a uniform combustion environ-

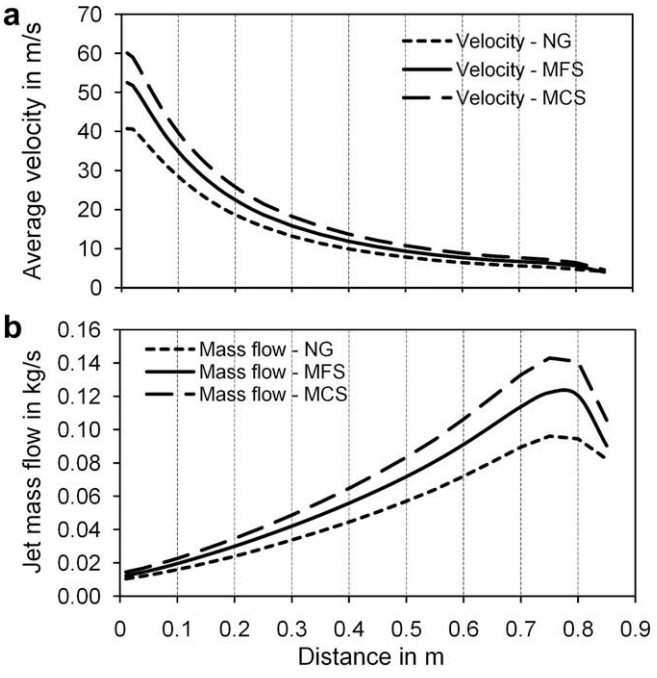

Fig. 4. Results of the CFD modelling of the combustion chamber for three different gaseous mixtures; (a) average velocity of the jet and (b) mass flow rate of the jet.

ment that allows comparison of ammonia behaviour in gases with significantly varying composition. The lower heating value of the fuel gas varies from 4.4 to 36 MJ/m^3 i.N. in these studies. Due to the burner flexibility and combustion stability, the comparison of ammonia decomposition can be done under very similar conditions for all of the tested fuels. The high dilution of the reaction zone caused by the recirculation of hot flue gases significantly decreases the temperature peaks in the combustion chamber [1]. Therefore, the combustion of the studied fuels occurs at very similar intermediate temperature conditions. Moreover, the hot recirculated gases include nitrogen oxides that influence the nitrogen chemistry in the jet.

4.1. Kinetic schemes and the effect of mixing

The analysis of modelling studies of the ammonia conversion using three different gas mixtures under flameless combustion conditions was performed. In order to validate the reactor network models, the predicted NO_x concentration values are compared with the experimental results of Schuster et al. [15]. The *ÅA* and GRI-Mech 3.0 kinetics mechanisms were used for modelling. However, the GRI-Mech 3.0 mechanism was used only together with the air-into-fuel mixing approach.

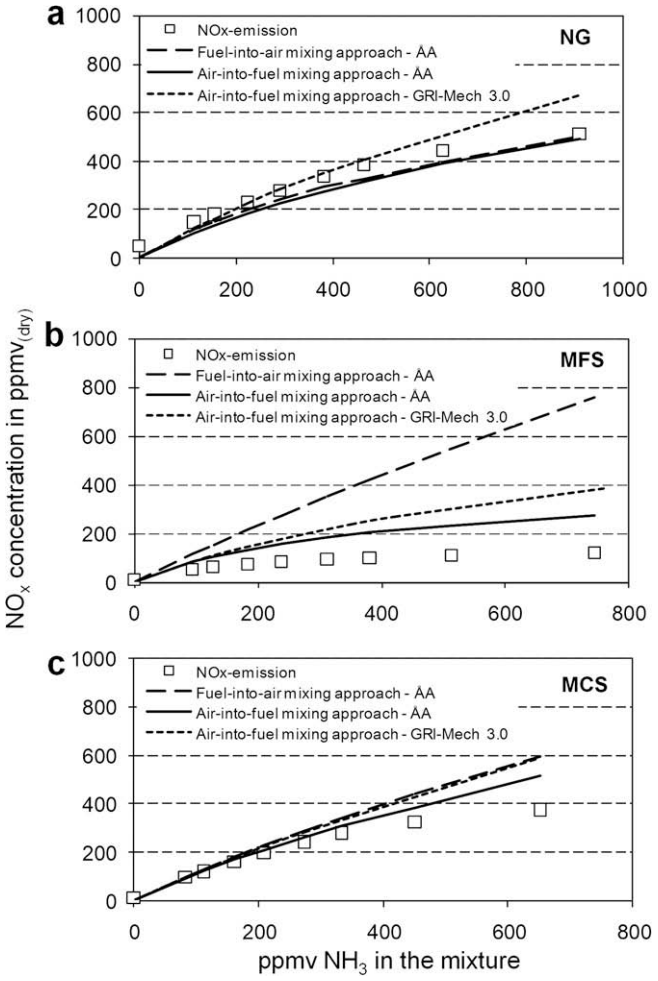

Fig. 5. Comparison between experimental results (Schuster et al. [15]) and model results versus inlet ammonia concentration; (a) results for ammonia-doped natural gas, (b) results for ammonia-doped methane-free syngas, and (c) results for ammonia-doped methane-containing syngas. Experimental conditions: $P = 18$ kW, $T = 1000$ °C, 50% excess air.

4.1.1. Modelling using the ÅA mechanism

The modelling results are shown in Fig. 5. In the case of ammonia-doped natural gas, both of the mixing models using the *ÅA* mechanism predicted the NO_x concentration very well over the whole range of ammonia input as shown in Fig. 5a. Here production of the nitrogen oxides occurs only via fuel-NO reaction pathways. Fig. 5c shows the modelled NO_x concentration for methane-containing syngas. The calculated values were slightly higher than the measured ones, whereas the model with the air-into-fuel mixing approach resulted in better agreement with the measured data. With decreasing methane content in the fuel, the overprediction of the NO_x with the fuel-into-air mixing approach increased. The predicted NO_x concentrations for the methane-free syngas were strongly overestimated as shown in Fig. 5b. Only the model with the air-into-fuel mixing approach was able to predict the trends for all experimentally tested gas compositions. For natural gas and methane-containing syngas, the modelled conversion of ammonia to NO_x was relatively high compared to the methane-free syngas, which was in good agreement with the measurements.

The main difference between the two mixing approaches is the local stoichiometric ratio λ along the modelled jet. In the case of the fuel-into-air approach, the entire combustion process takes place under overstoichiometric conditions. In the case of the air-into-fuel mixing approach, there exist substoichiometric conditions at the entrance and overstoichiometric conditions at the outlet. Therefore, the ammonia in the fuel reacts under a broad spectrum of conditions, going from very fuel rich, through to fuel lean, and to conditions of full mixing. This seems to be essential for the modelling of ammonia chemistry in the flameless jet.

4.1.2. Modelling using the GRI-Mech 3.0 mechanism

Additional calculations were carried out using the GRI-Mech 3.0 mechanism together with the air-into-fuel mixing approach. Fig. 5 shows that by using this kinetic scheme, the reactor network model was able to predict the trends satisfactorily: i.e. showing lower concentration of NO_x in the case of methane-free gas. However, in all cases the model overestimated the NO_x emissions. The discrepancy increased with increasing ammonia concentration in the fuel. The possible reasons for the discrepancies are discussed below.

4.2. Nitrogen-containing species behaviour along the jet

The proposed model with the air-into-fuel approach of mixing was able to predict the trends of ammonia conversion to NO_x quite well. Therefore, the analysis of the computed results for natural gas and methane-free syngas was performed in order to describe the chemical processes of ammonia decomposition and NO_x creation along the flameless jet.

In Fig. 6, profiles of the normalised fluxes of the main nitrogen-containing species and combustibles have been plotted as a function of the distance from the burner nozzle. Fig. 6a–d presents the results obtained using the *ÅA* kinetic scheme, whereas Fig. 6e–h displays the calculated results using the GRI-Mech 3.0 mechanism. Fig. 6a shows the normalised flux profiles of nitrogen-containing species while burning natural gas. The results indicate that along the first 20 cm ammonia does not react. At the same time the recirculated NO coming from the flue gas is slowly consumed. Since the recirculated part of NO has been extracted from the main flux, its negative value means, that the recirculated NO is consumed faster than it is produced at the burner entrance. The almost constant value of NO and NO_2 flux indicates, that the part of the NO is not reduced to N_2 but it is converted to NO_2.

Fig. 6b shows the profile of combustibles, while burning natural gas. When the methane ignites, ammonia rapidly decomposes and the initially created NO_2 reduces back to NO. These processes take place in the part of the jet where all of the combustion air has al-

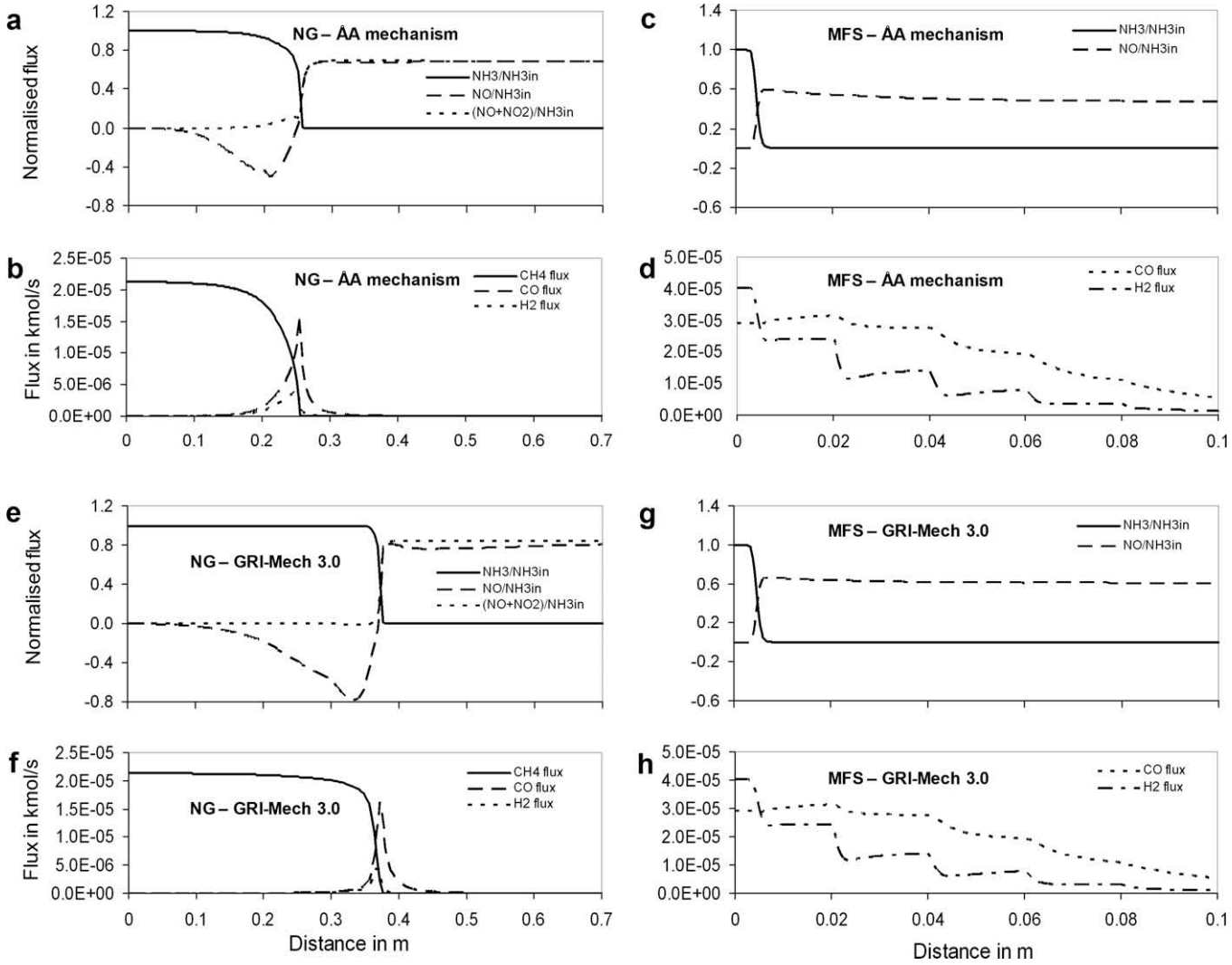

Fig. 6. Predicted flux profiles as a function of distance from burner nozzle. The fluxes of NH_3, NO and (NO + NO_2) have been normalised to the incoming flux of ammonia; in all cases the recirculated part of the flux has been removed from the total flux; (a) profile along the jet of normalised flux of NH_3, NO and (NO + NO_2) for ammonia-doped natural gas – *ÅA* mechanism; (b) flux of CH_4, CO and H_2 along the jet for natural gas – *ÅA* mechanism; (c) profile of NH_3 and NO normalised flux for methane-free syngas – *ÅA* mechanism; (d) profile of CO and H_2 flux for methane-free syngas – *ÅA* mechanism; (e) profile along the jet of normalised flux of NH_3, NO and (NO + NO_2) for ammonia-doped natural gas – GRI-Mech 3.0; (f) flux of CH_4, CO and H_2 along the jet for natural gas – GRI-Mech 3.0; (g) profile of NH_3 and NO normalised flux for methane-free syngas – GRI-Mech 3.0; and (h) profile of CO and H_2 flux for methane-free syngas – GRI-Mech 3.0. Conditions: 310 $ppmv_{(dry)}$ NH_3, $T = 1000$ °C, 50% excess air.

ready been introduced into the fuel stream. The conditions are overstoichiometric.

In quite the opposite manner, the ammonia contained in the methane-free syngas reacts rapidly after the gas nozzle under substoichiometric condition as shown in Fig. 6c. Therefore, the conversion of NH_3 to NO is much lower. Since the NO_2 was not present in significant concentrations in this case Fig. 6b and g shows only the behaviour of the NO. The profile of combustibles shown in Fig. 6d indicates that the combustion process is limited by mixing. Due to the assumption of discrete oxidizer entrainment, the flux of CO and H_2 decreases stepwise.

Similar results were observed using the GRI-Mech 3.0 mechanism. However, some differences could be noticed. The first difference was the longer ignition delay for NG, as shown in Fig. 6f, compared to that obtained using the *ÅA* mechanism. This caused more NO to be oxidised to NO_2, resulting in higher final NO_x emissions as shown in Fig. 6e. Another possible reason for the higher predicted NO_x emissions is the favouring of HNO over N formation in the mechanism. This was observed by Sullivan et al. [8], when studying non-premixed methane/air flames when using GRI-Mech 3.0.

The fluxes of combustibles for MFS, shown in Fig. 6h, were identical for both kinetic schemes. The behaviour of nitrogen species, shown in Fig. 6g, was also similar, although the GRI-Mech 3.0 showed higher NH_3 to NO_x conversion.

Both of the mechanisms overestimated the measured values for MCS and MFS. The differences were particularly big for MFS. The *ÅA* and GRI-Mech 3.0 schemes with the air-into-fuel mixing approach overestimated the results by a factor of two and three, respectively. A possible source for these errors could be the simplification of the turbulent mixing. Fig. 6c and g shows that the whole ammonia decomposition takes place in the first reactor. Therefore, the description of the mixing in the zone directly after the burner nozzle is of key importance.

For the NG the errors were much smaller, because the process was limited by the chemistry and the discretization of the mixing in the model was not as crucial. Because of the high speed of the jet and relatively long delay in ignition all reaction were taking place at the fuel lean side of the mixture. Therefore, also the fuel-into-air mixing model was able to predict the values correctly.

Another reason for the overestimation of the measured NO_x emissions for the MCS, particularly at higher concentrations of

ammonia could be missing reaction pathways in the kinetic mechanisms. Dean and Bozzelli [33] have identified an additional pathway of relevance in ammonia oxidation in the temperature range 1000–1300 K via the intermediate methylamine. Koger and Bockhorn [34] later showed that this pathway does play a role in ammonia oxidation at conditions where methane is present. However, Koger et al. showed that this pathway contributes only to 10% or less of ammonia conversion leading to additional HCN formation. Therefore, it is unlikely that the methylamine pathway would have a significant influence on the overall conclusions of our model calculations using the *ÅA* mechanism.

4.2.1. Reaction path analysis

A rate-of-production (ROP) analysis was performed in order to identify the main reaction routes for the formation and decomposition of nitrogen-containing species. The ROP analysis was performed using the *ÅA* mechanism, since there were no significant differences found in the main nitrogen species behaviour and the results using the *ÅA* mechanism were in better agreement with the measured data. Moreover, the analysis was carried out only for the reactors which are representative of the processes taking place along the jet. For the natural gas fuel, two reactors have been chosen. The first one corresponds to the distance, where the methane decomposition occurs very slowly and the nitrogen oxide is converted to NO_2. The second reactor corresponds to the place, where methane ignites and ammonia is rapidly consumed. In the case of methane-free syngas, the first reactor was essential for the NO_x formation. The main reaction pathways were drawn based on time integration of rate-of-production under ideal plug flow conditions. The most important pathways are indicated in Figs. 7 and 8 with thicker arrows.

In the pre-ignition zone of the natural gas/air flameless jet the NO–NO_2 conversion is taking place. Methane slowly converts to methyl radicals via the following reactions:

$$CH_4 + H \leftrightharpoons CH_3 + H_2 \quad (2)$$

$$CH_4 + O \leftrightharpoons CH_3 + OH \quad (3)$$

$$CH_4 + OH \leftrightharpoons CH_3 + H_2O \quad (4)$$

Those three reactions consume most of the H, O and OH radicals occurring in the jet. The CH_3 radical undergoes further reactions which via formaldehyde (CH_2O) and formyl radical (HCO) leading to hydroperoxyl radical (HO_2) formation. The HO_2 radical is responsible for the conversion of previously recirculated NO to NO_2 via the reaction:

$$NO + HO_2 \leftrightharpoons NO_2 + OH \quad (5)$$

At the same time, ammonia conversion does not proceed because of the lack of radicals able to react with NH_3 at 1000 °C.

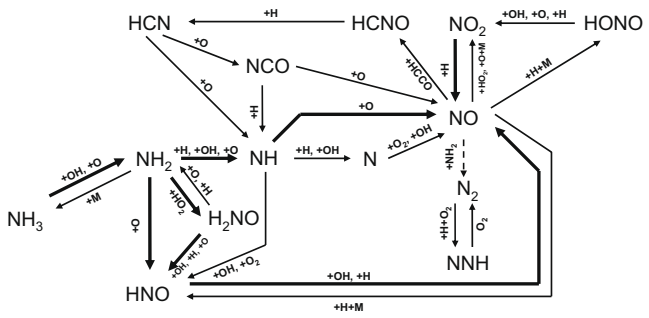

Fig. 7. Main chemical reaction pathways of NO creation and reduction in a flameless jet of ammonia-doped natural gas.

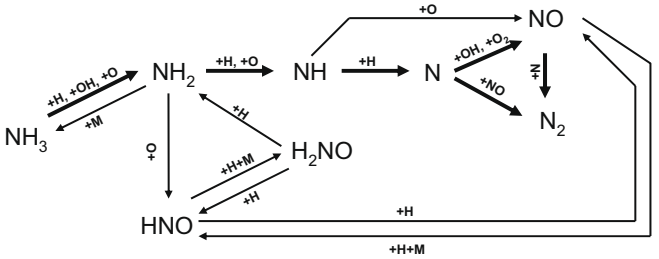

Fig. 8. Main chemical pathways of NO creation and reduction in flameless jet for ammonia-doped methane-free syngas.

Mancini et al. [27] have also reported the formation of NO_2 in the flameless combustion of methane/air mixture. However, they found that besides reaction (5), a reaction:

$$NO + O + M = NO_2 + M \quad (6)$$

generates around two-thirds of the total NO_2 produced, whereas in this work the contribution of this reaction was only minor.

As the methane ignites, ammonia decomposition progresses rapidly. In this part of the jet all of the combustion air has already been introduced into the fuel stream. The conditions are overstoichiometric. The abundant oxygen causes that almost all of the NH_3 is converted to NO. This makes the process different to the classical flames. Sullivan et al. [8] have investigated the ammonia conversion and NO_x formation in non-premixed methane-air flames. They found that ammonia is decomposed and NO is formed mainly in the ignition region, which occurs at the border between fuel reach and fuel lean mixture. In the flameless process, the high velocity of the jet causes the combustion mixture to be fuel lean when igniting. The main chemical pathways related to nitrogen conversion are shown in Fig. 7. The major part of the NO is created via oxidation of imidogen (NH), the nitroxide radical (H_2NO) and nitrosyl hydride (HNO). Although some reaction pathways via HCN are found active, they have a very small influence on the overall NO concentration. The NO_2 initially created in the pre-ignition zone is now converted back to NO. Some additional creation of NO_2 via HONO was found. The reduction of NO to N_2 during the ignition time was almost negligible.

The process of NH_3 decomposition and NO_x creation in the case of methane-free syngas is different to that observed for the natural gas. According to the model, all of the ammonia reacts rapidly in the substoichiometric region of the jet. The hydrogen contained in the fuel ignites directly after the nozzle and releases enough radicals to start the ammonia decomposition. The released radicals are not completely consumed by other combustibles and easily react with NH_3. The main chemical paths leading to NO creation and reduction are shown in Fig. 8.

The main part of the NO is created via oxidation of nitrogen radicals (N) which are formed via the reaction:

$$NH + H \leftrightharpoons N + H_2 \quad (7)$$

Simultaneously the same radicals react with nitrogen oxide forming N_2.

$$N + NO \leftrightharpoons N_2 + O \quad (8)$$

This reduction mechanism was found to be very important. The pathways via H_2NO and HNO are also active but the net contribution to NO creation is relatively small.

5. Conclusions

The presented kinetic modelling study shows the fate of ammonia and nitrogen-containing species in a flameless jet for different

gaseous fuels mixtures. Depending on the gas composition, there can be a large difference in the conversion of NH_3 to NO_x.

In the case of flameless natural gas combustion, the methane ignites with delay around the location where the oxidant is already completely mixed with the fuel. Before the ignition occurs, the ammonia conversion is inhibited due to the absence of radicals which are instead consumed by methane–methyl radical conversion. Recirculated NO is converted to NO_2 in this part of the jet. After methane ignition, ammonia oxidises mostly to NO.

In the flameless jet of methane-free gas, ignition occurs rapidly and ammonia decomposes in the substoichiometric region of the jet. The radicals needed for ammonia decomposition are generated from hydrogen oxidation. In contrast to the natural gas jet the radicals are not completely consumed by other combustibles. The reduction of NO to N_2 is very pronounced and result in significantly lower nitrogen oxides emissions.

Since the ignition delay depends on the fuel composition, the high velocity of the jet and the strong recirculation can lead to crucial changes in local stoichiometry under which the mixture ignites. The longer ignition delay the higher amount of air and recirculated gases are mixed with the fuel when igniting. Since the ignition zone is not stabilized in the flameless combustor, it can significantly influence the ammonia to NO_x conversion. The modelling results also showed that for the ammonia-doped fuel, a correct mixing approach is critical in order to successfully predict the concentration of nitrogen-containing species under flameless oxidation conditions.

Although, the choice of kinetic scheme had an influence on the final NO_x prediction, the results show similar behaviour of the main nitrogen species along the jet. The model is able to accurately predict the trends using both the *ÅA* and the GRI-Mech 3.0 kinetic mechanisms.

References

[1] J.A. Wünning, J.G. Wünning, Prog. Energy Combust. Sci. 23 (1997) 81–94.
[2] C. Galletti, A. Parente, L. Tognotti, Combust. Flame 151 (2007) 649–664.
[3] A. Cavaliere, M. de Joannon, Prog. Energy Combust. Sci. 30 (2004) 329–366.
[4] A. Schuster, M. Zieba, G. Scheffknecht, J.G. Wünning, Application of FLOX technology for the utilisation of low-grade biofuels, in: Proceedings of 15th European Biomass Conference, Berlin, Germany, 2007, pp. 1703–1706.
[5] J. Leppälahti, T. Koljonen, Fuel Process. Technol. 43 (1995) 1–45.
[6] M. Becidan, Ø. Skreiberg, J.E. Hustad, Energy Fuels 21 (2007) 1173–1180.
[7] J.A. Miller, C.T. Bowman, Prog. Energy Combust. Sci. 15 (4) (1989) 287–338.
[8] N. Sullivan, A. Jensen, P. Glarborg, M.S. Day, F.F. Grcar, J.B. Bell, C. Pope, R.J. Kee, Combust. Flame 131 (2002) 285–298.
[9] P. Glarborg, A.D. Jensen, J.E. Johnson, Prog. Energy Combust. Sci. 29 (2003) 89–113.
[10] C.P. Fenimore, G.W. Jenes, J. Phys. Chem. 65 (1961) 289–303.
[11] R.P. van der Lans, P. Glarborg, K. Dam-Johansen, Prog. Energy Combust. Sci. 23 (1997) 349–377.
[12] R.P. Lindstedt, F.C. Lockwood, M.A. Selim, Combust. Sci. Tech. 99 (1994) 253–276.
[13] Ø. Skreiberg, P. Kilpinen, P. Glarborg, Combust. Flame 136 (2004) 501–518.
[14] J.F. Grcar, P. Glarborg, J.B. Bell, M.s. Day, A. Loren, A.D. Jensen, Proc. Combust. Inst. 30 (2005) 1193–1200.
[15] A. Schuster, S. Erhardt, G. Scheffknecht, J. G. Wünning, Conversion of ammonia to NO_x for flameless oxidation of low calorific value gas, in: 7th High Temperature Air Combustion and Gasification International Symposium, Phuket, Thailand, 13–16 January 2008, Ref. No. HiTACG_163.
[16] Åbo Akademi University. <http://web.abo.fi/fak/ktf/cmc/research/r_schemes.html>.
[17] P. Glarborg, K. Dam-Johansen, P. Kristensen, Final Report, Gas Research Institute, 5091-260-2126, Nordic Gas Technology Center (89-03-11), 1993.
[18] P. Glarborg, D. Kubel, P. Kristensen, J. Hansen, K. Dam-Johansen, Combust. Sci. Technol. 110–111 (1995) 461–485.
[19] J.A. Miller, P. Glarborg, Springer Series in Chemical Physics, Springer Verlag, Berlin, Germany, 1996.
[20] E. Coda Zabetta, M. Hupa, Combust. Flame 152 (2008) 14–27.
[21] E. Coda Zabetta, Modelling of nitrogen oxides in combustion at atmospheric and elevated pressures: application to biomass- and oil-derived gaseous fuels, Academic Dissertation, Painotalo Gillot Oy, Åbo, Finland, 2002.
[22] E. Coda Zabetta, P. Kilpinen, M. Hupa, K. Ståhl, J. Leppälahti, M. Cannon, J. Nieminen, Energy Fuels 14 (2000) 751–761.
[23] R. Rota, F. Bonini, A. Servida, M. Moribidelli, S. Carra, Combust. Sci. Technol. 123 (1997) 83–105.
[24] P. Kilpinen, M. Hupa, Combust. Flame 85 (1991) 94–104.
[25] B. Leckner, M. Karlsson, K. Dam-Johansen, C. Weinell, P. Kilpinen, M. Hupa, Ind. Eng. Chem. Res. 30 (1991) 2396–2404.
[26] Gas Research Institute, GRI-Mech, Ver. 3.0. <http://www.me.berkely.edu/gri-mech/>.
[27] M. Mancini, P. Schwöppe, R. Weber, S. Orsino, Combust. Flame 150 (2007) 54–59.
[28] C.K. Westbrook, Y. Mizobuchi, T.J. Poinsot, P.J. Smith, J. Warnatz, Proc. Combust. Inst. 30 (2005) 125–157.
[29] M.U. Alzueta, R. Bilbao, A. Millera, P. Glarborg, M. Østberg, K. Dam-Johansen, Energy Fuels 12 (1998) 329–338.
[30] M. Oliva, M.U. Alzueta, A. Millera, R. Bilbao, Chem. Eng. Technol. 25 (2002) 417–419.
[31] W.P. Jones, R.P. Lindstedt, Combust. Flame 73 (1988) 233–249.
[32] B.F. Magnussen, B.H. Hjertager, in: Sixteenth Symposium (International) on Combustion, The Combustion Institute, Pittsburgh, PA, 1976, pp. 719–729.
[33] M. Dean, J.W. Bozzelli, in: W.C. Gardiner (Ed.), Combustion Chemistry II, Springer-Verlag, 2000, pp. 125–341.
[34] S. Koger, H. Bockhorn, Proc. Combust. Inst. 30 (2005) 1201–1209.

3 Discussion and Conclusions

The present work focuses on experimental and modelling studies on fuel-NO_x formation during flameless combustion of biogenous fuels. It covers the early research work on CFD-based design development, broad experimental studies on fuel N conversion as well as development of the two-step methodology for modelling of fuel N formation processes in flameless burners. In the following, the two major research objectives and results are discussed. Moreover, the modelling work is extended, and some additional results are presented and discussed that are complementary to the work published in the outlined papers.

3.1 On geometrical design

The early research presented in Chapters 2.1 and 2.2 was focused on the geometrical design optimization and the development of a new air-staged flameless burner design. Both were based on the multi-nozzle burner design proposed by Schuster [9]. The geometry was inspired by former designs developed for GT combustors presented in [102–104]. The original GT combustor consisted of a burner front plate with 12 single nozzles positioned on a reference circle. Each singe nozzle comprised a small diameter fuel inlet placed in the middle of an air nozzle. The fuel nozzle was positioned upstream of the air injection [102].

The design proposed for LCVG generated from gasification of solid biomass is similar, however, there are some important differences. The burner consisted of eight nozzles, as shown in Figure 23. The high velocity air jet was introduced in the center of each nozzle. The air inlet was thus surrounded by the fuel leaving the gasification zone and entering the burner.

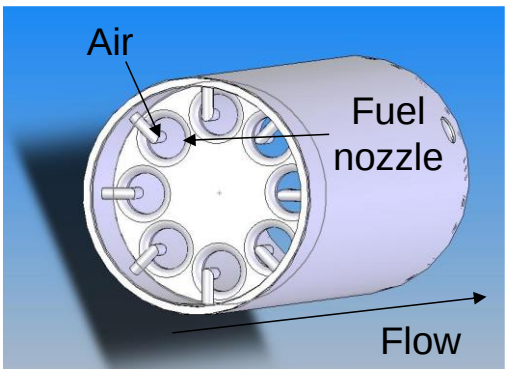

Figure 23 Flameless burner proposed by Schuster [9]

The main advantage of flameless burners in the combustion of LCVG is the flame stability, which is the direct result of the strong recirculation of hot product gases. Such reverse flow within the burner ensures that the combustion mixture is heated up above the self-ignition temperature. Therefore, one of the main parameters that is subject to CFD analysis is the recirculation ratio, which should be maximized. In Chapter 2.1, three different designs were proposed and simulated using the models described in Subchapter 1.5.2.1. The reported results

showed that, by using simple CFD analysis, it is possible to optimize the geometry and identify its limitations. In the presented paper, the results were evaluated qualitatively based on the flow patterns. Nevertheless, more detailed analysis is needed to quantitatively assess the results obtained.

For this reason, the recirculation ratio K, as defined in Subchapter 1.3.1, was adapted to evaluate the results by defining the local recirculation rate, which is the recirculation rate calculated for a certain cross-section along the burner axis. This means that, for each perpendicular cross-section of the burner volume, the mass flux flowing in the opposite direction (recirculation) was calculated and divided by the total mass flux entering the burner, including the air and the fuel.

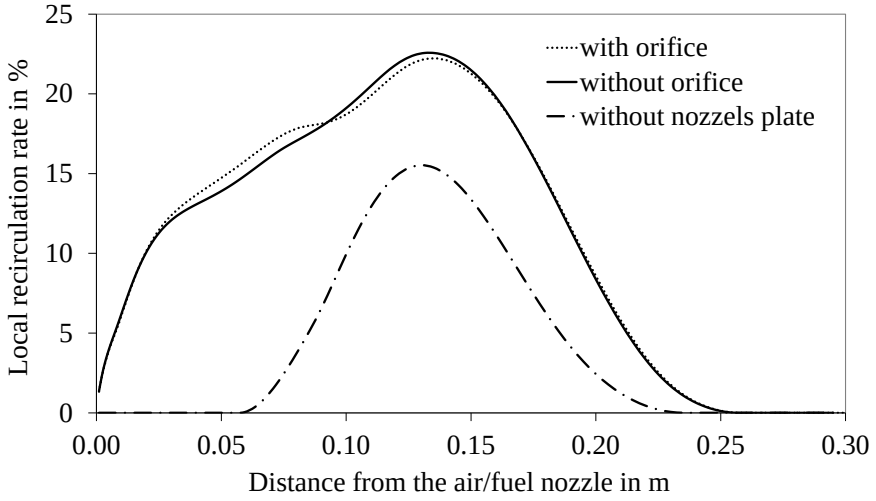

Figure 24 Local recirculation rate along the burner for the three analyzed multi-nozzle designs (Chapter 2.1)

The quantitative results showed that through the multi-nozzle design, the local recirculation ratios were limited, and the highest reachable values were of approx. 20–25 %, which is actually far lower than the level of recirculation described by Wünning and Wünning in [92], where values of 300 % were indicated as the minimum to reach the flameless conditions by combusting natural gas. The highest value was reached approximately 13 cm from the front nozzles' plate, where strong backflow in the burner axis takes place. The experimental results obtained showed that even such low recirculation was enough to reach perfect mixing conditions, resulting in complete combustion at relatively low excess oxygen levels. Nevertheless, it must be considered that the temperature of the product gas entering the burner is simultaneously the temperature of the pre-gasifier (approximately 900 °C), which is already above the ignition point of the product gas. Moreover, the combustion air is also highly preheated and was assumed to be 600 °C in the numerical model. If cold fuel and air would be applied to the burner, the recirculated heat would not be sufficient to maintain the combustion process. In this case, the burner would have to be designed differently, allowing much higher recirculation ratios.

This can principally be obtained using two strategies. The first one is to increase the momentum of the air jets by increasing their velocity. Each of the eight air/fuel jets entering the burner are following the law of conservation of momentum. As the velocity in the jet is much higher than in the surrounding volume, a pressure difference is created, causing a suction of the surrounding fluid into the jet. The jet grows and becomes slower according to the law of conservation of momentum. The velocity and the resulting pressure difference are therefore responsible for the quantity of the flue gas back-flow. However, as the applied velocity was already approximately 100 m/s, a further increase of this value would not be practical for such a combustion system.
An alternative strategy is to increase the volume of the burner. In the current design, the confined space of the burner resulted in a high internal flue gas velocity, which predefined the flow direction, forcing the flue gases to flow downstream in the burner, thus suppressing the recirculation. Moreover, the narrow space between the nozzle and the burner wall, and the small distances between the nozzles themselves, disturbed the formation of the recirculation.
Offering the flue gas more space decreases the average velocity in the chamber, and creates zones where recirculation can be efficiently built. Moreover, the introduction of flame tubes and modifications to the nozzle geometry may also have a positive effect on the recirculation. Such design optimization and its experimental validation is presented by Berger and Zieba [132] in the final report of the project focusing on the development of the LCVG burner for landfill residue gases. In this study, the same methodology as in Chapter 2.1 and 2.2 was used. The exemplary results of the CFD analysis are shown in Figure 25. In this case, a multi-nozzle geometry was also applied and adapted for the LCVG fuel. As the landfill gas and the combustion air were introduced in the combustion chamber at ambient temperature, the geometry of the burner had to be optimized to increase the recirculation rate and to ensure proper ignition and stable combustion of the applied LCVG fuel.

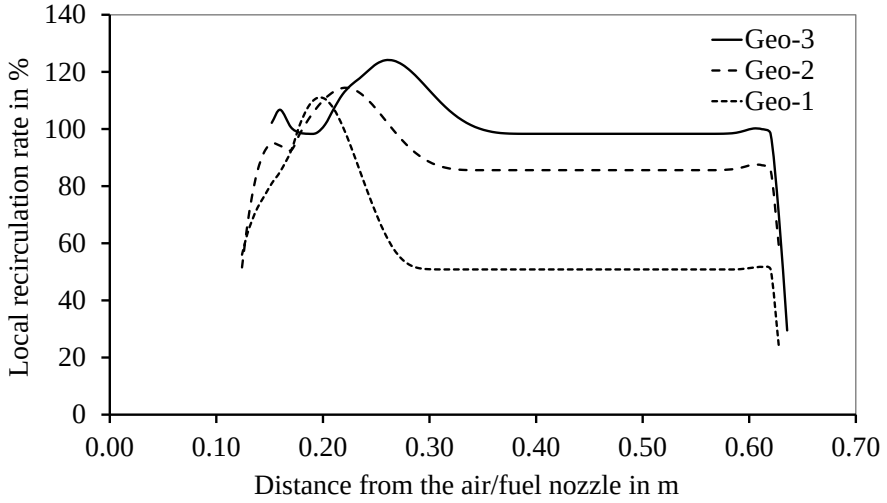

Figure 25 Local recirculation rate for three geometry variations of landfill residue gas burner. Based on results obtained in [132]

The CFD analysis showed that the geometry has a significant impact on the recirculation and thus plays a crucial role on the combustion process. By using an optimized flame tube and nozzle design (Geo-3), it was possible to increase the local recirculation up to approximately 120 %. The experimental results obtained and published in [132] confirmed the positive role of the recirculation rate on the combustion stability and the pollutant emissions. Nevertheless, also in this case, the multi-nozzle design showed its limitation when considering the local recirculation rate. A further increase of the burner volume or velocities of the air jets is necessary to increase the recirculation.

The optimum design studied within this thesis, and thus the highest recirculation rates, were obtained using a single nozzle burner used for the experimental and modelling studies in Chapters 2.3, 2.4 and 2.5. In this setup, the burner nozzle was arranged at the front wall of the combustion chamber of a much larger diameter than that of the nozzle itself. There is no interference with other nozzles. The entire combustion volume can be used to build the recirculation. If the combustion chamber is large enough, the centrally arranged jet can develop almost in an open space without disturbance of the wall. The comparison of the recirculation principle for multi-nozzle and single-nozzle design is shown in Figure 26.

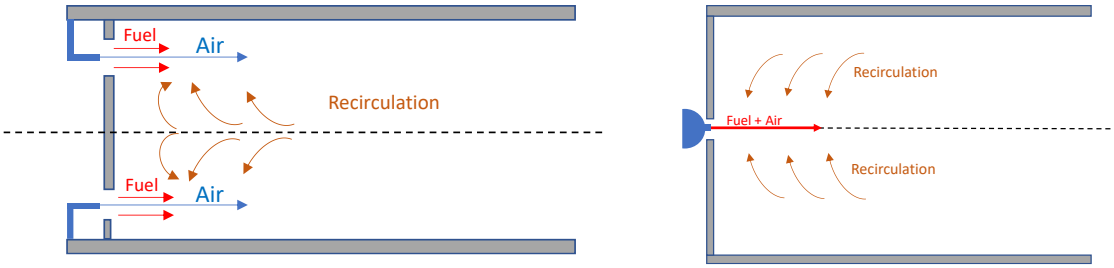

Figure 26 Comparison of the recirculation principle for multi-nozzle (left) and single-nozzle (right) design

The studies described in Chapter 2.5 showed that the recirculation ratios obtained using the 20 kW single-nozzle burner arranged in an isolated combustion chamber with a diameter of 0.6 m were significantly higher than for the multi-nozzle design analyzed in Chapters 2.1 and 2.2.

Such design is considered as being optimal to achieve the maximum recirculation ratios. The results presented in Chapter 2.5 showed that all modelled jets behaved in a very similar fashion, as it could be expected from the free jet theory. In all three cases, the jet grew until it faced the turn-back point placed near to the back wall of the combustion chamber. The mass flow of the jet at the maximum point was approximately 10 times bigger than the inlet mass flow of the fuel and air. From this perspective, a single-nozzle flameless burner in connection with a combustion chamber of high volume seems to be the most advantageous design for combustion of LCVG.

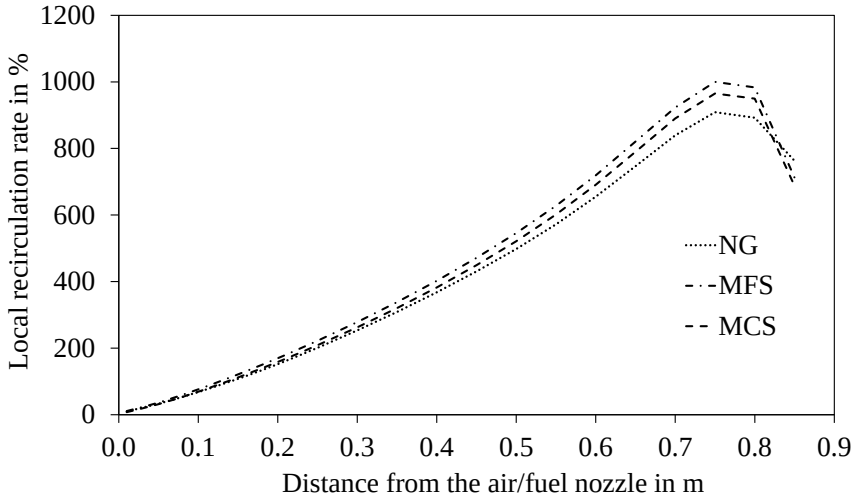

Figure 27 Local recirculation ratio for single-nozzle system according to the results described in Chapter 2.5 where NG – natural gas; MCS – methane containing syngas; MFS – methane-free syngas

3.2 On fuel-NO_x conversion in combustion systems with integrated flameless burners

The main topic of the research presented in this thesis is the fate of fuel N in combustion systems with integrated flameless burners. The early research on this topic was conducted by Schuster and is presented in the experimental part of the papers enclosed in Chapters 2.1 and 2.2. Detailed analysis of the data obtained during the experiments is further described by Schuster in [9]. The studies mentioned are the only sources found in the literature where a direct comparison of the same combustion system fuel with a conventional and flameless burner is provided. In both cases, the systems were fired with the same fuels: stem wood (wood chips), wheat husks and rapeseed cake pellets. For all fuels, the combustion parameters such as stability, burn-out and excess oxygen were improved. Only for the NOx, there was a very minor improvement for woody fuels but a general worsening for high N-content fuels when a flameless burner was applied. The experimental work done by Schuster was realized using a multi-nozzle burner design described in detail in Subchapter 3.1.

In this thesis research, further experimental work was performed in a test rig consisting of a gasifier and a single-nozzle flameless burner (see Chapter 2.4). Two fuels, pellets made of spruce wood and rapeseed cake pellets (very similar fuels were used in the experiments of Schuster) were gasified and the generated syngas was subsequently combusted. For better comparison of the obtained NO_x emissions with the data published in other literature sources, the data provided in Chapter 2.4 were recalculated in terms of the conversion of the N contained in the fuel to the N emitted in the flue gases as NO_x. For this purpose, the fuel data for the

spruce wood pellets used were supplemented with more detailed information about the N content of N_{dry} = 0.15 % [10].

The fuel-N conversion ratios allow the assessment of the entire process, beginning with the solid fuel as input into the conversion process and ending with the flue gas as the output of the flameless combustion step. The resulting conversion ratios are shown in
Figure 28.

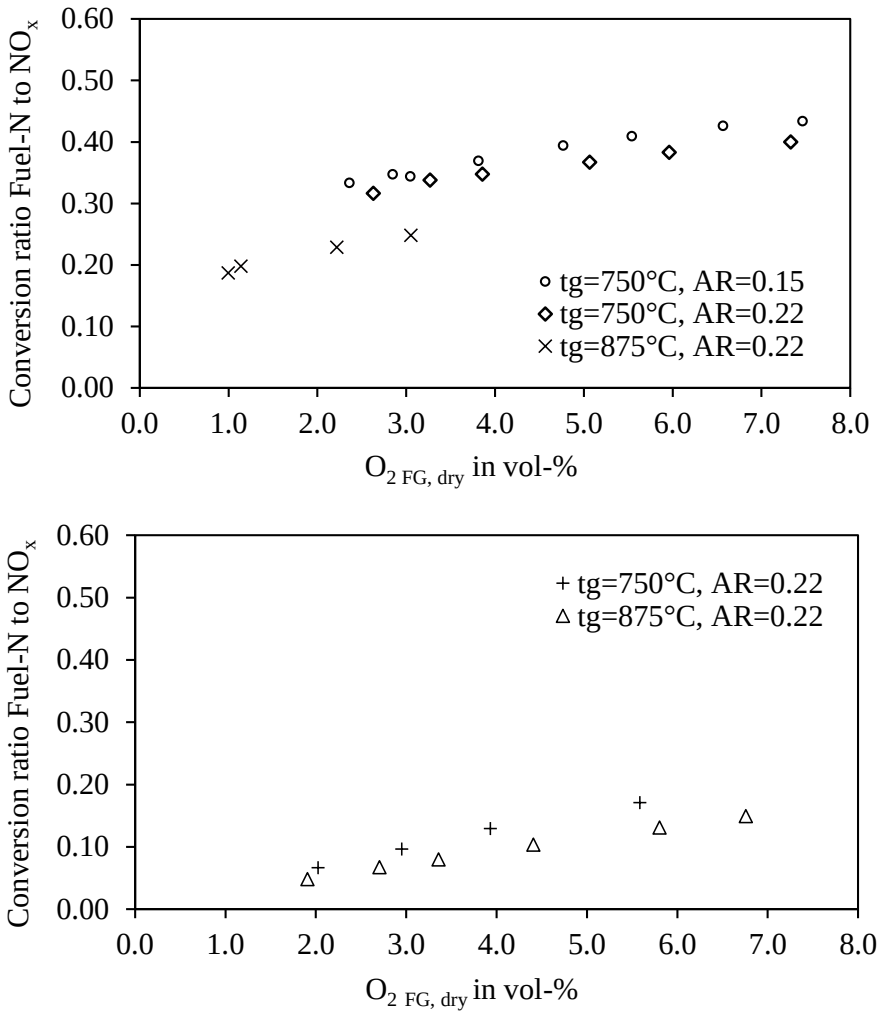

Figure 28 N conversion ratios for wood pellets and rapeseed cake pellets calculated based on data from Chapter 2.4

The fuel-N conversion ratios were plotted against the excess oxygen content in the flue gas. The conversion ratios obtained for the woody biomass were between 0.2 and 0.4, while the conversion ratios obtained for the rapeseed cake pellets were lower and were between 0.05 and 0.15. The NO_x emissions, and consequently the conversion ratios, were strongly dependent on the gasifier temperature and the burner stoichiometry at which the gasifier product gases were combusted. The best values of 0.05 were recorded for higher gasifier temperatures of 850 °C

and very low excess oxygen of approximately 2 %. At these low O_2 levels, the combustion was still very robust, and the emissions of CO (not presented here) were very low (below the detection limit of the analyzer). Firstly, at oxygen levels significantly below 2 %, the CO levels rapidly increased and the combustion process became unstable. Despite much higher O_2 levels in the pre-gasifier, the results reported by Schuster [9] for the rapeseed cake pellets were similar. The fuel-N conversion ratio of 0.049 – 0.051 at very low CO levels was also observed.

For woody biomass, the NO_x emissions obtained in a single-nozzle burner were between 100 and 125 mg/m^3_{stp} and were thus slightly lower than the emissions reported by Schuster in [9], which were up to 150 mg/m^3_{stp}. Both values were recalculated to O_2 = 13 % reference O_2 level in the flue gas. Schuster did not publish the fuel-N conversion ratios for this fuel.

In a similar fashion to what was observed for rapeseed cake pellets, a stable combustion took place at very low excess O_2, and the first CO peaks were observed at excess O_2 levels below 1 %. Therefore, it must be considered that all reported NO_x emissions for the single nozzle flameless burner were at almost zero CO levels and very low excess O_2 levels. Such efficient operation and completeness of combustion is not achievable for any conventional biomass combustion systems found in the literature. On the other hand, in the tested combustion system there is no further possibility to decrease the NO_x by increasing the CO emissions, as these occur rapidly and are of very high levels due to very low oxygen concentration. At such conditions, the combustion cannot be controlled any more.

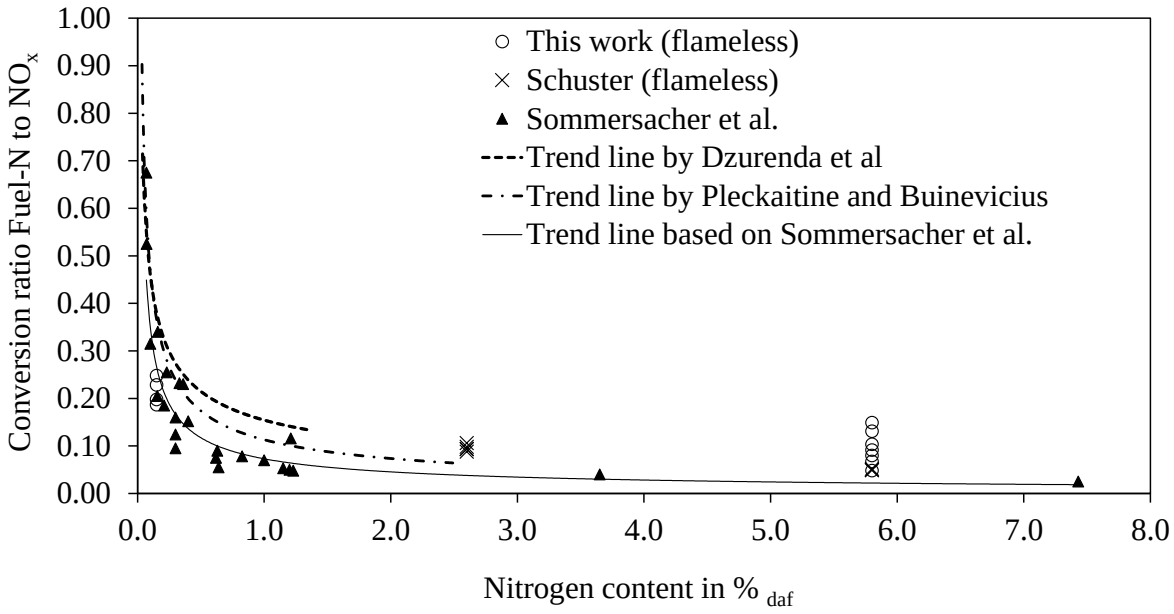

Figure 29 Fuel-N conversion for various fuels and combustion systems based on data obtained in this work in comparison to data published in [9, 22, 133–135]

A comparison of the data obtained for flameless combustors with other literature data for conventional solid biomass combustion systems is shown in Figure 29. The trend line proposed

by Dzurenda et al. [134] is based on the results from the operation of 16 different modern grate boilers with a thermal output between 300 – 2500 kW_{th}. The N content of the solid fuels tested was in the range between N_{daf} = 0.04 – 1.3 %. All boilers were operated at CO levels of approximately 500–600 $mg/m^3_{stp.}$ at 11 % O_2. The trend line proposed by Pleckaitine and Buinevicius is based on data obtained from a small-sized boiler installation with staged air. The N content of the solid fuels tested was in the range between N_{daf} = 0,021–2,5 %. The measured CO concentrations were spread between a few hundred up to 2000 $mg/m^3_{stp.}$ at 11 % O_2. The data published by Sommersacher et al. [22] contained results from pilot- and real-scale combustion tests on large facilities. All combustion plants were based on grate firing and have geometrically separated primary and secondary combustion zones for efficient air staging. The primary air ratio was typically between 0.6 and 0.9, and the overall air ratio applied was between 1.4 and 1.6. The size of the real scale facilities was up to 110 MW_{th}. The N content of the tested fuels was up to N_{daf} = 7.5 %. All the facilities used in the cited study represent the current state-of-the-art technology.

The results for low fuel-N fuel such as wood pellets showed that the conversion ratios are at a similar level to the results obtained in state-of-the-art large-scale grate boilers. The results obtained were better than the conversion ratios reported by Dzurenda et al. [134] or Pleckaitine and Buinevicius [135]. However, the results for high N content fuels obtained in this work or by Schuster [9] were higher than the data reported by Sommersacher et al. [22]. Particularly when considering the data obtained using higher burner air ratios, the difference becomes significant. Nevertheless, as mentioned above, the recorded conversion ratios were obtained at excellent burn-out at a very low O_2 level. Therefore, it became apparent that the advantage of the excellent mixing, which is responsible for complete oxidation of all residual combustibles in the flue gas, is also responsible for "good" oxidation of the NO_x precursors contained in the syngas.

3.3 On NO_x formation and the role of gas composition and mixing process

The results of the experimental work presented in Chapter 2.3 showed that the CH_4 presence in the fuel has a significant effect on the oxidation rate of NH_3 in the tested burner. The NH_3 conversion to NO_x increases rapidly when increasing the CH_4 content. When no CH_4 is present in the fuel, the NH_3 mostly converts to N_2, which results in very low NO_x emissions. On the other hand, the CO/H_2 ratio seems to not influence the NH_3 oxidation process at the investigated concentrations.

The detailed analysis of this phenomenon is described in the paper included in Chapter 2.5. It has been clearly shown that, depending on the CH_4 concentration, the combustion regime changes from mixing-controlled to kinetic-controlled when CH_4 is present in the fuel. This occurs due to much slower CH_4 oxidation process in comparison to pure CO/H_2 mixtures. Moreover, as the CH_4 decomposition process prohibits the NH_3 breakdown, the location of NH_3

conversion is pushed deeper in the combustion chamber towards lean combustion conditions, resulting in higher oxidation rates to NO_x. For a better visualization of this phenomenon, the NH_3 normalized flux and the local air ratio along the jet was plotted against the distance from the burner nozzle in Figure 30.

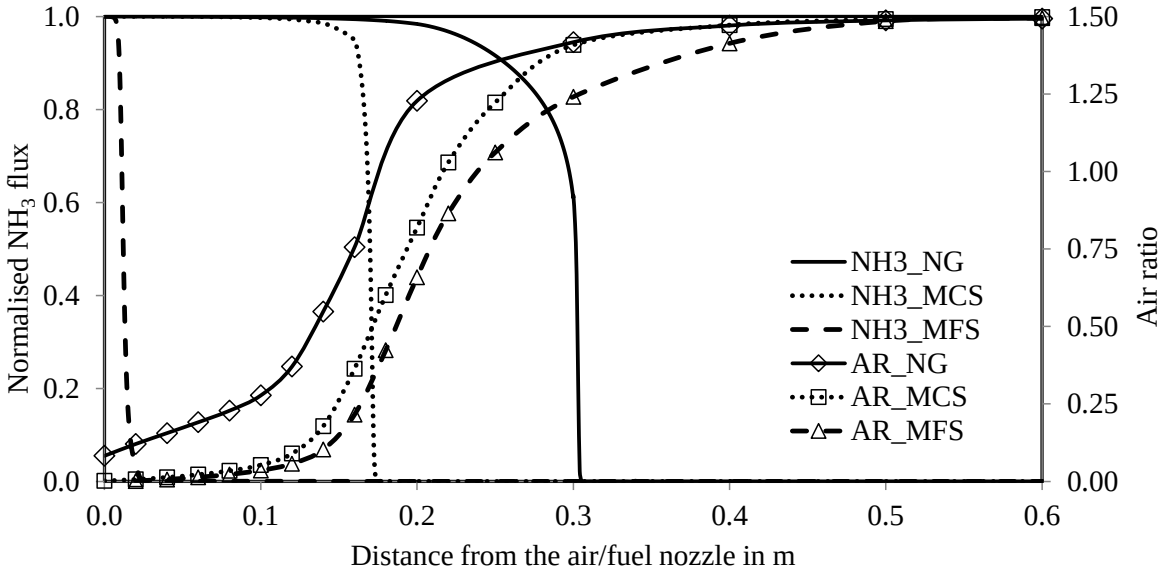

Figure 30 Normalized flux of NH_3 and local air ratio against the distance from the air/fuel nozzle, as based on the results from Chapter 2.5 where NG – natural gas; MCS – methane containing syngas; MFS – methane-free syngas

The fact that the combustion and the NO_x formation for natural gas are kinetic-controlled processes, also explains the good level of agreement between the experimental data and both fuel-into-air and air-into-fuel mixing approaches as shown in Figure 5 in Chapter 2.5. With the declining content of CH_4, the deviation between experiments and the modelling results for the fuel-into-air mixing approach increased. It can therefore be concluded that the less CH_4 in the fuel, the more important the correct representation of the mixing process becomes, as this controls the overall NO_x formation. Only the air-into-fuel mixing approach could correctly reproduce the experimental results.

In the framework of additional scientific work, the air-into-fuel mixing approach was reconsidered and revalidated to achieve even better NO_x prediction performance. Instead of linear air distribution along the modelled jet, it was proposed to distribute the air according to the mixture fraction value ξ (see Eq 3) derived from the CFD modelling. The origin approach systematically overestimated the in-mixing process of the air, and thus led to higher O_2 concentrations at the beginning of the jet. Using the new approach, here called the "advance mixing approach," the air was introduced slower as shown in Figure 31.

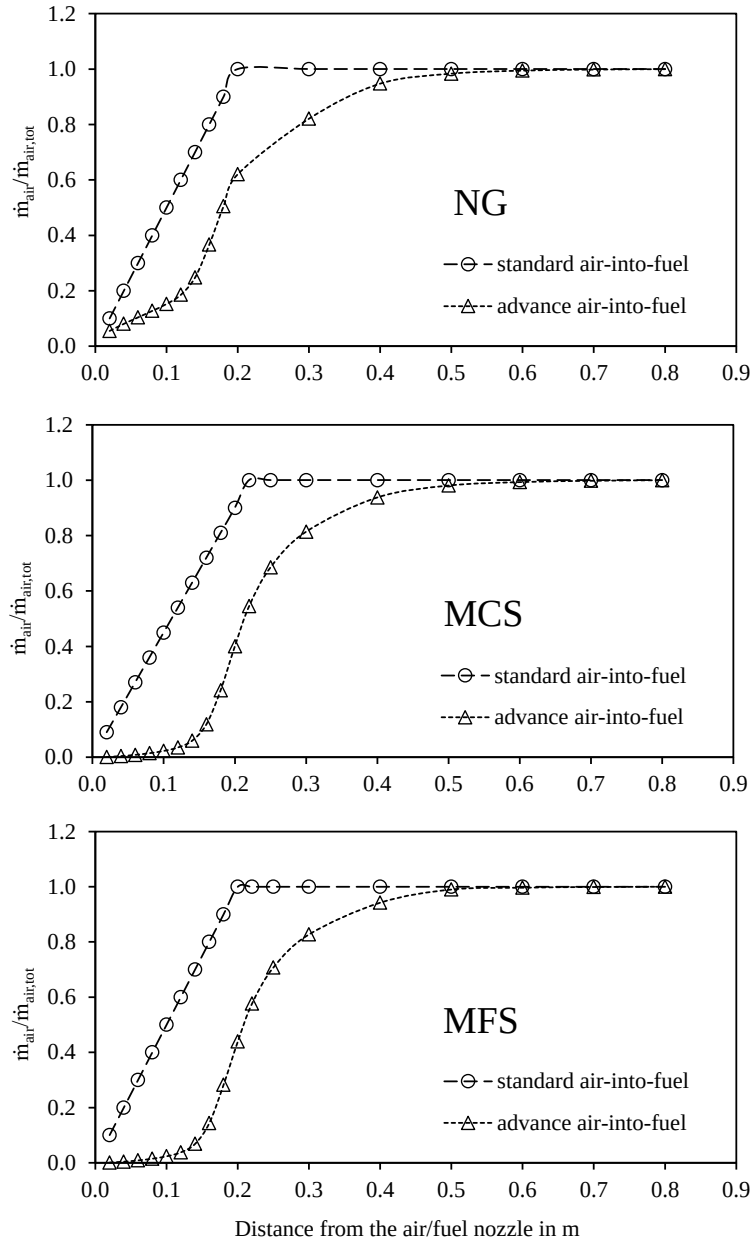

Figure 31 Comparison of the normalized air distribution for the standard (as used in Chapter 2.5) and advanced mixing approach for NG, MCS and MFS where NG – natural gas; MCS – methane containing syngas; MFS – methane-free syngas

The slightly different air distribution led to lower NOx emission predictions for all simulated NH_3 concentrations and fuel compositions. For the NG, the application of the advanced mixing approach caused an underestimation of NO_x values in the whole range of tested NH_3 concentrations, and this increased with increasing NH_3 content. When considering the MCS and MFS, much better results were achieved using the new mixing approach. As this type of

fuel is much more representative of real processes, the advanced mixing approach was regarded as being the best choice when modelling the NO_x emissions for flameless burners.

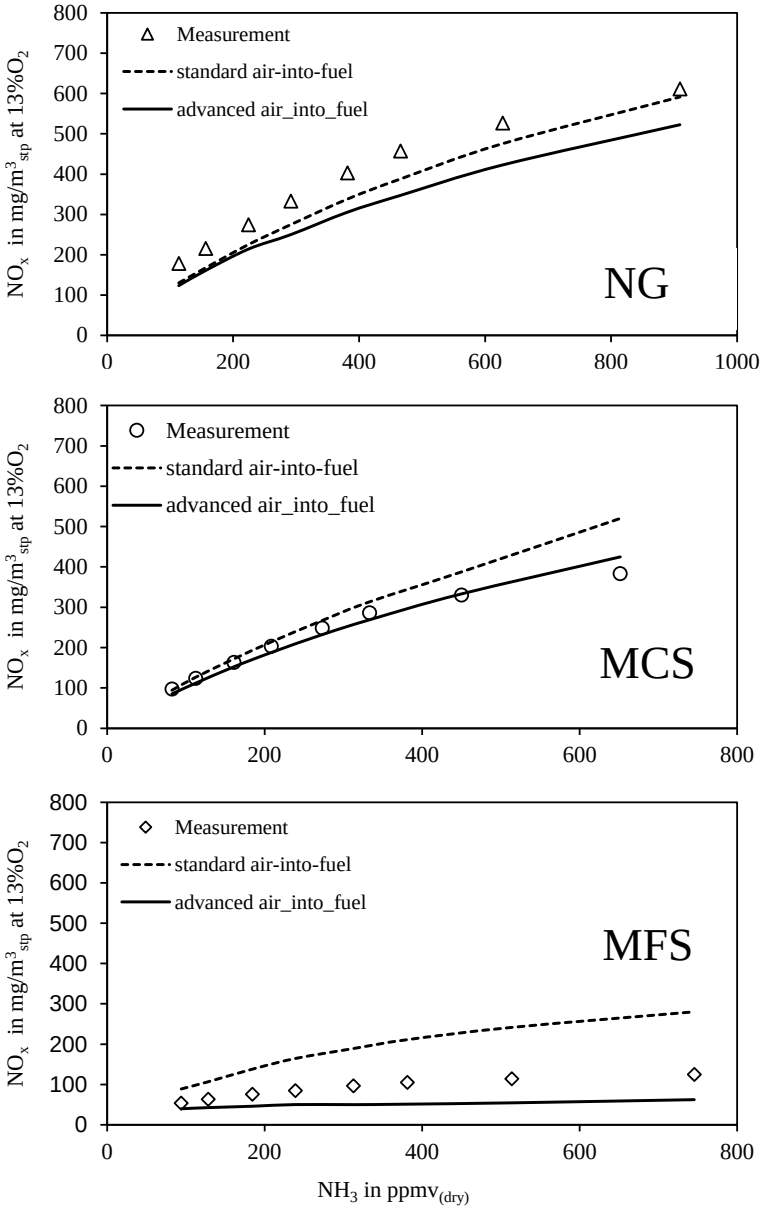

Figure 32 Comparison of the experimental and modelling results for NG, MCS and MFG using the standard and advanced mixing approach where NG – natural gas; MCS – methane containing syngas; MFS – methane-free syngas

3.4 Outlook – next steps towards the development of low-NO_x flameless burners

Because it is not practically possible to significantly decrease the CH_4 content in syngases to decrease the NO_x, the only way to achieve better emissions is to optimize the gasifier parameters and to apply an air staging in the burner itself. The influence of the gasifier parameters on the

NO_x levels were shown and discussed in Chapter 2.4. The first work on the air-staged burner was presented in the Chapter 2.2. However, this study was limited to the investigation of the flow pattern only, without any prediction on the NO_x emission reduction due to the lack of correct numerical models. Because the two-step model proposed in Chapter 2.5 was successfully validated against the experimental data, its further development should be considered to predict the possible impact of the air staging under flameless conditions on the NO_x emissions and to derive the optimum geometry and operating parameters.
The rector network model can be reconsidered to represent two independent combustion volumes, each with its own air distribution and flue gas recirculation, as outlined in Figure 33.

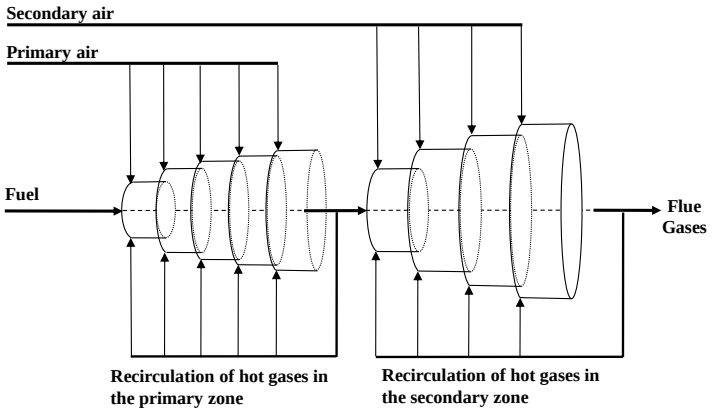

Figure 33 Schematic representation of a reactor network model for air-staged flameless combustion

The parameters for the air and flue gas distribution could be derived from additional CFD modelling or could be considered to be the same for the first combustion stage as it was already applied in the model presented in Chapter 2.5. The parameters for the second stage can be set up as assuming that a new jet is formed in the separate combustion volume that behaves similarly (jet propagation and mixing ratio) to the initial jet in the primary zone.
As a further measure to decrease the NO_x, the separation of the main fuel inlet from the air injection point should be considered. The positive effect of such separation was already observed by the development of the flameless burners for pulverized coal [96]. The respective reactor network model representation must consider the initial mixing of the air with the recirculated flue gases before the mixing with the fuel jet. This measure can be applied together with the air staging to intensify the effect of NO_x reduction.

4 Summary

In the present work, experimental and modelling studies on the development and optimization of the flameless technology for low-grade biofuel applications were presented. The work built on the experimental results reported by Schuster [9] related to the development of the multi-nozzle flameless burner combined with the biomass pre-gasifier.
The investigation presented within this work covers research results from the application of the CFD modelling for simple flow pattern studies, via experimental work on the fuel-NOx formation using two different test rigs, up to the development and validation of a two-step numerical model for detailed analysis of NOx formation and reduction mechanisms. The results also provided an explanation for the relatively high NOx emissions observed during the experimental work. The main conclusion and achievements can be summarized as follows:

Conclusions and achievements concerning technology development

- The recirculation built in the combustion volume using a single nozzle design burner was much greater than what was observed when modelling the multi-nozzle design.

- A lab-scale infrastructure for flameless combustion of synthetic gases from different sources (mixing station, gasifier) with the possibility of additional NH_3 doping of fuels was developed.

- When combusting NH_3 doped synthetic gases, the NH_3 to NO_x conversion was highly dependent on the CH_4 concentration in the fuel. It significantly increased with the CH_4 content. The CO/H_2 ratio had no measurable influence on the NH_3 conversion.

- When increasing the CH_4 content, the combustion regime and thus the NH_3 conversion process is changing from mixing-controlled to kinetic-controlled causing NH_3 to react under O_2 rich conditions.

- When gasifying solid biomass and combusting the product gases in the flameless burner, it was observed that the final NO_x emission depended on the initial N content in the fuel, the gasifier parameters, and the final stoichiometry of the burner.

- For the fuels with lower N content (for example wood), the NOx emissions, thus N to NOx conversion ratios, were comparable (or even better) to other combustion technologies.

- For high-N content fuels, the conversion ratios were higher in comparison to other combustion technologies.

- The higher temperature in the gasifier and higher stoichiometry, the better NO_x emission can be achieved in the flameless burner.

- Due to perfect mixing conditions, it is possible to operate the flameless burners for LCVG at very low excess oxygen, simultaneously achieving CO emissions at the level of a few ppm. This makes the comparison of the recorded NO_x emissions with other combustion technologies difficult where significant CO concentrations are reported.

Conclusions and achievements concerning mathematical modeling

- CFD analysis with a global chemistry model is a suitable tool for the proper geometry design to optimize the fluid flow in a flameless combustor.

- The methodology to calculate the recirculation was introduced to the software code by the calculation of the local recirculation rate for quantitative analysis of the flue gas flow pattern.

- A two-stage numerical model was developed for the combustion and pollutant formation analysis.

- Two different detailed chemistry schemes were validated, identifying both suitable to predict NOx emissions for methane containing gases

- Three different mixing approaches were applied and validated, showing that the proper mixing representation is crucial when modelling gases with lower CH_4 content.

Due to the excellent combustion performance, the flameless technology seems to be perfectly suitable for utilization of difficult LCVG fuels, even if there is still some work necessary to decrease the potential NO_x emission from fuel bound N. It must be considered that the NO_x emissions reported in this work were measured at CO concentrations at the levels of detection limit using a commercial type of burner that was developed for the combustion of NG. A possible way for further NO_x emission reduction is the application of primary measures such as air and fuel staging. The optimal design and operating parameters could be derived using the tools and methods developed and validated within this work.

5 Bibliography

[1] EUROPEAN COMMISSION: *2030 Climate Target Plan - Stepping up Europe's 2030 climate ambition Investing in a climate-neutral future for the benefit of our people* (idF v. COM/2020/562 final) (2020), EUR-Lex - 52020DC0562 - EN

[2] PRICEWATERHOUSECOOPERS EU: *Sustainable and optimal use of biomass for energy in the EU beyond 2020*. URL https://ec.europa.eu/energy/sites/default/files/documents/biosustain_report_final.pdf. – Aktualisierungsdatum: 2018-02-16

[3] FEHRENBACH, Horst ; GIEGRICH, Jürgen ; KÖPPEN, Susanne ; WERN, Bernhard ; PERTAGNOL, Joachim ; BAUR, Frank ; HÜNECKE, Katja ; DEHOUST, Günter ; BULACH, Winfried ; WIEGMANN, Kirsten: *BioRest: Verfügbarkeit und Nutzungsoptionen biogener Abfall- und Reststoffe im Energiesystem (Strom-, Wärme- und Verkehrssektor)*. In: *Texte Umweltbundesamt* (2019), Nr. 115

[4] NUSSBAUMER, Thomas: *Potenzial und Technik zur Holzenergie-Nutzung* : *17. September 2010, ETH Zürich*. Bern : ENET, 2010

[5] VICENTE, E. D. ; ALVES, C. A.: *An overview of particulate emissions from residential biomass combustion*. In: *Atmospheric Research* 199 (2018), S. 159–185

[6] TISSARI, J. ; LYYRÄNEN, J. ; HYTÖNEN, K. ; SIPPULA, O. ; TAPPER, U. ; FREY, A. ; SAARNIO, K. ; PENNANEN, A. S. ; HILLAMO, R. ; SALONEN, R. O. ; HIRVONEN, M.-R. ; JOKINIEMI, J.: *Fine particle and gaseous emissions from normal and smouldering wood combustion in a conventional masonry heater*. In: *Atmospheric Environment* 42 (2008), Nr. 34, S. 7862–7873

[7] KLIPPEL, N. ; NUSSBAUMER, T. ; ETA-RENEWABLE ENERGIES ; WIP-RENEWABLE ENERGIES: V2B.V.9 Health Relevance of Combustion Particles from Automatic Wood Furnaces and Diesel Engines Indicated by Cytotoxicity. In: . Florence:, Paris : ETA srl,, 2005, S. 1292–1295

[8] OZGEN, S. ; CERNUSCHI, S. ; CASERINI, S.: *An overview of nitrogen oxides emissions from biomass combustion for domestic heat production*. In: *Renewable and Sustainable Energy Reviews* 135 (2021), S. 110113

[9] SCHUSTER, Anja: *Entwicklung eines Schwachgasbrenners basierend auf der Flammlosen Oxidation zur Optimierung einer Vorofenfeuerung und thermischen Verwertung von biogenen Reststoffen im dezentralen Bereich*. Zugl.: Stuttgart, Univ., Diss., 2011. 1. Aufl. Göttingen : Cuvillier, 2011

[10] KALTSCHMITT, Martin (Hrsg.); HARTMANN, Hans (Hrsg.); HOFBAUER, Hermann (Hrsg.): *Energie aus Biomasse* : *Grundlagen, Techniken und Verfahren*. 3., aktualisierte Aufl. 2016. Berlin, Heidelberg : Springer Berlin Heidelberg, 2016 (SpringerLink : Bücher)

[11] *DIN EN ISO 17225-1:2014-09, Biogene Festbrennstoffe_- Brennstoffspezifikationen und -klassen_- Teil_1: Allgemeine Anforderungen (ISO_17225-1:2014); Deutsche Fassung EN_ISO_17225-1:2014*

[12] HARTMANN, Hans: Solid Biofuels, Fuels, and Their Characteristics. In: MEYERS, Robert A. (Hrsg.): *Encyclopedia of Sustainability Science and Technology*. New York, NY : Springer New York, 2017, S. 1–36

[13] ISLAS, Jorge ; MANZINI, Fabio ; MASERA, Omar ; VARGAS, Viridiana: Solid Biomass to Heat and Power. In: *The Role of Bioenergy in the Bioeconomy* : Elsevier, 2019, S. 145–177

[14] GARCÍA, Roberto ; PIZARRO, Consuelo ; LAVÍN, Antonio G. ; BUENO, Julio L.: *Spanish biofuels heating value estimation. Part I: Ultimate analysis data*. In: *Fuel* 117 (2014), S. 1130–1138

[15] GARCÍA, Roberto ; PIZARRO, Consuelo ; LAVÍN, Antonio G. ; BUENO, Julio L.: *Spanish biofuels heating value estimation. Part II: Proximate analysis data*. In: *Fuel* 117 (2014), S. 1139–1147

[16] VASSILEV, Stanislav V. ; BAXTER, David ; ANDERSEN, Lars K. ; VASSILEVA, Christina G.: *An overview of the chemical composition of biomass*. In: *Fuel* 89 (2010), Nr. 5, S. 913–933

[17] ELTROP, Ludger ; HARTMANN, Hans ; HEINRICH, Peter ; JAHRAUS, Birgit ; KALTSCHMITT, Martin ; RAAB, Konrad ; SCHNEIDER, Sven ; SCHRÖDER, Gerd: *Leitfaden Bioenergie* : *Planung, Betrieb und Wirtschaftlichkeit von Bioenergieanlagen*. 4., vollständig überarbeitete Auflage. Gülzow b Güstrow : Fachagentur Nachwachsende Rohstoffe, 2014

[18] FRANCO-NAVARRO, Juan D. ; ROSALES, Miguel A. ; CUBERO-FONT, Paloma ; CALVO, Purificación ; ÁLVAREZ, Rosario ; DIAZ-ESPEJO, Antonio ; COLMENERO-FLORES, José M.: *Chloride as a macronutrient increases water-use efficiency by anatomically driven reduced stomatal conductance and increased mesophyll diffusion to CO2*. In: *The Plant journal : for cell and molecular biology* 99 (2019), Nr. 5, S. 815–831

[19] NUSSBAUMER, Thomas: *Combustion and Co-combustion of Biomass: Fundamentals, Technologies, and Primary Measures for Emission Reduction †*. In: *Energy & Fuels* 17 (2003), Nr. 6, S. 1510–1521

[20] MICHAËL BECIDAN: *Experimental Studies on Municipal Solid Waste and Biomass Pyrolysis*. Theses at NTNU, 2007:125

[21] CONESA, J. A. ; FULLANA, A. ; FONT, R.: *Thermal decomposition of meat and bone meal*. In: *Journal of Analytical and Applied Pyrolysis* 70 (2003), Nr. 2, S. 619–630

[22] SOMMERSACHER, Peter ; BRUNNER, Thomas ; OBERNBERGER, Ingwald: *Fuel Indexes: A Novel Method for the Evaluation of Relevant Combustion Properties of New Biomass Fuels*. In: *Energy & Fuels* 26 (2012), Nr. 1, S. 380–390

[23] STEENARI, B.-M. ; LINDQVIST, O.: *High-temperature reactions of straw ash and the anti-sintering additives kaolin and dolomite*. In: *Biomass and Bioenergy* 14 (1998), Nr. 1, S. 67–76

[24] KOPPEJAN, Jaap ; VAN LOO, Sjaak: *Handbook of biomass combustion and co-firing* : *Prepared by Task 32 of the Implementing Agreement on Bioenergy*. Reprinted with minor corr. Enschede : Twente Univ. Press, 2003

[25] KNUDSEN, Jacob N. ; JENSEN, Peter A. ; DAM-JOHANSEN, Kim: *Transformation and Release to the Gas Phase of Cl, K, and S during Combustion of Annual Biomass*. In: *Energy & Fuels* 18 (2004), Nr. 5, S. 1385–1399

[26] FACHAGENTUR NACHWACHSENDE ROHSTOFFE E.V.: *Biomethane*. URL https://mediathek.fnr.de/media/downloadable/files/samples/b/i/biomethane.pdf

[27] VOHRA, Mustafa ; MANWAR, Jagdish ; MANMODE, Rahul ; PADGILWAR, Satish ; PATIL, Sanjay: *Bioethanol production: Feedstock and current technologies*. In: *Journal of Environmental Chemical Engineering* 2 (2014), Nr. 1, S. 573–584

[28] SADHUKHAN, Anup Kumar ; GUPTA, Parthapratim ; GOYAL, Tripurari ; SAHA, Ranajit Kumar: *Modelling of pyrolysis of coal-biomass blends using thermogravimetric analysis*. In: *Bioresource technology* 99 (2008), Nr. 17, S. 8022–8026

[29] ROY, Poritosh ; DIAS, Goretty: *Prospects for pyrolysis technologies in the bioenergy sector: A review*. In: *Renewable and Sustainable Energy Reviews* 77 (2017), S. 59–69

[30] AMENAGHAWON, Andrew N. ; ANYALEWECHI, Chinedu L. ; OKIEIMEN, Charity O. ; KUSUMA, Heri Septya: *Biomass pyrolysis technologies for value-added products: a state-of-the-art review*. In: *Environment, Development and Sustainability* (2021)

[31] MOLINO, Antonio ; CHIANESE, Simeone ; MUSMARRA, Dino: *Biomass gasification technology: The state of the art overview*. In: *Journal of Energy Chemistry* 25 (2016), Nr. 1, S. 10–25

[32] STRZALKA, Rafal ; SCHNEIDER, Dietrich ; EICKER, Ursula: *Current status of bioenergy technologies in Germany*. In: *Renewable and Sustainable Energy Reviews* 72 (2017), S. 801–820

[33] PATUZZI, Francesco ; BASSO, Daniele ; VAKALIS, Stergios ; ANTOLINI, Daniele ; PIAZZI, Stefano ; BENEDETTI, Vittoria ; CORDIOLI, Eleonora ; BARATIERI, Marco: *State-of-the-art*

of small-scale biomass gasification systems: An extensive and unique monitoring review. In: *Energy* 223 (2021), S. 120039

[34] SIEDLECKI, Marcin ; JONG, Wiebren de ; VERKOOIJEN, Adrian H.M.: *Fluidized Bed Gasification as a Mature And Reliable Technology for the Production of Bio-Syngas and Applied in the Production of Liquid Transportation Fuels—A Review*. In: *Energies* 4 (2011), Nr. 3, S. 389–434

[35] BRIDGWATER, A.V: *Renewable fuels and chemicals by thermal processing of biomass*. In: *Chemical Engineering Journal* 91 (2003), 2-3, S. 87–102

[36] LEPAGE, Thibaut ; KAMMOUN, Maroua ; SCHMETZ, Quentin ; RICHEL, Aurore: *Biomass-to-hydrogen: A review of main routes production, processes evaluation and techno-economical assessment*. In: *Biomass and Bioenergy* 144 (2021), S. 105920

[37] DAHMEN, Nicolaus ; ABELN, Johannes ; EBERHARD, Mark ; KOLB, Thomas ; LEIBOLD, Hans ; SAUER, Jörg ; STAPF, Dieter ; ZIMMERLIN, Bernd: *The bioliq process for producing synthetic transportation fuels*. In: *WIREs Energy and Environment* 6 (2017), Nr. 3

[38] SEINFELD, John H. ; PANDIS, Spyros N.: *Atmospheric chemistry and physics* : *From air pollution to climate change*. 3rd edition. Hoboken, New Jersey : Wiley, 2016

[39] ZELDOVICH, Y. B. ; SADOVNIKOV, P. Y. AND FRANK-KAMENETSKII, D. A.: *The oxidation of nitrogen in combustion and explosions*. In: *Acta Physicochemica USSR* (1946), Nr. 21, S. 577–628

[40] LAVOIE, GEORGE A. ; HEYWOOD, JOHN B. ; KECK, JAMES C.: *Experimental and Theoretical Study of Nitric Oxide Formation in Internal Combustion Engines*. In: *Combustion Science and Technology* 1 (1970), Nr. 4, S. 313–326

[41] FENIMORE, C. P.: *Formation of nitric oxide in premixed hydrocarbon flames*. In: *Symposium (International) on Combustion* 13 (1971), Nr. 1, S. 373–380

[42] MILLER, James A. ; BOWMAN, Craig T.: *Mechanism and modeling of nitrogen chemistry in combustion*. In: *Progress in Energy and Combustion Science* 15 (1989), Nr. 4, S. 287–338

[43] GLARBORG, Peter ; MILLER, James A. ; RUSCIC, Branko ; KLIPPENSTEIN, Stephen J.: *Modeling nitrogen chemistry in combustion*. In: *Progress in Energy and Combustion Science* 67 (2018), S. 31–68

[44] GLARBORG, P. ; JENSEN, A.D ; JOHNSSON, J.E: *Fuel nitrogen conversion in solid fuel fired systems*. In: *Progress in Energy and Combustion Science* 29 (2003), Nr. 2, S. 89–113

[45] GREUL, Ulrich: *Experimentelle Untersuchung feuerungstechnischer NOx-Minderungsverfahren bei der Kohlenstaubverbrennung*. Zugl.: Stuttgart, Univ., Diss. Düsseldorf : VDI Verl., 1998 (Fortschritt-Berichte / VDI Reihe 6, Energietechnik 388)

[46] GIUNTOLI, Jacopo ; JONG, Wiebren de ; VERKOOIJEN, Adrian H. M. ; PIOTROWSKA, Patrycja ; ZEVENHOVEN, Maria ; HUPA, Mikko: *Combustion Characteristics of Biomass Residues and Biowastes: Fate of Fuel Nitrogen*. In: *Energy & Fuels* 24 (2010), Nr. 10, S. 5309–5319

[47] LEPPÄLAHTI, Jukka: *Behaviour of fuel-bound nitrogen in gasification and in high-temperature NH_3 removal processes*. Zugl.: Espoo, Univ., Diss., 1998. Espoo : Technical Research Centre of Finland, 1998 (VTT publications 369)

[48] DI NOLA, Gianluca: *Biomass fuel characterization for NO_x emissions in cofiring applications*. Phd dissertation : Delft University of Technology, 2007

[49] GIUNTOLI, Jacopo: *Characterization of 2nd generation biomass under thermal conversion and the fate of nitrogen*. [Delft] : Process and Energy, Faculty 3mE, Delft University of Technology, 2010

[50] WINTER, F. ; WARTHA, C. ; HOFBAUER, H.: *NO and N_2O formation during the combustion of wood, straw, malt waste and peat*. In: *Bioresource technology* 70 (1999), Nr. 1, S. 39–49

[51] ABELHA, P. ; GULYURTLU, I. ; CABRITA, I.: *Release Of Nitrogen Precursors From Coal And Biomass Residues in a Bubbling Fluidized Bed*. In: *Energy & Fuels* 22 (2008), Nr. 1, S. 363–371

[52] WERTHER, J. ; SAENGER, M. ; HARTGE, E.-U. ; OGADA, T. ; SIAGI, Z.: *Combustion of agricultural residues*. In: *Progress in Energy and Combustion Science* 26 (2000), Nr. 1, S. 1–27

[53] HANSSON, Karl-Martin ; SAMUELSSON, Jessica ; TULLIN, Claes ; ÅMAND, Lars-Erik: *Formation of HNCO, HCN, and NH_3 from the pyrolysis of bark and nitrogen-containing model compounds*. In: *Combustion and Flame* 137 (2004), Nr. 3, S. 265–277

[54] BECIDAN, Michaël ; SKREIBERG, Øyvind ; HUSTAD, Johan E.: *NO_x and N_2O Precursors (NH_3 and HCN) in Pyrolysis of Biomass Residues*. In: *Energy & Fuels* 21 (2007), Nr. 2, S. 1173–1180

[55] RIAZA, Juan ; MASON, Patrick ; JONES, Jenny M. ; GIBBINS, Jon ; CHALMERS, Hannah: *High temperature volatile yield and nitrogen partitioning during pyrolysis of coal and biomass fuels*. In: *Fuel* 248 (2019), S. 215–220

[56] HANSSON, K.: *Pyrolysis of poly-L-leucine under combustion-like conditions⋆*. In: *Fuel* 82 (2003), Nr. 6, S. 653–660

[57] REN, Qiangqiang ; ZHAO, Changsui: *Evolution of fuel-N in gas phase during biomass pyrolysis*. In: *Renewable and Sustainable Energy Reviews* 50 (2015), S. 408–418

[58] BASSILAKIS, R. ; CARANGELO, R.M ; WÓJTOWICZ, M.A: *TG-FTIR analysis of biomass pyrolysis*. In: *Fuel* 80 (2001), Nr. 12, S. 1765–1786

[59] DE JONG, W. ; PIRONE, A. ; WOJTOWICZ, M.: *Pyrolysis of Miscanthus Giganteus and wood pellets: TG-FTIR analysis and reaction kinetics*. In: *Fuel* 82 (2003), Nr. 9, S. 1139–1147

[60] DE JONG, W. ; DINOLA, G. ; VENNEKER, B. ; SPLIETHOFF, H. ; WOJTOWICZ, M.: *TG-FTIR pyrolysis of coal and secondary biomass fuels: Determination of pyrolysis kinetic parameters for main species and NOx precursors*. In: *Fuel* 86 (2007), Nr. 15, S. 2367–2376

[61] GIUNTOLI, J. ; JONG, W. de ; ARVELAKIS, S. ; SPLIETHOFF, H. ; VERKOOIJEN, A.H.M.: *Quantitative and kinetic TG-FTIR study of biomass residue pyrolysis: Dry distiller's grains with solubles (DDGS) and chicken manure*. In: *Journal of Analytical and Applied Pyrolysis* 85 (2009), 1-2, S. 301–312

[62] DI NOLA, G. ; DE JONG, W. ; SPLIETHOFF, H.: *The fate of main gaseous and nitrogen species during fast heating rate devolatilization of coal and secondary fuels using a heated wire mesh reactor*. In: *Fuel Processing Technology* 90 (2009), Nr. 3, S. 388–395

[63] BROER, Karl M. ; BROWN, Robert C.: *The role of char and tar in determining the gas-phase partitioning of nitrogen during biomass gasification*. In: *Applied Energy* 158 (2015), S. 474–483

[64] CODA ZABETTA, Edgardo ; KILPINEN, Pia ; HUPA, Mikko ; STÅHL, Krister ; LEPPÄLAHTI, Jukka ; CANNON, Michael ; NIEMINEN, Jorma: *Kinetic Modeling Study on the Potential of Staged Combustion in Gas Turbines for the Reduction of Nitrogen Oxide Emissions from Biomass IGCC Plants*. In: *Energy & Fuels* 14 (2000), Nr. 4, S. 751–761

[65] LIU, Xiaorui ; LUO, Zhongyang ; YU, Chunjiang: *Conversion of char-N into NOx and N2O during combustion of biomass char*. In: *Fuel* 242 (2019), S. 389–397

[66] KARLSTRÖM, Oskar ; BRINK, Anders ; HUPA, Mikko: *Biomass Char Nitrogen Oxidation—Single Particle Model*. In: *Energy & Fuels* 27 (2013), Nr. 3, S. 1410–1418

[67] GARIJO, Elena García ; JENSEN, Anker Degn ; GLARBORG, Peter: *Kinetic Study of NO Reduction over Biomass Char under Dynamic Conditions*. In: *Energy & Fuels* 17 (2003), Nr. 6, S. 1429–1436

[68] KARLSTRÖM, Oskar ; PERANDER, Magnus ; DEMARTINI, Nikolai ; BRINK, Anders ; HUPA, Mikko: *Role of ash on the NO formation during char oxidation of biomass*. In: *Fuel* 190 (2017), S. 274–280

[69] WILLIAMS, A. ; JONES, J. M. ; MA, L. ; POURKASHANIAN, M.: *Pollutants from the combustion of solid biomass fuels*. In: *Progress in Energy and Combustion Science* 38 (2012), Nr. 2, S. 113–137

[70] NUSSBAUMER, T.: Primary and Secondary Measures for the Reduction of Nitric Oxide Emissions from Biomass Combustion. In: BRIDGWATER, A. V.; BOOCOCK, D. G. B. (Hrsg.): *Developments in Thermochemical Biomass Conversion*. Dordrecht : Springer Netherlands, 1997, S. 1447–1461

[71] LAMBERG, Heikki ; SIPPULA, Olli ; TISSARI, Jarkko ; JOKINIEMI, Jorma: *Effects of Air Staging and Load on Fine-Particle and Gaseous Emissions from a Small-Scale Pellet Boiler*. In: *Energy & Fuels* 25 (2011), Nr. 11, S. 4952–4960

[72] HOUSHFAR, Ehsan ; SKREIBERG, Øyvind ; TODOROVIĆ, Dušan ; SKREIBERG, Alexandra ; LØVÅS, Terese ; JOVOVIĆ, Aleksandar ; SØRUM, Lars: *NO_x emission reduction by staged combustion in grate combustion of biomass fuels and fuel mixtures*. In: *Fuel* 98 (2012), S. 29–40

[73] HOUSHFAR, Ehsan ; SKREIBERG, Øyvind ; LØVÅS, Terese ; TODOROVIĆ, Dušan ; SØRUM, Lars: *Effect of Excess Air Ratio and Temperature on NO_x Emission from Grate Combustion of Biomass in the Staged Air Combustion Scenario*. In: *Energy & Fuels* 25 (2011), Nr. 10, S. 4643–4654

[74] HOUSHFAR, Ehsan ; LØVÅS, Terese ; SKREIBERG, Øyvind: *Experimental Investigation on NO_x Reduction by Primary Measures in Biomass Combustion: Straw, Peat, Sewage Sludge, Forest Residues and Wood Pellets*. In: *Energies* 5 (2012), Nr. 2, S. 270–290

[75] CARVALHO, Lara ; WOPIENKA, Elisabeth ; POINTNER, Christian ; LUNDGREN, Joakim ; VERMA, Vijay Kumar ; HASLINGER, Walter ; SCHMIDL, Christoph: *Performance of a pellet boiler fired with agricultural fuels*. In: *Applied Energy* 104 (2013), S. 286–296

[76] LIU, Hao ; CHANEY, Joel ; LI, Jinxing ; SUN, Chenggong: *Control of NO_x emissions of a domestic/small-scale biomass pellet boiler by air staging*. In: *Fuel* 103 (2013), S. 792–798

[77] CARROLL, J. P. ; FINNAN, J. M. ; BIEDERMANN, F. ; BRUNNER, T. ; OBERNBERGER, I.: *Air staging to reduce emissions from energy crop combustion in small scale applications*. In: *Fuel* 155 (2015), S. 37–43

[78] SKREIBERG, Øyvind ; KILPINEN, Pia ; GLARBORG, Peter: *Ammonia chemistry below 1400 K under fuel-rich conditions in a flow reactor*. In: *Combustion and Flame* 136 (2004), Nr. 4, S. 501–518

[79] OLUWOYE, Ibukun ; ALTARAWNEH, Mohammednoor ; GORE, Jeff ; DLUGOGORSKI, Bogdan Z.: *Products of incomplete combustion from biomass reburning*. In: *Fuel* 274 (2020), S. 117805

[80] HAN, Kuihua ; NIU, Shengli ; LU, Chunmei: *Experimental study on biomass advanced reburning for nitrogen oxides reduction*. In: *Process Safety and Environmental Protection* 88 (2010), Nr. 6, S. 425–430

[81] BALLESTER, J. ; ICHASO, R. ; PINA, A. ; GONZÁLEZ, M. A. ; JIMÉNEZ, S.: *Experimental evaluation and detailed characterisation of biomass reburning*. In: *Biomass and Bioenergy* 32 (2008), Nr. 10, S. 959–970

[82] CHEN, Qun ; ZHANG, Xiaohui ; ZHOU, Jue ; SHARIFI, Vida N. ; SWITHENBANK, Jim: *Effects of Flue Gas Recirculation on Emissions from a Small Scale Wood Chip Fired Boiler*. In: *Energy Procedia* 66 (2015), S. 65–68

[83] LONDERVILLE, Steve ; ANDERSON, Kevin ; BAUKAL, Charles ; BUSSMAN, Wes: Water/Steam Injection for NO_x Reduction in Process Burners. In: *Water/Steam Injection for NOx Reduction in Process Burners* : *Volume 8A: Heat Transfer and Thermal Engineering* : American Society of Mechanical Engineers, 11092018

[84] MATHIOUDAKIS, K.: *Evaluation of steam and water injection effects on gas turbine operation using explicit analytical relations*. In: *Proceedings of the Institution of Mechanical Engineers, Part A: Journal of Power and Energy* 216 (2002), Nr. 6, S. 419–431

[85] KANE, Mitchell: *Effect of water injection on boiler performance* : Loughborough's Research Repository, 2019

[86] PRONOBIS, Marek: Reduction of nitrogen oxide emissions. In: *Environmentally Oriented Modernization of Power Boilers* : Elsevier, 2020, S. 79–133

[87] SCHREIFELS, Jeremy J. ; WANG, Shuxiao ; HAO, Jiming: *Design and operational considerations for selective catalytic reduction technologies at coal-fired boilers*. In: *Frontiers in Energy* 6 (2012), Nr. 1, S. 98–105

[88] INSTITUTE OF CLEAN AIR COMPANIES, INC: *Selective catalytic reduction (SCR) control of NOx emissions from fossil fuel-fired electric power plants* : *WHITE PAPER*, 2009

[89] WEINBERG, F. J.: *Combustion temperatures: the future?* In: *Nature* 233 (1971), Nr. 5317, S. 239–241

[90] WEINBERG, FELIX: *Heat-Recirculating Burners: Principles and Some Recent Developments*. In: *Combustion Science and Technology* 121 (1996), 1-6, S. 3–22

[91] WEBER, Roman ; GUPTA, Ashwani K. ; MOCHIDA, Susumu: *High temperature air combustion (HiTAC): How it all started for applications in industrial furnaces and future prospects*. In: *Applied Energy* 278 (2020), S. 115551

[92] WÜNNING, J.: *Flameless oxidation to reduce thermal no-formation*. In: *Progress in Energy and Combustion Science* 23 (1997), Nr. 1, S. 81–94

[93] CAVALIERE, Antonio ; JOANNON, Mara de: *Mild Combustion*. In: *Progress in Energy and Combustion Science* 30 (2004), Nr. 4, S. 329–366

[94] TSUJI, Hiroshi (Hrsg.); GUPTA, Ashwani K. (Hrsg.); HASEGAWA, Toshiaki (Hrsg.); KATSUKI, Masashi (Hrsg.); KISHIMOTO, Ken (Hrsg.): *High temperature air combustion* : *From energy conservation to pollution reduction*. Boca Raton : CRC Press, 2019

[95] WÜNNING, J. (Hrsg.): *Flameless Oxidation* : *Proceedings of the 6th HiTACG Symposium; 17th - 19th October 2005, Essen*, 2005

[96] RISTIC, Dragisa: *Feasibility and NO_x reduction potential of flameless oxidation in pulverised coal combustion*. Zugl.: Stuttgart, Univ., Diss., 2012. 1. Aufl. Göttingen : Cuvillier, 2012

[97] WEBER, Roman ; SMART, John P. ; KAMP, Willem vd: *On the (MILD) combustion of gaseous, liquid, and solid fuels in high temperature preheated air*. In: *Proceedings of the Combustion Institute* 30 (2005), Nr. 2, S. 2623–2629

[98] DERUDI, Marco ; ROTA, Renato: *Experimental study of the mild combustion of liquid hydrocarbons*. In: *Proceedings of the Combustion Institute* 33 (2011), Nr. 2, S. 3325–3332

[99] AZEVEDO, Cláudia Gonçalves de ; ANDRADE, José Carlos de ; SOUZA COSTA, Fernando de: *Flameless compact combustion system for burning hydrous ethanol*. In: *Energy* 89 (2015), S. 158–167. URL https://www.sciencedirect.com/science/article/pii/S0360544215009445

[100] LUHMANN, H. ; MALDONADO, F. Carrasco ; SPÖRL, R. ; SCHEFFKNECHT, G.: *Flameless Oxidation of liquid fuel oil in a reverse-flow cooled combustion chamber*. In: *Energy Procedia* 120 (2017), S. 222–229

[101] UHLIG, Dieter (Hrsg.); BERGER, Roland (Hrsg.): *Advantages of using recuperative FLOX combustion for the thermal treatment of landfill gas*, 2017

[102] LÜCKERATH, Rainer ; MEIER, Wolfgang ; AIGNER, Manfred: *FLOX® Combustion at High Pressure With Different Fuel Compositions*. In: *Journal of Engineering for Gas Turbines and Power* 130 (2008), Nr. 1

[103] SCHÜTZ, H. ; LÜCKERATH, R. ; KRETSCHMER, T. ; NOLL, B. ; AIGNER, M.: *Analysis of the Pollutant Formation in the FLOX® Combustion*. In: *Journal of Engineering for Gas Turbines and Power* 130 (2008), Nr. 1

[104] BRIGITTE ROSENDAHL: *Untersuchung der flammlosen Oxidation für die thermische Nutzung schwachkaloriger Gase in Mikro-Gasturbinen*. Ruhr-Universität Bochum, Universitätsbibliothek. Doctoralthesis. 2006

[105] DANON, B. ; DE JONG, W. ; ROEKAERTS, D. J. E. M.: *Experimental and Numerical Investigation of a FLOX Combustor Firing Low Calorific Value Gases*. In: *Combustion Science and Technology* 182 (2010), Nr. 9, S. 1261–1278

[106] DERUDI, Marco ; VILLANI, Alessandro ; ROTA, Renato: *Sustainability of mild combustion of hydrogen-containing hybrid fuels*. In: *Proceedings of the Combustion Institute* 31 (2007), Nr. 2, S. 3393–3400

[107] COLORADO, A. F. ; HERRERA, B. A. ; AMELL, A. A.: *Performance of a flameless combustion furnace using biogas and natural gas*. In: *Bioresource technology* 101 (2010), Nr. 7, S. 2443–2449

[108] EFFUGGI, Alessandro ; GELOSA, Davino ; DERUDI, Marco ; ROTA, Renato: *Mild Combustion of Methane-Derived Fuel Mixtures: Natural Gas and Biogas*. In: *Combustion Science and Technology* 180 (2008), Nr. 3, S. 481–493

[109] MLADENOVIC, Milica ; DAKIC, Dragoljub ; NEMODA, Stevan ; PAPRIKA, Milijana ; KOMATINA, Mirko ; REPIC, Branislav ; ERIC, Aleksandar: *The combustion of biomass - the impact of its types and combustion technologies on the emission of nitrogen oxide*. In: *Hemijska industrija* 70 (2016), Nr. 3, S. 287–298

[110] JOHANSSON, Linda S. ; LECKNER, Bo ; GUSTAVSSON, Lennart ; COOPER, David ; TULLIN, Claes ; POTTER, Annika: *Emission characteristics of modern and old-type residential boilers fired with wood logs and wood pellets*. In: *Atmospheric Environment* 38 (2004), Nr. 25, S. 4183–4195

[111] FELLIN, Marco ; NEGRI, Martino ; ANTOLINI, Daniele ; BAGGIO, Paolo ; PIERATTI, Elisa: *Biomass use best practices: monitoring biomass and process emissions for sustainable use: a case study*. In: *Contemporary Engineering Sciences* 9 (2016), S. 1535–1546

[112] FACHINGER, Friederike ; DREWNICK, Frank ; GIERÉ, Reto ; BORRMANN, Stephan: *How the user can influence particulate emissions from residential wood and pellet stoves: Emission factors for different fuels and burning conditions*. In: *Atmospheric Environment* 158 (2017), S. 216–226

[113] MORÁN, Jorge C. ; MÍGUEZ, José. L. ; PORTEIRO, Jacobo ; PATIÑO, David ; GRANADA, Enrique: *Low-Quality Fuels for Small-Scale Combustion Boilers: An Experimental Study*. In: *Energy & Fuels* 29 (2015), Nr. 5, S. 3064–3081

[114] KIM, Ju Pyo: *Numerical modeling of MILD combustion*. Zugl.: Stuttgart, Univ., Diss., 2008. Aachen : Shaker, 2008 (Berichte aus der Energietechnik)

[115] CELLEK, Mehmet Salih: *Flameless combustion investigation of CH_4/H_2 in the laboratory-scaled furnace*. In: *International Journal of Hydrogen Energy* 45 (2020), Nr. 60, S. 35208–35222

[116] FORTUNATO, Valentina ; GIRALDO, Andres ; ROUABAH, Mehdi ; NACEREDDINE, Rabia ; DELANAYE, Michel ; PARENTE, Alessandro: *Experimental and Numerical Investigation of a MILD Combustion Chamber for Micro Gas Turbine Applications*. In: *Energies* 11 (2018), Nr. 12, S. 3363

[117] KURZ, Dominik: *Numerische Simulation industrieller Rostfeuerungen nach der Euler-Euler Methode*. Zugl.: Stuttgart, Univ., Diss., 2014. Aachen : Shaker, 2014 (Berichte aus der Energietechnik)

[118] LEISER, Simon: *Numerical simulation of oxy-fuel combustion*. Zugl.: Stuttgart, Univ., Diss., 2010. Aachen : Shaker, 2011 (Berichte aus der Energietechnik)

[119] SCHNEIDER, Rolf: *Beitrag zur numerischen Berechnung dreidimensional reagierender Strömungen in industriellen Brennkammern*. Zugl.: Stuttgart, Univ., Diss., 1997. Als Ms. gedr. Düsseldorf : VDI-Verl., 1998 (Fortschritt-Berichte VDI Reihe 6, Energieerzeugung 385)

[120] JONES, W.P ; LAUNDER, B.E: *The prediction of laminarization with a two-equation model of turbulence*. In: *International Journal of Heat and Mass Transfer* 15 (1972), Nr. 2, S. 301–314

[121] FÖRTSCH, D.: *A kinetic model of pulverised coal combustion for computational fluid dynamics: Ein kinetisches Modell der Kohlenstaubverbrennung für die numerische Strömungsberechnung*, 2003

[122] HOWARD, J. B. ; WILLIAMS, G. C. ; FINE, D. H.: *Kinetics of carbon monoxide oxidation in postflame gases*. In: *Symposium (International) on Combustion* 14 (1973), Nr. 1, S. 975–986

[123] MAGNUSSEN, B.: On the structure of turbulence and a generalized eddy dissipation concept for chemical reaction in turbulent flow. In: *19th Aerospace Sciences Meeting*. Reston, Virigina : American Institute of Aeronautics and Astronautics, 1981

[124] JONES, W. P. ; LINDSTEDT, R. P.: *Global reaction schemes for hydrocarbon combustion*. In: *Combustion and Flame* 73 (1988), Nr. 3, S. 233–249

[125] MAGNUSSEN, B. F. ; HJERTAGER, B. H.: *On mathematical modeling of turbulent combustion with special emphasis on soot formation and combustion*. In: *Symposium (International) on Combustion* 16 (1977), Nr. 1, S. 719–729

[126] BRINK, Anders: *Eddy break-up based models for industrial diffusion flames with complex gas phase chemistry*. Zugl.: Åbo, Akad., Diss., 1998. Åbo, 1998 (Report/Åbo Akademi, Kemisk-tekniska Fakulteten, Förbänningskemska Forskargruppen 98-7)

[127] MANCINI, Marco: *Numerische Untersuchung von Mild-Verbrennung von Erdgas mit vorgewärmter Luft*. Zugl.: Clausthal, Techn. Univ., Diss., 2006. 1. Aufl. Clausthal-Zellerfeld : Papierflieger-Verl., 2011

[128] LIU, Shijie: *Bioprocess Engineering* : *Kinetics, Sustainability, and Reactor Design*. 2nd ed. San Diego : Elsevier Science, 2016

[129] OLIVA, M. ; ALZUETA, M. U. ; MILLERA, A. ; BILBAO, R.: *An Approach to the Analysis of Mixing in Reactive Systems*. In: *Chemical Engineering & Technology* 25 (2002), Nr. 4, S. 417–419

[130] ALZUETA, María U. ; BILBAO, Rafael ; MILLERA, Angela ; GLARBORG, Peter ; ØSTBERG, Martin ; DAM-JOHANSEN, Kim: *Modeling Low-Temperature Gas Reburning. NO_x Reduction Potential and Effects of Mixing*. In: *Energy & Fuels* 12 (1998), Nr. 2, S. 329–338

[131] ZWIETERING, Th.N.: *The degree of mixing in continuous flow systems*. In: *Chemical Engineering Science* 11 (1959), Nr. 1, S. 1–15

[132] BERGER, Roland ; ZIEBA, Mariusz: *FLOX-Schwachgasbrenner für niederkalorische Restgase aus Deponien* : *Abschlussbericht über ein Entwicklungsprojekt*. 2010 (FKZ 25491-24/0)

[133] DZURENDA, Ladislav ; LADOMERSKY, Juraj ; HRONCOVÁ, Emília: *Conversion Factor of Fuel-Bound Nitrogen to Oxides in the Process of Spruce Wood Combustion in Boiler Grate Furnaces*. In: *Polish Journal of Environmental Studies* 24 (2015)

[134] DZURENDA, Ladislav ; HRONCOVÁ, Emília ; LADOMERSKÝ, Juraj: *Extensive Operating Experiments on the Conversion of Fuel-Bound Nitrogen into Nitrogen Oxides in the Combustion of Wood Fuel*. In: *Forests* 8 (2017), Nr. 1, S. 1

[135] PLECKAITINE, Raminta ; BUINEVICIUS, Kestutis: *The factors which have influence on nitrogen conversion formation*. In: *8th International Conference on Environmental Engineering, ICEE 2011* (2011)